From the
Walter-Brendel-Zentrum für Experimentelle Medizin
of the Ludwig-Maximilians-Universität München
Interim Director: Prof. Dr. med. Markus Sperandio

Circadian Control of Leukocyte Numbers in the Circulation

Dissertation
zum Erwerb des Doctor of Philosophy (PhD)
an der Medizinischen Fakultät der
Ludwig-Maximilians-Universität

submitted by

Sophia Martina Hergenhan

from

Bad Neustadt a.d. Saale, Germany

München, 2020

Supervisor: Prof. Dr. Christoph Scheiermann

Second evaluator: Prof. Dr. Markus Sperandio

Dean: Prof. Dr. med. dent. Reinhard Hickel

Date of oral defense: 25.03.2020

Acknowledgements

First of all, I want to thank my supervisor Christoph Scheiermann. His passion for science is catching and convinced me from the first second to work in a research field that I hardly heard of before. His door was always open for any concern and I highly appreciate that I was never afraid to ask potentially stupid questions. I am also very glad that the whole group was a great team and we were able to work together very well, especially during several night-time experiments. I am especially thankful for the help and discussions with Louise Ince, Alba de Juan, Chien-Sin Chen, Wenyan He, Jasmin Weber, Stephan Holtkamp, Robert Pick, David Druzd and Kerstin Kraus representing current and former members of the Munich Lab. Without them, this work would not have been possible. But also the support from Geneva was amazing, although we only met once or twice in person.

Additionally, many PhD students, postdocs and also PIs from our institute, but also from the two graduate schools IMPRS and IRTG914 that I was associated with, took great care of me and my project, which made me feel very comfortable. Particularly my TAC members Markus Sperandio and Reinhard Fässler as well as my collaborators supported me a lot. The whole campus forms an incredible network and makes it very hard for me to leave.

Of course, a PhD is never easy-going and probably the most important thing during tough times is the support of your friends and family. I am so incredibly grateful for my best friends Saskia and Peter who were always there for me, no matter what happened. I could have never done this without you. Also, colleagues became friends and enriched my life so much during the last months and years, always giving me a reason to get up in the morning and come to the lab with (almost) always a smile on my face although the project was difficult at that time. I will miss our productive get-togethers so much.

Last but not least, I want to thank my parents. They supported me from day one, not only during my PhD but already my whole life, no matter how tiring I was, and encouraged me to do whatever my gut feeling told me to. This achievement was only possible because I knew that you would be there for me if I failed and I feel so blessed to have your silent but constant support. Danke!

Abstract

Circadian rhythms play an important role in determining the strength of the immune response. Key entrainment factors for these oscillations are light, behaviour and food intake. It has previously been shown that leukocyte mobilization from the bone marrow fluctuates over the course of the day. In addition, leukocyte homing to organs contributes to an oscillatory cell count in the circulation. However, it is currently unclear which factors determine oscillations in blood cellularity.

Leukocyte numbers were investigated after altering the main entrainment factors and timed feeding was able to phase-shift rhythms in white blood cell numbers in blood, while light was only able to shape these rhythms. Additionally, germ-free animals exhibited lower leukocyte counts at specific times and reduced oscillations in overall cellularity. Serum transfer experiments revealed increased leukocyte numbers in the circulation at specific times. These increases could be prevented by genetic ablation of toll-like receptor adaptor molecule MyD88 or pharmacological targeting of inflammatory cytokines. On a molecular level, time-restricted feeding (TRF) phase-shifted clock gene expression in peripheral organs that receive input from the gut and leukocytes from germ-free animals exhibited altered expression of migratory factors.

It is known that TRF induces circadian rhythms in microbiota composition, orchestrated by the central clock. Additionally, commensal bacteria influence the immune system by priming innate immune cells for potential infections. Taken together, these data propose a daily steady-state inflammation as part of normal host physiology, leading to rhythmic leukocyte numbers in blood. This physiological immune priming is mediated by rhythms in commensal bacteria, controlled by timed food uptake.

Table of contents

List of figures

List of tables

List of abbreviations

ABX	Antibiotics-depleted
AMP	Anti-microbial peptide
APC	Antigen presenting cell
ARNTL1	Aryl hydrocarbon receptor nuclear translocator-like protein 1
bHLH	Basic helix-loop-helix
BIR	Baculovirus Inhibitor of apoptosis protein Repeat
BM	Bone marrow
BMAL	Brain and Muscle ARNT-Like 1
bp	Base pair
BrdU	Bromodeoxyuridine
bZIP	Basic region leucine zipper
CARD	Caspase activation and recruitment domain
CBA	Cytokine bead array
cDC	Conventional DC
cDNA	Complementary DNA
CLOCK	Circadian Locomotor Output Cycles Kaput
CLR	C-type lectin receptors
Co	Control
CRY	Cryptochrome
DAMP	Danger-associated molecular pattern
DAPI	4',6-diamidino-2-phenylindole buffer
DBP	D site of albumin promoter (albumin D-box) binding protein
DC	Dendritic cell
DD	Constant darkness
DNA	Deoxyribonucleic acid
DRF	Dark-restricted feeding
dsRNA	Double stranded RNA
EAE	Experimental autoimmune encephalomyelitis
EC	Endothelial cell
EDTA	Ethylenediaminetetraacetic acid
FACS	Fluorescence activated cell sorting
FADD	Fas-associated protein with death domain
FBS	Fetal bovine serum
FEO	Food-entrainable oscillator
FITC	Fluorescein isothiocyanate
GAPDH	Glyceraldehyde-3-phosphate dehydrogenase
GF	Germ-free
HPA	Hypothalamic-pituitary-adrenal
i.p.	Intraperitoneal
i.v.	Intravenous
ICAM-1	Intercellular adhesion molecule-1
IEC	Intestinal epithelial cell

IFN	Interferon
Ig	Immunoglobulin
IGF-1	Insulin-like growth factor-1
IKK	Inhibitor of κ-B kinase
IL	Interleukin
IL1R	IL-1 receptor
IM	Inflammatory monocytes
ipRGC	Intrinsically photosensitive retinal ganglion cells
IRAK	Interleukin-1 receptor associated kinase
IRF	Interferon regulatory factor
JAM1	Junction adhesion molecule 1
KEGG	Kyoto Encyclopedia of Genes and Genomes
KO	Knockout
LBP	LPS binding protein
LFA-1	Leukocyte function associated molecule-1
LL	Constant light
LN	Lymph node
LPS	Lipopolysaccharide
LRF	Light-restricted feeding
LTA	Lipoteichoic acid
MAMP	Microbial activating molecular pattern
MAPK	Mitogen-activated protein kinase
MB	Microbiota
MD-2	Myeloid differentiation factor-2
MHC	Major histocompatibility complex
mRNA	Messenger RNA
MyD88	Myeloid differentiation primary response 88
NEMO	Nuclear factor κ-B essential modulator
NFIL3	Nuclear Factor, Interleukin 3 Regulated
NFκb	Nuclear factor κ-B
NIM	Non-inflammatory monocytes
NK	Natural killer
NLR	NOD-like receptor
OUT	Operational taxonomic units
PAF	Platelet-activated factor
PAMP	Pathogen-associated molecular pattern
PBS	Phosphate buffered saline
PCR	Polymerase chain reaction
pDC	Plasmacytoid DC
PEB	Protein extraction buffer
PECAM-1	Platelet endothelial adhesion molecule-1
PER	Period
PRR	Pattern recognition receptor
qPCR	Quantitative real-time PCR

RBC	Red blood cell
RHT	Retinohypothalamic tract
RIP	Receptor-interacting protein
RLR	RIG-I-like receptors
RNA	Ribonucleic acid
rRNA	Ribosomal RNA
RT	Reverse transcription
RT	Room temperature
SCN	Suprachiasmatic nuclei
SDS	Sodium dodecyl sulphate
SEM	Standard error of the mean
SPF	Specific pathogen free
ssRNA	Single stranded RNA
STAT1	Signal transducer and activator of transcription 1
TAB	TAK-1 binding protein
TAK-1	Transforming growth factor β-activated kinase-1
TBK1	TANK-binding kinase 1
TE	Tris EDTA
TLR	Toll-like receptor
TNF	Tumour necrosis factor
TRADD	TNF receptor type 1-associated DEATH domain protein
TRAF	TNF receptor associated factor
TRF	Time-restricted feeding
TRIF	TIR-domain-containing adapter-inducing interferon-β
UPEC	Uropathogenic *E.coli*
VCAM-1	Vascular cell adhesion molecule-1
VLA-4	Very late antigen-4
WBC	White blood cell
WT	Wild-type

1. Introduction

1.1. Circadian Rhythms

The earth's rotation leads to light and dark phases that are following a 24 h rhythm, marking our day and night. The term "circadian" originates from the Latin words "circa" and "dies" and means "approximately/about a day", therefore describing what takes place within these 24 h. Since early development of life, the niches between the light and dark phase were used to optimize life's adaption to the environmental cues. Most strikingly, these adjustments are encoded within the genome and evolutionary conserved among the different taxonomic kingdoms including bacteria, plants, insects and of course mammals (Bell-Pedersen et al., 2005).

1.1.1. Molecular clock

It was already known in the 18th century that some daily rhythms in plants are persisting without external entrainment factors, such as light (Gardner et al., 2006). These freely running rhythms were also described in animals at the beginning of the 20th century, leading to the assumption that there must be some internal master coordination underlying this effect (Bruce, 1957; Pittendrigh, 1993). However, it was not before 1971 and 1984 until this hypothesis could be proven by discovering and isolating the first clock gene *period* in Drosophila by Jeffrey C. Hall and Michael Rosbash (Reddy et al., 1984; Zehring et al., 1984). Together with Michael W. Young, they were awarded the Nobel Prize in Medicine and Physiology in 2017, highlighting the importance of this research.

Soon after these discoveries, clock genes were also detected in multiple other species, including cyanobacteria, plants, and also mammals (Albrecht et al., 1997; Kurosawa et al., 2006; Nagy F, 1988). Interestingly, these genes are able to maintain a circadian rhythm although they function in different ways throughout diverse species. The clock proteins of cyanobacteria are even able to maintain their approximate 24h rhythm in a test tube without any other ingredient except for ATP (Nakajima et al., 2005).

In mammals, the molecular clock persists of three transcriptional feedback loops that contain at least ten genes. The most important gene here is *Arntl1* or *Bmal1* since a knock-out of this gene alone completely abolishes the internal rhythms (Bunger et al., 2000). BMAL1 is a basic helix-loop-helix (bHLH) transcription factor and forms a heterodimer with CLOCK, another bHLH transcription factor. These two proteins form the positive branch of the feedback system by binding to E-boxes in promoters of different target genes and inducing their transcription (Ohno et al., 2007; Yoo et al., 2005). Hereby, they also induce the expression of their own repressors, PER1, PER2 and PER3 as well as CRY1 and CRY2. The PER-CRY heterodimer then inhibits the expression of *Bmal1* and *Clock* on a transcriptional level, forming the negative branch of the feedback loop (**Figure 1-1**) (Griffin et al., 1999; Sangoram et al., 1998). Moreover, there is a third loop existing that increases the stability and precision of the internal clock. This branch consists of Rev-Erbα/β

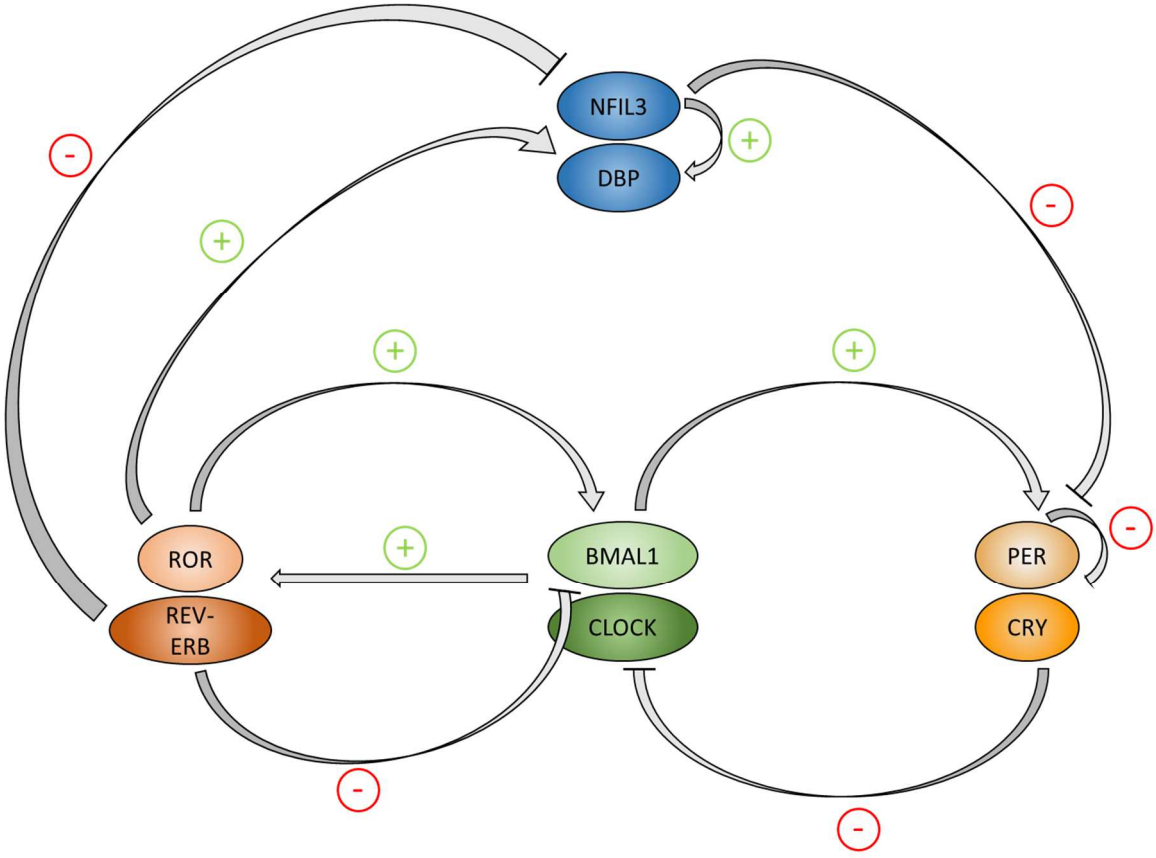

Figure 1-1: Interactions in the molecular clock. BMAL1 is the central clock component that forms a heterodimer with CLOCK. Both induce the transcription of their own repressors PER and CRY, forming a first loop. RORs competes with REV-ERBs for binding to RORE-elements in the promoter of BMAL1, where ROR induces its expression and REV-ERB inhibits it. BMAL1 in turn activates expression of both genes, establishing a second loop. In a third loop, DBP expression is activated by ROR and NFIL3. NFIL3 additionally functions as repressor of the PER:CRY heterodimer while being repressed itself by REV-ERBα. These three loops together form a central oscillatory network.

and Ror-α/-β/-γ, whose expression is under the control of E-boxes and therefore regulated by BMAL1:CLOCK directly. REV-ERB and ROR proteins compete for RORE-binding sites in promoter regions, such as in the gene locus of *Bmal1*. However, they have different effects upon binding: Binding of ROR elements leads to the induction of transcription of *Bmal1* while binding of REV-ERB proteins inhibits this process (**Figure 1-1**) (Guillaumond et al., 2005).

Another influencing feedback loop is formed by the D-box binding PAR bZIP transcription factors. Two representatives are D-Box binding protein (DBP) and NFIL3. Both bind to D-box containing promoters, such as the Period genes and hence regulate their transcription in an additional manner (**Figure 1-1**) (Ueda et al., 2005).

These regulatory mechanisms affect the genome, rendering about 10% under direct circadian regulation (Panda et al., 2002; Storch et al., 2002). Due to multiple additional mechanisms on a post-transcriptional level, it is suggested that even a higher percentage of daily rhythmicity is present at the protein level (Robles et al., 2014).

This molecular clock is present in every nucleated mammalian cell so far investigated, however, it still requires external *Zeitgebers* to synchronize these rhythms to a functional system (Stratmann and Schibler, 2006). *Zeitgeber* (ZT) is a German term and means “time giver”, therefore describing the entrainment factors that are influencing and regulating the molecular clocks.

1.1.2. Central clock

To organize all the different, peripheral clocks in one organism, there is the need of a central clock or conductor, which records the external entrainment factors from the environment and subsequently instructs the molecular clocks in various tissues. In mammals, this master pacemaker is localized in the suprachiasmatic nuclei (SCN) in the hypothalamus of the brain (Moore, 1973). The SCN receive direct photic input from the intrinsically photosensitive retinal ganglion cells (ipRGCs) in the retina via the retinohypothalamic tract (RHT). Hence, they process the main entrainment factor light (Do and Yau, 2010). Moreover, the about 20 000 neurons in the SCN show circadian electrical activity *in vitro* on a single cell level, due to their spontaneous action potentials (Green and Gillette, 1982; Yamazaki et al., 1998).

Together with input from other photoreceptors, the ipRGC-RHT-SCN axis therefore provides a very robust master pacemaker that is also able to absorb perturbations to a certain extent. Lesion of the SCN has been clearly shown to abrogate the synchronization of the peripheral clocks, leading to arrhythmic behaviour and body temperature (Eastman et al., 1984; Stephan and Zucker, 1972).

The influence on organ clocks occurs via humoral and neuronal pathways via the hypothalamic-pituitary-adrenal (HPA) axis. For the humoral output, the SCN induces the production of adrenocorticotropic hormone (ACTH) from the pituitary gland, thus influencing the rhythmic release of glucocorticoid hormones from the adrenal gland (Rosenfeld et al., 1993). These hormones then form entraining signals for peripheral clocks since the core clock genes *Bmal1*, *Cry1*, *Per1* and *Per2* exhibit the respective response elements (So et al., 2009). However, almost every mammalian cell expresses the glucocorticoid nuclear hormone receptors, leading to a global influence on gene expression (**Figure 1-2**).

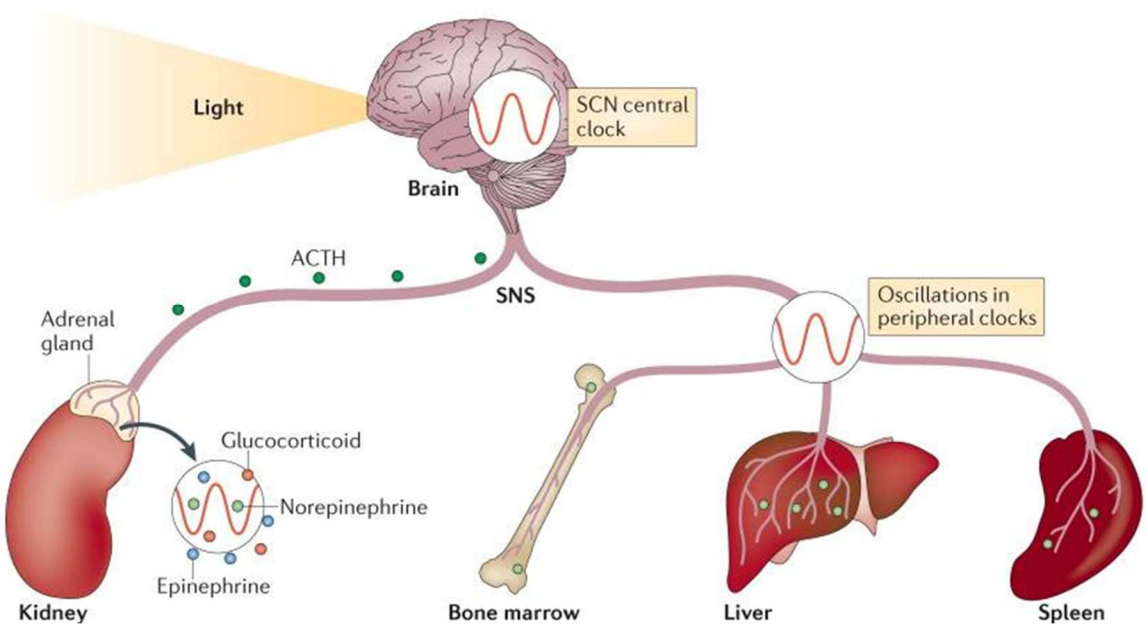

Figure 1-2: Orchestration of peripheral clocks by the central clock. Light is sensed by the eye and this signal is further processed in the suprachiasmatic nuclei (SCN) of the hypothalamus in the brain. This central clock orchestrates and synchronizes peripheral clocks via two main pathways. On the one hand, adrenocorticotropic hormone (ACTH) regulates the rhythmic release of glucocorticoid hormones from the adrenal gland, forming a humoral pathway. On the other hand, the sympathetic nervous system (SNS) influences the sensitivity of peripheral organs to these hormones and hence builds a nervous output pathway.

Furthermore, the sympathetic nervous system (SNS) affects this humoral output by regulating the sensitivity of the adrenal gland to ACTH (Oster et al., 2006). Also,

direct sympathetic innervation of tissues adjusts the peripheral rhythms by a circadian, local release of noradrenaline.

Taken together, this system provides a central conductor that synchronizes via multiple ways the peripheral clocks analogous to a well-coordinated orchestra, perfectly adapted to external entrainment factors.

1.1.3. Food as Entrainment Factor

The 24h oscillation in light and dark phases is not the only entrainment factor since another very important *Zeitgeber* is food intake. In mice lacking a functional clock, e.g. by SCN lesion, and therefore exhibiting desynchronized peripheral clocks and dysfunctional behavioural rhythms, it was possible to rescue these oscillations via time-restricted feeding (Krieger et al., 1977). Furthermore, using mice with a functional clock but applying food restriction to the resting phase, desynchronization between the central clock and some peripheral clocks could be achieved (Damiola et al., 2000; Pezuk et al., 2010). Further studies were even able to prospect the presence of a food-entrainable oscillator (FEO), which can anticipate food availability (Stephan et al., 1979). This observed increase in activity is still present after fasting, after SCN lesion or in mice with a dysfunctional molecular clock, therefore indicating an additional internal oscillating mechanism. While the existence of a FEO, especially anatomically, is controversial (Pendergast and Yamazaki, 2018), a recent publication claims that insulin and insulin-like growth factor-1 (IGF-1) mediate the effects of timed feeding on a cell-autonomous and hence SCN-independent level (Crosby et al., 2019). However, there are more factors to be considered as underlying mechanism between food intake and its influence on circadian rhythms.

1.1.4. Relevance

Circadian rhythms are not just a rudiment from evolution, but still very important for our whole physiology. Misalignment of internal rhythms with external *Zeitgebers*, for instance, leads to various clinical and subclinical symptoms such as fatigue, insomnia, digestive troubles, cardiovascular diseases, reduced performance of the immune system and even cancer (Alibhai et al., 2015; Leproult et al., 2014; Litinski

et al., 2009; Stevens et al., 2007). This strong link to pathophysiology shows that almost every branch in physiology is influenced by these oscillations.

For example, about 25% of all metabolites underlie circadian cycles due to rhythms in many rate-limiting enzymes in metabolic processes (Dallmann et al., 2012). Disruption in these rhythms lead to severe alterations such as an increase in glucose and lipids and further also an increase in body mass. Several clock gene knockouts have shown that these genes are closely related with the regulation of metabolism and alterations in either clock gene expression or also desynchronization by e.g. shift work can predispose for the development of metabolic syndrome and obesity (Carvas et al., 2012; Delezie et al., 2012; Marcheva et al., 2010).

In the cardiovascular system, the heart beat presents a clear circadian oscillation. During the active phase, frequencies and cardiac output are higher, hence leading to a rhythm of blood supply in the tissue that coincides with oscillations in oxygen and nutrient reserves. Moreover, there is a significant peak in cardiovascular events at the beginning of the behavioural active phase and desynchronization of daily rhythms increases the pathogenesis of cardiovascular diseases (Durgan et al., 2010; Larochelle, 2002).

Disruption of circadian rhythms was also found to be associated with a higher cancer risk in basically every organ system tested (Kubo et al., 2006; Lahti et al., 2008; Schernhammer et al., 2003; Stevens, 2009; Viswanathan et al., 2007). Moreover, circadian interruptions are linked with poor therapeutic responses and early mortality (Kim et al., 2012; Levi et al., 2007; Sephton et al., 2000). This is why the World Health Organization's International Agency for Research on Cancer (IARC) listed shift work with circadian disruption as carcinogen in 2007 (Fu and Kettner, 2013).

Most importantly for this project, however, are the oscillations in the immune system. Many processes, such as the distribution of leukocytes, their migration and their function show clear circadian rhythms. Since this a key part of this project, these effects will be explained in detail later.

1.2. Immune system

Every day, our body faces multiple threats to our health, such as bacteria, viruses, but also fungi, parasites and other pathogens. It is our highly developed immune system that manages to keep these pathogens under control - most of the time. This regulation can be classified into an innate and an adaptive immune response with both of them being dependent on the activity of white blood cells, the leukocytes.

1.2.1. Innate immune system

The innate immune system is defined as providing a quick and unspecific immune response to conserved structures across a broad range of microorganisms. The recognition receptors for these pathogenic patterns are encoded in the DNA and similar mechanisms exist in many different organisms, such as vertebrates but also insects (Zhang et al., 2010). The response is limited to the preserved recognition of ligands and mediated by different cell types, which are mainly professional phagocytes and killer cells.

1.2.1.1. Pattern recognition receptors

Pattern recognition receptors (PRRs) are germline encoded receptors that recognize pathogen-associated molecular patterns (PAMPs) and damage- or danger-associated molecular patterns (DAMPs). PAMPs for example are components of bacterial cell membranes or viral nucleic acid while DAMPs present self-molecules that are only exposed during cell damage (Seong and Matzinger, 2004). Activation of these receptors leads to the production of pro-inflammatory cytokines, type I interferons, chemokines and antimicrobial peptides.

1.2.1.1.1. Toll-like receptors

The most prominent PRRs are toll-like receptors (TLRs). In humans, ten TLRs were detected so far while in mouse, twelve TLRs have been described. These receptors are membrane-bound and either located at the outside of the cell (TLR1, 2, 4, 5, 6, and 11) or in endosomes and lysosomes (TLR3, 7, 9, and 10; see also **Table 1-1**).

TLR	Location	Ligands	Pathogen	Cell type	Characteristics	Ref.
TLR1	cell surface	Diacyl lipoproteins, peptidoglycans, lypotechoic acids, tymosan, mannan, mucin	Gram+ bacteria	Monocytes, macrophages, DCs, microglia	Heterodimer with TLR2	(Kawai and Akira, 2010; Takeuchi et al., 2002)
TLR2	cell surface	Diacyl and triacyl lipoproteins, peptidoglycans, lypotechoic acids, tymosan, mannan, mucin	Gram+ bacteria	Monocytes, macrophages, DCs, microglia	Heterodimer with TLR1 and TLR6	(Kawai and Akira, 2010; Takeuchi et al., 2002)
TLR3	endosomal	dsRNA, polyI:C	Virus (reovirus)	DCs, stromal cells	Only TLR without MyD88	(Zhang et al., 2007)
TLR4	cell surface	LPS	Gram- bacteria	DCs, neutrophils, mast cells, B cells, epithelial cells	Switch between MyD88 and TRIF pathway possible	(Yamamoto et al., 2003)
TLR5	cell surface	flagellin	Flagellated bacteria	DCs, macrophages in lamina propria, IECs	Intestinal homeostasis	(Uematsu et al., 2008)
TLR6	cell surface	Triacyl lipoproteins, peptidoglycans, lypotechoic acids, tymosan, mannan, mucin	Gram+ bacteria	Monocytes, macrophages, DCs, microglia	Heterodimer with TLR2	(Kawai and Akira, 2010; Takeuchi et al., 2002)
TLR7/8	endosomal	ssRNA (bacterial RNA), imidazoqionolines	Virus, (bacteria)	pDCs, B cells (cDCs)	TLR7: murine, TLR8: human	(Mancuso et al., 2009)
TLR9	endosomal	Unmethylated CpG-DNA	Virus, bacteria	DCs, macrophages, B cells	Role in malaria, circadian	(Coban et al., 2010; Silver et al., 2012b)

TLR	Loca-tion	Ligands	Pathogen	Cell type	Charac-teristics	Ref.
TLR10	cell surface	Not yet identified		B cells, DCs, eosinophils, neutrophils	Only in humans, Anti-inflammatory	(Oosting et al., 2014)
TLR11	endo-somal	Flagellin, UPEC-component, profilin-like molecule	Uropathogenic *E.coli* (UPEC), *Toxoplasma gondii*	Macro-phages, DCs, epithelial cells in liver, bladder, kidney	Only in mice	(Lauw et al., 2005; Yarovinsky et al., 2005)
TLR12	endo-somal	profilin	*Toxoplasma gondii*	Myeloid cells	Only in mice	(Koblansky et al., 2013)
TLR13	endo-somal	23S rRNA Unknown components	Bacteria Vesicular stomatitis virus	DCs, macro-phages	Only in mice	(Oldenburg et al., 2012; Shi et al., 2011)

Table 1-1: Location, ligands of stimulating pathogens and characteristics of different TLRs.

Every receptor has a different ligand and binding can induce different inflammatory responses, also depending on the expressing cell type (**Table 1-1**) (Akira, 2006).

TLR2 mainly binds diacyl and triacyl lipoproteins that are present in many pathogens. It is expressed on many cells of the innate immune system, such as monocytes and macrophages, dendritic cells (DCs), microglia, but also on cells of the adaptive immune response and on epithelia of the respiratory tract, the gastrointestinal tract and the skin. TLR2 can form heterodimers with TLR1 and TLR6, therefore varying the specificity (Barbalat et al., 2009; Cario, 2008).

TLR4 is probably the most prominent representative of TLRs, known for binding lipopolysaccharide (LPS), a key component in the wall of Gram-negative bacteria. For detecting LPS, LPS binding protein (LBP) has to attach to LPS and transfer to membrane-bound CD14. This complex can then be recognized by myeloid differentiation factor-2 (MD-2), which is associated with the extracellular part of TLR4. Activation leads to the homodimerization of TLR4 and the activation of downstream pathways (**Figure 1-3**) (Lu et al., 2008).

Another surface-expressed TLR is TLR5, which is highly expressed on dendritic cells and macrophages of the lamina propria in the small intestine. Its ligand is bacterial flagellin and it is crucial for maintaining intestinal homeostasis. TLR11 is a TLR5 homologue in mice that is highly expressed in liver, bladder and kidney, therefore probably recognizing uropathogenic bacteria and other pathogens typical for these areas (Uematsu et al., 2006).

On the other side, the intracellular TLRs bind nucleic acid structures from viruses and bacteria, but also detect endogenous nucleic acids that are present in a pathogenic context. Their activation additionally induces the expression of type I interferons, hence generating an anti-viral immune response. TLR3 binds viral dsRNA and is the only TLR, which is not signalling through Myeloid differentiation primary response 88 (MyD88) but only via TIR-domain-containing adapter-inducing interferon-β (TRIF) (O'Neill and Bowie, 2007). It is mostly expressed on hematopoietic cells, subsets of DCs and also stromal cells. Murine TLR7 or the human analogue TLR8 recognize ssRNA and also bacterial RNA in plasmacytoid DCs (pDCs) and B cells while TLR9 is able to identify unmethylated DNA in CpG motifs (Mancuso et al., 2009). TLR7 and TLR9 are highly expressed in pDCs and induce a high response in type I interferons due to viral infections. For the recognition of endogenous nucleic acid, however, is the localization crucial to avoid autoimmunity. For that reason, intracellular TLRs are localized close to the endoplasmic reticulum and only recruited to endolysosomes after ligand binding where they additionally undergo further processing (**Table 1-1**) (Ewald et al., 2008).

1.2.1.1.2. Signalling pathways

Binding of the according ligand to its receptor activates mainly two different signalling pathways. On the one hand is the MyD88 adaptor molecule activated and on the other hand TRIF.

MyD88 is a crucial adaptor molecule for all TLRs except TLR3. Upon TLR activation, MyD88 interacts with interleukin-1 receptor associated kinase-4 (IRAK-4), a serine/threonine kinase that in turn stimulates IRAK-1 and IRAK-2. These kinases then cooperate with TNF receptor associated factor 6 (TRAF6), which has an E3 ubiquitin protein ligase function (Kawagoe et al., 2008). TRAF6 together with an E2 ubiquitin-conjugation enzyme complex next builds up a K63-poly-ubiquitin chain that activates transforming growth factor β-activated kinase-1 (TAK-1). TAK-1 is a

mitogen-activated protein kinase (MAPK) and works together with TAK-1 binding proteins (TAB) 1, 2, and 3 to phosphorylate inhibitor of κ-B kinase β (IKKβ) and MAPK6 (Dong et al., 2006). The IKK complex, consisting of IKKα, IKKβ and nuclear factor κ-B essential modulator (NEMO), subsequently phosphorylates inhibitor of κ-B (IκBα) and hence leads to its degradation. Therefore, nuclear factor κ-B (NF-κB) is free to translocate to the nucleus and induce the expression of pro-inflammatory genes (**Figure 1-3**) (Oeckinghaus and Ghosh, 2009).

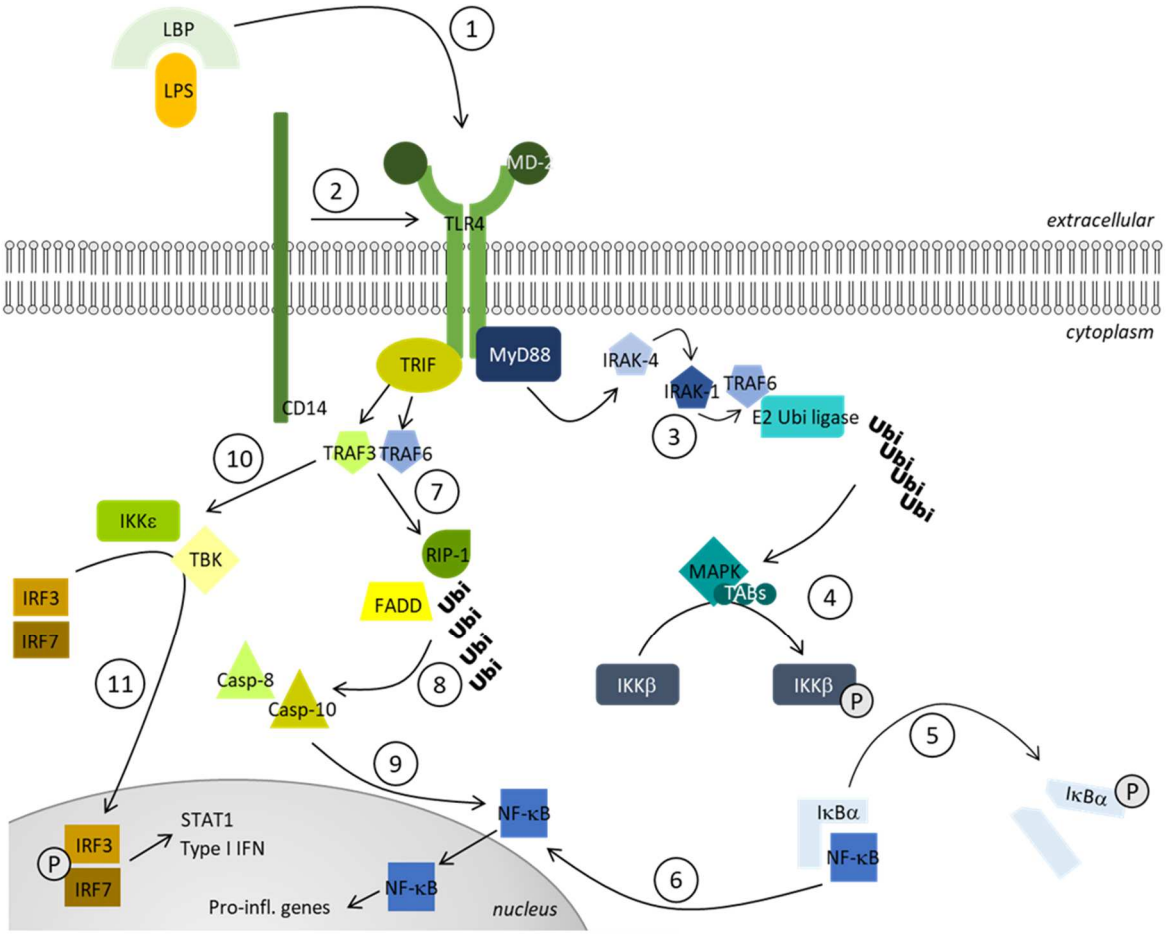

Figure 1-3: TLR4 signalling pathways. (1) TLR4 ligand LPS is bound by LPS-binding protein (LBP) in the extracellular space. Together, they are recognized by the TLR4:MD-2 complex, which leads to recruitment of CD14 (2). This hence allows downstream signalling via two adaptor molecules: MyD88 (shadows of blue) and TRIF (shadows of green). (3) MyD88 next interacts with IRAK-4, which next activates IRAK-1 and TRAF6. TRAF6 associates with an E2 ubiquitin ligase and self-ubiquitination activates a MAPK. (4) This MAPK phosphorylates IKKβ, which subsequently phosphorylates IκBα, the inhibitor of NF-κB. (5) Phosphorylated IκBα becomes instable and is degraded while NF-κB can translocate to the nucleus and induce the expression of pro-inflammatory molecules (6). (7) The other TLR adaptor molecule, TRIF, associates with TRAF3 and TRAF6, which activate RIP-1. (8) Interaction of RIP-1 with FADD results in auto-ubiquitination, which activates caspase-8 and -10. (9) These caspases also induce translocation of NF-κB into the nucleus to induce gene expression. (10) TRAF3 additionally activates kinases IKKε and TBK, resulting in phosphorylation of IRF3 and IRF7. (11) This allows their translocation into the nucleus, where they induce gene expression of STAT1 and type I interferons (IFN).

In the TRIF pathway, TRIF associates with TRAF3 and TRAF6 upon receptor engagement. Moreover, this complex next interacts with receptor-interacting protein (RIP) -1 and -3. Using the adaptor molecule TNF receptor type 1-associated DEATH domain protein (TRADD), RIP-1 forms a complex with Fas-associated protein with death domain (FADD). This association next ubiquitinates RIP-1 and additionally activates caspase-8 and -10. Both leads to the translocation of NF-κB to the nucleus, where it can induce the translation of its target genes (Pobezinskaya et al., 2008; Takahashi et al., 2006). Moreover, TRAF3, which associates with TRIF after receptor binding, activates the IKK-related kinases TANK-binding kinase 1 (TBK1) and IKKε (Hacker et al., 2006). The targets of these kinases are interferon regulatory factor (IRF) 3 and IRF7, which translocate into the nucleus after their phosphorylation. There, they induce the transcription of type I interferons while IKKε additionally phosphorylates signal transducer and activator of transcription 1 (STAT1) to facilitate the transcription of these genes (**Figure 1-3**) (Tenoever et al., 2007).

1.2.1.1.3. Other PRRs

Besides TLRs, there are a couple of other PRRs existing. Firstly, the C-type lectin receptors (CLRs) that are characterized by their carbohydrate binding domain. The recognized carbohydrates mostly derive from fungi, but also carbohydrates from bacteria and viruses are identified (van Kooyk, 2008). Some examples are mannose, a carbohydrate expressed by viruses, fungi and mycobacteria, fucose, which is present on certain bacteria and also helminths, and glucan, originating from mycobacteria and fungi (Rothfuchs et al., 2007). CLRs are mainly expressed on DCs and macrophages and remarkably influence the adaptive immune response. This link between the innate and adaptive immune system is achieved by internalization, degradation and presentation of the pathogen due to receptor activation. The exact signalling pathways are complex and also depend on interactions with other PRRs as well as the cell type, but they mainly lead to the activation and modulation of transcription factor NF-κB (Sato et al., 2006).

Secondly, NOD-like receptors (NLRs) function as additional cytoplasmic pathogen sensors with a nucleotide-binding domain. They recognize peptidoglycans from Gram-negative and Gram-positive bacteria and interact with adaptor molecules

via N-terminal binding motifs, such as caspase activation and recruitment domains (CARDs), pyrin domains or Baculovirus Inhibitor of apoptosis protein Repeat (BIR) domains (Caruso et al., 2014). The signal transduction also targets MAPKs and NF-κB via RIP2. The most prominent representatives of NLRs are NLRP3 and NLRP4, which are known for activating inflammasomes (Ip and Medzhitov, 2015).

Lastly, cytoplasmic RIG-I-like receptors (RLRs) recognize dsRNA and ssRNA of viruses. They are typically expressed on fibroblasts and conventional DCs (cDCs) and their activation triggers the expression of type I interferons (Mahla et al., 2013).

1.2.1.2. Cytokines

Cytokines are small proteins that are secreted in response to a distinct stimulus by various cells. Upon activation of PRRs, macrophages and other innate immune cells mostly secrete pro-inflammatory cytokines such as interleukin-1 (IL-1), IL-6 and tumour necrosis factor α (TNFα), which act not only locally, but also systemically.

IL-1 activates the vascular endothelium and lymphocytes, and facilitates the access of effector cells to the site of infection. Systemically, it induces fever and the production of IL-6. Most prominent members of the IL-1 family are IL-1α and IL-1β representing the bound and hence locally operating form as well as the secreted and systemically active form, respectively. Both bind to the IL-1-receptor (IL-1R) that is associated with the adaptor molecule MyD88 and hence leads to further activation of NF-κB (Dinarello, 2009). Moreover, IL-1 affects bone marrow (BM) stem cells and induces the differentiation of myeloid progenitor cells as well as the mobilization of neutrophils into the circulation (van Damme et al., 1986).

IL-6 has similar effects with activating lymphocytes, inducing fever and increasing the production of acute-phase proteins. Likewise, it is also able to stimulate the mobilization of neutrophils from the bone marrow (Suwa et al., 2000).

TNFα allows easier entry of IgG and effector cells into tissues by increasing the permeability of the vascular endothelium. Furthermore, it also induces fever and plays a critical role in shock. Under steady-state conditions, it is crucial for monocyte survival (Wolf et al., 2017).

Altogether, these cytokines guide the inflammation after an infection, however, they are all also expressed under steady-state conditions and probably manage different roles in this situation (Van Bezooijen et al., 1998).

1.2.1.3. Mechanical barriers

The very first defence mechanism is built by epithelial surfaces. Using multiple mechanisms, such as tight junctions between the epithelial cells, this barrier is a mechanistic hurdle for pathogens to enter the organism. Since a potential infection mostly takes place at internal epithelial surfaces, these barriers are often additionally covered with mucus to hinder the adherence of pathogens. Epithelia also frequently produce antimicrobial and antifungal substances by specific secretory cells to reduce the pathogen load directly upon contact that cover the pathogens to allow an easy opsonisation and therefore phagocytosis by the innate immune cells (Janeway CA, 2001).

Another mechanism to avoid infections is the colonization of epithelial surfaces with non-pathogenic bacteria, the so-called commensal bacteria or also microbiota. These bacteria not only cover the intestinal tract and help for the digestion, but they also occupy ecological niches and hence provide competition with pathogenic bacteria for resources (Janeway CA, 2001).

1.2.1.4. Cellular components

Nevertheless, these mechanistic barriers can be injured and many microorganisms developed strategies to overcome this very first defence. This is why the innate immune system also includes a lot of different cell types that recognize a broad variety of pathogens, namely neutrophils, monocytes or macrophages, natural killer (NK) cells, eosinophils, basophils, mast cells and also dendritic cells (DC) (Janeway CA, 2001).

The first category of cells that is present at the site of a bacterial or fungal infection are usually neutrophils. They are the most abundant cell type in human blood, terminally differentiated from the bone marrow and short-lived. Neutrophils circulate in blood for less than one day and also exhibit a big marginal pool with loose attachment to the wall of low flow exchange vessels, allowing a rapid mobilization into blood and recruitment to sites of infection. The inflamed epithelium expresses molecules, such as platelet-activating factor (PAF), leukotriene B4 and chemokines (i.e. chemotactic cytokines) that prime the neutrophils to extravasate into the infected tissue (Adams and Shaw, 1994). Initial rolling on the vessel wall is mediated

by the interaction of neutrophil-expressed L-selectin and PSGL-1 with P- and E-selectin, which are both expressed by endothelial cells (**Figure 1-4**). P-selectin is induced by histamine, thrombin and oxygen radicals while E-selectin is upregulated in response to cell stimulation with IL-1, TNFα or LPS. L-selectin on the other side is constantly expressed on many circulating leukocytes to allow rapid recruitment from blood (McEver and Cummings, 1997; Premack and Schall, 1996). The different pro-inflammatory factors present at this site, such as chemokines, cytokines and also bacterial products, next lead to the priming of the neutrophil and hence also to a switch in β1 and β2 integrins to a high affinity state. β1 integrin, also known as CD29, associates with integrin α subunits -1 (CD49a), -2 (CD49b) and -3 to form heterodimers with different binding specificities while β2 integrin (CD18) heterodimerizes with subunit α-L (CD11a), α-M (CD11b), α-X (CD11c) and α-D (CD11d). The different heterodimers represent receptors for respective antigens on other cells or endothelial cells to execute variable functions. Such, the heterodimer αLβ2, also leukocyte function associated molecule-1 (LFA-1), allows interactions with intercellular adhesion molecule-1 (ICAM-1), which is highly expressed on endothelial cells, and mediates firm adhesion and spreading of the neutrophil

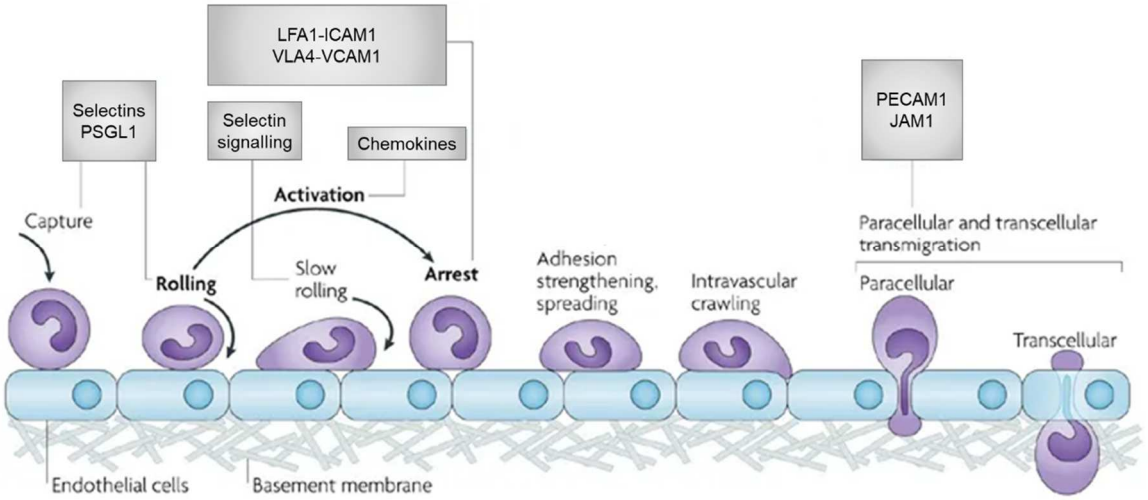

Figure 1-4: Leukocyte adhesion cascade. The three main steps of leukocyte adhesion are depicted in bold. Initial capture and rolling is mediated by the interaction of leukocyte L-selectin and PSGL-1 with endothelial P- and E-selectin. Next, the leukocyte is activated by chemokines and other pro-inflammatory stimuli at this site and this hence leads to a switch in the formation of integrins. Different integrin subunits form heterodimers, such as LFA-1 and VLA-4, to allow specific interaction with molecules on endothelial cells, such as ICAM-1 and VCAM-1, respectively. This leads to firm arrest of the leukocyte. In further steps, adhesion is strengthened and spreading takes place, to allow intravascular crawling. Extravasation is dependent on PECAM-1 and JAM1 and follows a gradient of chemoattractants. Modified from (Ley et al., 2007).

(**Figure 1-4**) (Anderson et al., 1984). Another integrin-based interaction in this step is the binding of very late antigen-4 (VLA-4), which is the $\alpha 4\beta 1$ integrin dimer, with vascular cell adhesion molecule-1 (**Figure 1-4**) (VCAM-1). Extravasation then takes places through the tight junctions of the endothelial cells and requires platelet endothelial adhesion molecule-1 (PECAM-1 or also CD31) and junction adhesion molecule 1 (JAM1) (**Figure 1-4**) (Muller et al., 1993). Migration into tissue takes place via haptotaxis, meaning migration along a gradient of cellular adhesion sites or substrate bound chemoattractants, that is additionally dependent on $\beta 1$ and $\beta 3$ integrins (Basan et al., 2013).

This whole process is not only crucial for neutrophil extravasation into inflamed tissues, but with small variations also important for mostly all leukocyte subsets and for this reason, it is termed the leukocyte adhesion cascade. Once the neutrophil has finally reached the source of infection, it recognizes the pathogen via its PRRs, opsonizes it and – in the case of bacteria - kills it by fusing the phagosome with its lysozyme-containing granula.

While the neutrophil is usually dying soon after phagocyting pathogen, macrophages are able to produce new lysosomes (Gekle M, 2010). A macrophage precursor is the monocyte that circulates in blood for one to three days. There are two main monocyte subsets known in mouse. Firstly, inflammatory or also Ly6C+ monocytes (IM) are very efficient in extravasating from blood and responding to local signals. They are moreover crucial for initiating an inflammation (Sunderkotter et al., 2004). Secondly, non-inflammatory or Ly6C- monocytes (NIM) maintain the steady-state condition of the IMs and mostly remain within the vasculature, often adherent to the vascular endothelium (Janeway CA, 2001). These latter cells act as scavengers and patrol along the blood endothelium. Monocytes differentiate into macrophages once they enter different tissues and every tissue has its own type of macrophages. In some cases, these are monocyte derived, in some cases they arise from yolk sac macrophages (Epelman et al., 2014). In macrophages, pathogen recognition also takes place via PRRs and macrophages are even able to present pathogen antigens to other immune cells after phagocytosis. Unless neutrophils, which often induce tissue damage due to the release of cytotoxic granula, macrophages can stimulate wound healing (Gekle M, 2010).

Another important cell type of innate immunity is the NK cell. This cell is actually a lymphocyte that matures and differentiates mostly in the bone marrow. NK cells

recognize cells that are missing major histocompatibility complex class I (MHCI) on their cell surface, which is often downregulated after a viral infection. By integrating perforins into these cells' membranes, NK cells are able to insert granzyme B leading to an induction of cell death of the infected cell. NK cells are activated by IFNα and IFNβ, which is mainly produced after recognition of viral components (Gekle M, 2010).

Eosinophils are present in high frequencies in the mucosa of the gastrointestinal and respiratory tract. They contain granula with cytotoxic proteins and secrete these upon infection with parasites, such as worms. They produce leukotriene C4 and IL-3 to trigger a parasite-specific immune response but can also play a pathological role in allergies (Gekle M, 2010).

Two other cell types are also linked to an immune response against parasites and hence to pathologic reactions in allergy: Basophils and mast cells. Both cells express high affinity IgE-receptors and derive from the same progenitor cell. Upon IgE-receptor binding, they produce histamine, prostaglandin, leukotrienes and also platelet-activated factor (PAF) (Gekle M, 2010).

Lastly, DCs form a bridging cell type between innate and adaptive immunity. They are resident in most tissues and live rather long with a slow turnover rate. Deriving from the same precursor as macrophages in the bone marrow, DCs also are professional phagocytes. However, they are not mainly working on eliminating the pathogens, but presenting the degraded antigens on their surface to activate the adaptive immune system. DCs are mostly present in peripheral tissues where they not only recognize and phagocyte pathogens, but where they also constantly take up extracellular material including potential viral or bacterial components using the receptor-independent process of micropinocytosis. Once the DC is activated, it travels via the afferent lymph to the regional lymph node where it presents its ingested antigens to cells of the adaptive immune response. This highly effective antigen presenting cell (APC) is now also able to activate lymphocytes specific for the presented antigens. Moreover, it secretes cytokines that are not only stimulating adaptive immune cells, but also cells of innate immunity and hence connects these two branches of the immune system with each other (Janeway CA, 2001).

1.2.2. Adaptive immune system

The adaptive immune system is characterised by an extremely specific and hence very efficient response. However, this reaction takes about two weeks to develop its full potential but is also able to acquire a memory to reduce this lag in reaction time significantly upon a second infection with the same pathogen.

The main cells of adaptive immunity are T and B lymphocytes. T cells represent the effector cells of the cellular immune response while B cells are responsible for antibody production. After their development in thymus (T cells) and bone marrow (B cells), lymphocytes migrate to secondary lymphoid organs such as lymph nodes and spleen to scan the APCs there for matching antigens from tissues and blood, respectively (Janeway CA, 2001). For antigen recognition, both T and B cells express highly diverse receptors on their cell surface with one cell representing one clone of this receptor. The generation of these receptors is highly complex and can create up to 10^{12} potential clones to maximize a precise pathogen recognition. Upon matching with a presented antigen, naïve T lymphocytes can differentiate into two different subsets. Is the antigen presented on a MHC class I molecule, such as most of the intracellular peptides from pathogens due to an infection of this cell, the T cell is activated to become a CD8+ cytotoxic T cell and kills the target cell. Is the pathogenic antigen presented on a MHC class II molecule like on professional APCs, however, differentiation into a CD4+ T helper cell takes place (Bonilla and Oettgen, 2010). Depending on different additional stimuli, the T helper cells can be further sub-differentiate into Th1 and Th2 cells, fighting intracellular and extracellular antigens, respectively. In general, CD4+ cells next activate B cells to become highly efficient plasma cells that produce large amounts of highly specific antibodies (Bonilla and Oettgen, 2010). These processes are reviewed in detail by den Haan et al (den Haan et al., 2014) and can also be further pursued in Janeway's immunobiology (Janeway CA, 2001). This project, however, will focus on the innate part of the immune system.

1.3. Microbiota

The human microbiome consists of about 10^{14} bacteria consisting of about 1000 different species, hence outnumbering the number of cells in the human body by a ratio of about 3:1 (Sender et al., 2016). 98% of these commensal bacteria, archaea, fungi, protists and viruses are present in the gut where they reach a density of about 10^{11}-10^{12} mostly bacteria per millilitre (Bengmark, 1998; Whitman et al., 1998). Microbiota contribute to many physiological functions of the host, such as maintenance of the mucosal structure, host defence against pathogens, activation of the host immune response, fermentation of dietary fibres, vitamin production, and also metabolism of peptides and xenobiotics (Bengmark, 1998; Illing, 1981; Littman and Pamer, 2011; Stappenbeck and Gordon, 2001; Stevens and Hume, 1998). The composition was found to be crucial for physiological homeostasis of the host in many areas and a misbalance is associated with multiple diseases, such as obesity, inflammatory gut diseases, neurological and autoimmune diseases, hypertension, thrombosis and atherosclerosis, and also cancer (Dicksved et al., 2008; Koeth et al., 2013; Lampe, 2008; Marques et al., 2017; Sampson et al., 2016; Wen et al., 2008; Zhao, 2013). The major phyla present in the gut are Firmicutes (Gram+, ca. 40%), Bacteroidetes (Gram-, about 25%), Actinobacteria (about 3%), Proteobacteria (about 1%) and Verrucomicrobia (about 1%). They fulfil diverse functions and are also composed differently in distinct areas of the intestine (Arumugam et al., 2011).

1.3.1. Influence of microbiota on host physiology

Since the microbiota co-evolved with its host organism, there are multiple examples of symbiotic relationships. Most importantly, it was shown that the host is able to ingest microbial patterns to modulate several beneficial physiological processes. These signals from the commensal bacteria are suggested to be called microbial activating molecular patterns (MAMPs), analogous to the earlier described PAMPs. The MAMPs contribute to host development and immune function and their beneficial signalling is mediated by PRRs (Chu and Mazmanian, 2013).

The influence of the microbiota occurs in two different ways: locally and systemically. In direct proximity, commensal products, such as microbial substances or metabolites, bind to PRRs on innate immune cells but also on intestinal epithelial

cells (IECs). This activation leads to a low-level expression of cytokines and anti-microbial peptides (AMPs), thus maintaining tolerance and intestinal homeostasis (**Figure 1-5**) (Manicassamy and Pulendran, 2009; Round et al., 2010). Beside the classical recognition pathways, some special identifications processes developed to distinguish non-pathogenic from pathogenic organisms. For instance, IECs not only express TLRs on their basolateral site to detect invading bacteria, but also on their apical site to regulate commensal influence (Cario et al., 2000). Also, polysaccharide A found within the human microbiota is specifically detected on TLR2 of intestinal DCs to induce the development of regulatory T cells (Shen et al., 2012).

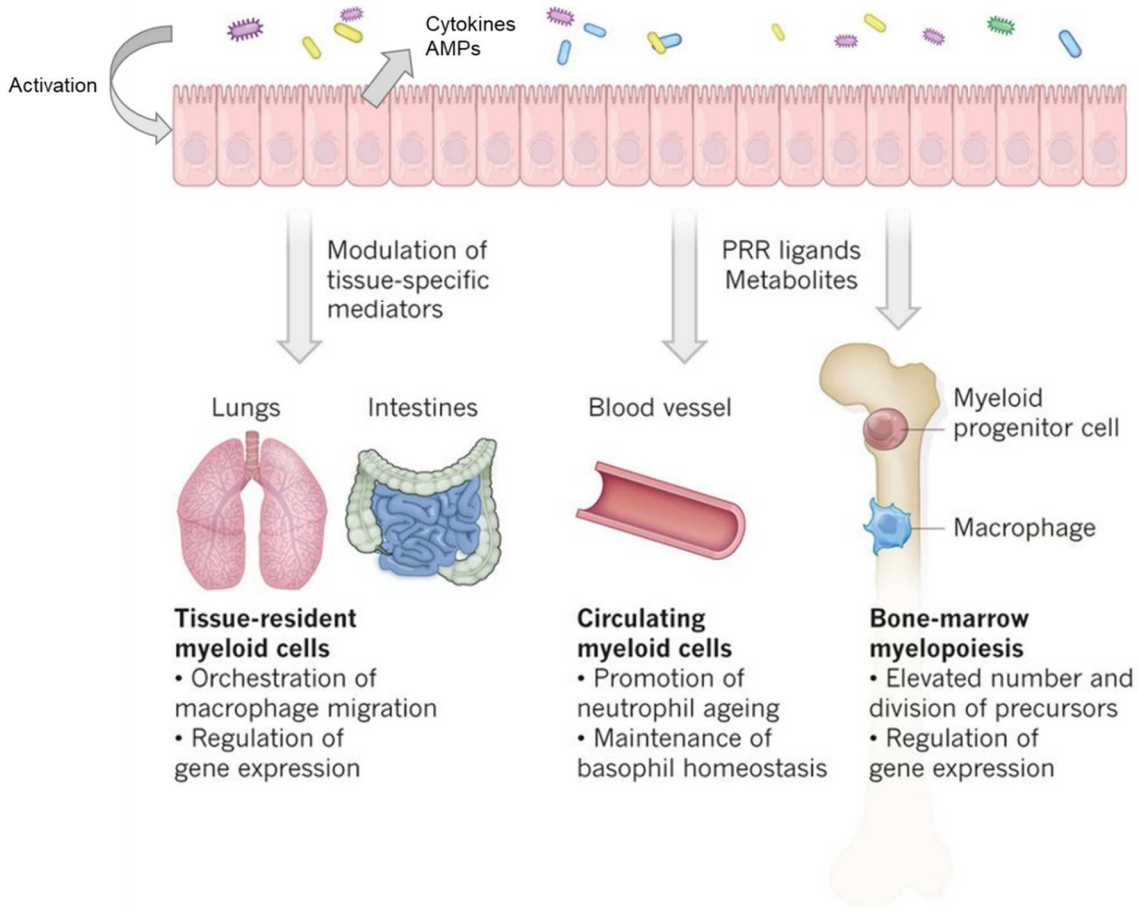

Figure 1-5: Influence of the microbiome on host physiology. Locally, intestinal commensal bacteria activate intestinal epithelial cells to produce cytokines and anti-microbial peptides (AMPs) that maintain intestinal homeostasis. On a systemic level, PRR ligands and metabolites can leak into the host organism and influence multiple physiological pathways far away from the gut. Modified from (Thaiss et al., 2016b).

Moreover, some microbial products can be found systemically, far away from the intestine. Peptidoglycan, for example, is present in serum and in the bone marrow and primes the innate immune system by activating the function of neutrophils via Nod1 (Clarke et al., 2010). Also, germ-free mice were found to have a reduced

myeloid cell development in the bone marrow and the level of myelopoiesis was dependent on the complexity of the commensal bacteria (Balmer et al., 2014). Likewise, the ageing of neutrophils depends on microbiota-derived TLR agonists as well as circulating basophils and tissue-resident macrophages are influenced by these factors (**Figure 1-5**) (Corbitt et al., 2013; Hill et al., 2012; Zhang et al., 2015).

Therefore, microbial signalling via PRRs provides beneficial signals by priming the respective receptors and helping to keep a healthy balance between tolerance and an inflammatory response.

1.3.2. Influence of the host on the microbiome

A symbiosis is always bidirectional, in this case meaning that the host also influences the commensal bacteria. Thus, the host PRRs can also shape the microbial composition in the intestine. It was shown that a knockout of crucial innate recognition receptors, such as NOD2, NLRP6 or TLR5, leads to dysbiosis and some polymorphisms in these genes are even associated with inflammatory bowel disease. This effect is probably due to an impaired secretion of AMPs, which induces pathogenic alterations in the commensal composition. This shift can also be induced by antibiotic depletion of microbiota and be rescued by feeding microbial products, such as LPS or lipoteichoic acid (LTA).

Moreover, the host is able to support the commensal organisms in fasting periods by shedding fucosylated proteins into the intestinal lumen, hence providing an energy source for the microbiota.

1.4. Role of circadian rhythms

1.4.1. Circadian rhythms in the immune system

As already mentioned above, circadian rhythms play a crucial role in many physiological aspects including an influence on the immune system. These rhythms most likely exist to minimize the cost of the immune response and potential side effects, such as tissue injuries at specific times, while maximizing the benefits. Accordingly, a temporal coordination prevents parallel activation of multiple parts of the immune system to reduce the risk for e.g. septic pathology, Moreover, oscillations in immunological features control the duration of an inflammatory response. Disturbances in these rhythms influence the peak response of the immune system as they can increase the activity at the rest period and hence prolong the inflammation (Curtis et al., 2015; Gibbs et al., 2012). However, it was also shown that mice lacking core clock protein *Bmal1* in their T cells displayed a reduced score in an experimental murine model of multiple sclerosis, the Experimental autoimmune encephalomyelitis (EAE). This indicates that also a reduced immune response can result from disturbed circadian rhythms, increasing complexity in this interaction.

Also, migration of immune cells is under circadian control and temporal relocation decreases the risk for tissue injuries while an inflammatory response takes place (Nguyen et al., 2013; Scheiermann et al., 2012).

It had been discovered about 50 years ago that the immune system shows daily variations in the response to a lethal LPS challenge. While mice challenged during their resting phase were able to survive a critical endotoxin injection, mice challenged at the onset of their active phase did not (Halberg et al., 1960; Shackelford and Feigin, 1973). Until this day, it was demonstrated that almost every part of the immune system is under circadian control (Curtis et al., 2014).

Maybe most obvious, leukocyte numbers in blood exhibit a very strong oscillation over the course of the day with peaks during the rest phase and a trough at the onset of the active phase. This effect is due to increased recruitment of the cells to tissues at the active phase and increased mobilization from the bone marrow during the resting phase (**Figure 1-6**) (Scheiermann et al., 2012). Both is mediated by the rhythmic expression of adhesion molecules and chemokines (He et al., 2018). On a

functional level, bacterial clearance, cytokine and inflammatory response, and phagocytosis are more effective during the active phase, potentially correlating with an increased infection risk during that time (Gibbs et al., 2012; Hayashi et al., 2007). Also, TLR9 and down-stream molecules of TLR4, such as Cd14, IκBα, p65 and Fos and Jun, were shown to underlie circadian gating and are higher expressed at the respective active period (**Figure 1-6**) (Keller et al., 2009).

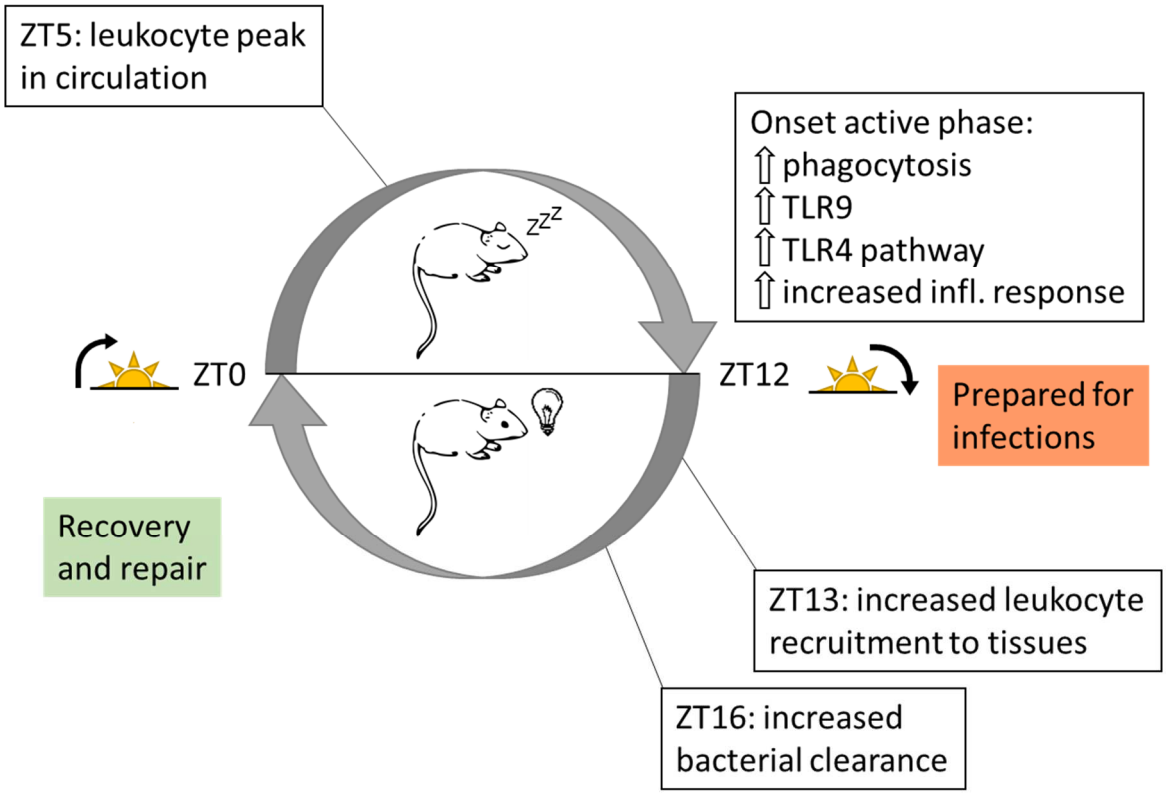

Figure 1-6: Circadian rhythms in the immune system. Mice exhibit a peak in their leukocyte numbers in the circulation during their resting phase (ZT5). At the onset of the active phase, immunological features, such as phagocytosis, TLR9 expression and activity of the TLR4 pathway, are increased. Moreover, there is a general more sensitive inflammatory response upon immune system activation at that time. At ZT13, leukocytes are predominantly recruited to tissues, leading to a trough of leukocyte numbers in the circulation. This effect is due to increased expression of adhesion and pro-migratory molecules. Also, the clearance of bacterial pathogens is increased during the active phase at ZT16. To conclude, the immune system is more active at the time of highest infection risk while recovery, repair and homeostatic functions are taking place during the rest phase of the organism.

While every immune cell thus far investigated carries a functional molecular clock (Adrover et al., 2019; Arjona and Sarkar, 2005; Curtis et al., 2015; Druzd et al., 2017; Nguyen et al., 2013; Silver et al., 2012a), these intrinsic rhythms are additionally modulated by extrinsic factors, orchestrated by the master clock and the environment. The cell-intrinsic, autonomous clock mainly controls trafficking of

myeloid cells and the inflammatory response, especially in the innate part of the immune system (Haspel et al., 2014; Nguyen et al., 2013). The cell-extrinsic factors, on the other side, influence the rhythmic migration of leukocytes and their recruitment under homeostatic conditions. Moreover, they also control rhythms in the adaptive immune response, such as the response to antigen and also trafficking of lymphocytes to lymphoid tissues (Druzd et al., 2017; Fortier et al., 2011; Mendez-Ferrer et al., 2008).

Strikingly, these rhythms are adapted to the respective activity- and rest-phases of different organisms and hence inverted in humans as diurnal organisms and mice as nocturnal animals (Zhao et al., 2017).

1.4.2. Circadian rhythms in microbiota

Recent studies have shown that the microbiota itself exhibit circadian rhythms. About 20-83% of the mice microbial taxa present a day-night-rhythmicity and in humans, about 10% of the operational taxonomic units (OTUs) are oscillating (Liang et al., 2015; Thaiss et al., 2014b). This rhythmic abundance is mostly present in the gram+ Lactobacillales, Clostridiales and Firmicutes, but also in the gram- Bacteroidales, and Proteobacteria. The total biomass in murine microbiota is higher in the active phase than in the resting phase, as well as the adherence of commensal bacteria is increased at the dark phase (Liang et al., 2015; Thaiss et al., 2016a). Additional to the compositional changes, also functional variabilities are present over the course of the day, which concerns about 23% of the Kyoto Encyclopedia of Genes and Genomes (KEGG) pathways with a 24h rhythm. KEGG pathways are utilized in bioinformatics research and describe a database that maps cellular and organismal functions. During the active phase, processes such as energy metabolism, DNA repair or growth are increased, probably due to the higher availability of nutrients during that time, boosting the metabolism of the commensals. On the other side, pathways of detoxification, environmental sensing and motility are peaking during the rest phase of the host organism, to allow closer proximity to the mucus and hence using this as nutrient (Thaiss et al., 2014b).

Although these rhythms are lost in microbiota of Per1/2 double knockout (KO) mice, time-restricted feeding can restore the bacterial oscillations. Interestingly, food restriction to the light phase leads to inverted rhythms compared to ad libitum

feeding in clock intact mice, indicating a crucial role of nutrient uptake for the oscillations in commensal bacteria (Thaiss et al., 2014b; Zarrinpar et al., 2014).

Despite dramatic variabilities in microbiota composition due to different animal facilities, environments and individuals, these rhythms are strikingly stable (Rausch et al., 2016). This points out the significance of oscillations in commensal bacteria, although the precise mechanism remains poorly understood so far.

1.5. Hypothesis

Although there are many studies about the role of circadian rhythms in the immune system and this field of research is constantly increasing, it is still not known what actually drives the leukocyte oscillation in the circulation. Light as main entrainment factor can be excluded since it was shown that these rhythms were still persistent in mice kept in complete darkness (Scheiermann et al., 2012). The publications about circadian microbiota hence made us hypothesize that low-dose microbial factors might induce a circadian leukocyte mobilization from the bone marrow. Interesting studies have already shown an influence of MAMP-sensing TLRs on IECs on the circadian clock in these cells (Mukherji et al., 2015). Moreover, microbial ablation is able to alter clock gene expression in hepatocytes (Leone et al., 2015; Montagner et al., 2016). However, none of these studies investigated the influence of altered commensal bacteria or altered MAMP-sensing pathways in the context with leukocyte numbers in the circulation.

2. Materials and methods

2.1. Animals

2.1.1. Mouse strains

Bmal1$^{flox/flox}$, *Lyz2*Cre, *Vil1*Cre and *MyD88*$^{-/-}$ animals were obtained from The Jackson Laboratory (Bar Harbor, ME, USA). *Cdh5*CreERT2 mice were kindly provided from Ralf Adams and Eloi Montañez. *Bmal1*$^{flox/flox}$ animals were crossed with *Lyz2*Cre, *Vil1*Cre and *Cdh5*CreERT2 animals to generate tissue-specific *Bmal1* knockout mice, lacking this gene in myeloid cells (*Lyz2*Cre x *Bmal1*$^{fl/fl}$), intestinal epithelial cells (*Vil1*Cre x *Bmal1*$^{fl/fl}$) or endothelial cells (*Cdh5*CreERT2 x *Bmal1*$^{fl/fl}$). C57BL6/N and C57BL6/J wild-type animals were purchased from Charles River Laboratories (Sulzfeld, Germany) and Janvier Labs (Saint Berthevin Cedex, France).

Germ-free animals as well as *VE-Cadherin*-Cre x *Tlr4*$^{fl/fl}$ and *VE-Cadherin*-Cre x *Tlr2*$^{fl/fl}$ animals were kindly provided from Christoph Reinhardt at the university of Mainz, Germany. Data from *TNF*$^{-/-}$ animals was provided from Daniel Lucas at Michigan University, Ann Arbor, USA.

All mice were housed under 12h:12h light-dark conditions with *ad libitum* access to food and water and rested seven days after shipment before usage for experiments. All experiments were performed with age and gender-matched groups, performed according to German legislation and approved by the Regierung of Oberbayern or the respective legislation at the universities where experiments were performed.

2.1.2. Light experiments

To obtain information without daily light influence, mice were kept under either constant darkness conditions or in constant light in cyclers (manufactured by Parkbio, Graveland, MA, USA and Ventilated cabinet ARIA BIO-C36, Tecniplast, Buguggiate, Italy) for 24 h before the first harvest time point. Samples were then harvested every 6 h over a time period of 24 h. For jetlag experiments, light-dark cycles were acutely shifted for 12 h and samples were harvested 24 h after jetlag induction every 6 h over a time period of 24 h. Mice had *ad libitum* access to food and water during the whole experimental procedure.

2.1.3. Time-restricted feeding

For 12 h-time restricted feeding (TRF), data was provided by Roee Gutman in at the Tel-Hai College in Tel Aviv, Israel. Mice received food access for 12 h either during the light or during the dark phase with *ad libitum* access to water for two weeks. After two weeks, blood was harvested every 6 h over a time period of 24 h and analysed. Subsequently, mice were shifted back to *ad libitum* feeding for two weeks after which blood was harvested every 6 h over a time period of 24 h and analysed after another two weeks. Before, during and after TRF, behavioural activity was recorded.
For 6 h-TRF, mice had access to food for 6 h, during the middle of the day or night, i.e. either from ZT 15 to ZT 21 during dark-restricted feeding (DRF) or from ZT 3 to ZT 9 during light-restricted feeding (LRF). After two weeks, samples were harvested every 6 h over a time period of 24 h.
During experimental procedure, all animals had *ad libitum* access to water and were housed under 12 h: 12 h light-dark conditions.

2.1.4. Antibiotics treatment

Mice received 1 g/l Neomycin, 1 g/l Ampicillin, 1 g/l Metronidazol and 0.5 g/l Vancomycin in their drinking water over a period of four weeks. Water was provided in black bottles to protect antibiotics from light exposure and exchanged twice a week. Water was supplied with sterile filtered liquid sweetener in a dilution of 1:1500 to reduce bitterness and increase water uptake of the animals. Control animals also received sweetened drinking water.

2.1.5. Tamoxifen treatment

*Cdh5*CreERT2 mice were injected i.p. with tamoxifen for five consecutive days to induce Cre-recombination. Animals were started to be analysed from day six onwards after treatment. Tamoxifen was dissolved in corn oil at a final concentration of 20 ng/ml at 37 °C for up to 5 h while constant rotation until all precipitates were suspended.

2.2. Genotyping

Biopsies from ears were digested overnight in lysis buffer (5 mM EDTA, 200 mM NaCl, 0.2% SDS in 100 mM Tris-HCl, pH 8.5) containing proteinase K (1 µl, 1.5 U per sample) at 55 °C while shaking. The next day, samples were centrifuged for 10 min at room temperature (RT) and 18 000 x g and supernatant was transferred to a new tube containing 200 µl isopropanol to induce DNA precipitation. Samples were again centrifuged for 10 min at 18 000 x g at RT and supernatant was removed. The DNA pellet was allowed to dissolve in 100 µl Tris EDTA (TE)-buffer for 1 h at 37 °C before being used for polymerase chain reaction (PCR).

For PCR, 1 µl of extracted DNA in TE-buffer was mixed with 8.6 µl nuclease-free H_2O, 10 µl 2x FastGene master mix, 0.2 µl forward and 0.2 µl reverse primer (each at 10 µM, sequences in **Table 2-1**). DNA was amplified according to the PCR protocol in **Table 2-2** on a Mastercycler Epgradient S.

Primer	Sequence (5' → 3')
Bmal1 forward	ACT GGA AGT AAC TTT ATC AAA CTG
Bmal1 reverse	CTG ACC AAC TTG CTA ACA ATT A
Generic *Cre* forward	GCG GTC TGG CAG TAA AAA CTA TC
Generic *Cre* reverse	GTG AAA CAG CAT TGC TGT CAC TT

Table 2-1: Primer sequences for genotyping PCR

Step	Temperature	Time	Cycles	Gene
Initial denaturation	94°C	3 min	1x	*Bmal1*
Denaturation	94°C	30 sec	35x	
Primer annealing	55°C	30 sec		
Polymerization	72°C	30 sec		
Final extension	72°C	2 min	1x	
Initial denaturation	95°C	3 min	1x	*Cre*
Denaturation	95°C	20 sec	38x	
Primer annealing	62°C	30 sec		
Polymerization	72°C	30 sec		
Final extension	72°C	10 min	1x	

Table 2-2: PCR protocols. Different PCR steps for amplification of *Bmal1* or *Cre* gene.

10 µl of PCR product were applied on a 1 % agarose gel including Midori Green (1:25 000) to visualize DNA. Samples ran for 30 min at 200 V together with FastGene 100bp DNA Marker and the gel was imaged under ultraviolet light using

an UV Transilluminator. *Bmal1* flox-bands were detected at the size of 431 bp, while wild-type (WT) products lacking the floxed sites were detected at 327 bp. Heterozygous animals showed both bands. PCR product of *Cre* genotyping could be found at the size of 324 bp while wild-type DNA did not show an amplified DNA product (**Figure 2-1**).

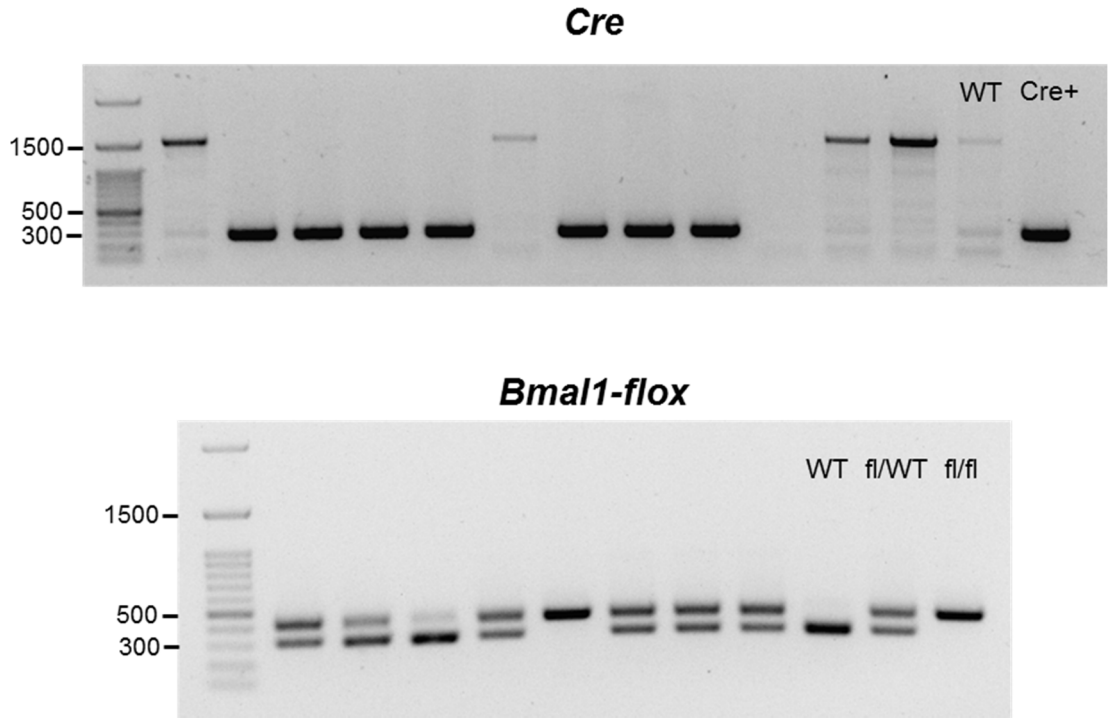

Figure 2-1: PCR products visualized on a 1% agarose gel. Top: exemplary samples as well as WT control and Cre+ control on the right. Cre+ bands were detected at the size of 324 bp. Bottom: exemplary samples as well as WT control with no flox-bands, heterozygous control (fl/WT) and homozygous flox-control (fl/fl) on the right. Flox-bands were detected at the size of 431 bp, while WT products were detected at the size of 327 bp. Numbers on the left indicate size of DNA marker.

2.3. Flow cytometry

2.3.1. Tissue harvest and processing

Upon tissue harvest, mice were anesthetized using isoflurane, blood was harvested into tubes supplemented with 1:100 0.5 M EDTA using microhematocrit tubes and mice were euthanatized under anaesthesia by cervical dislocation. Whole blood was counted using a ProCyte Dx™ blood counter.

Thymus, spleen and inguinal lymph nodes were directly smashed through a 70 µm cell strainer, rinsed with 5 ml protein extraction buffer (PEB, 2 mM EDTA and 2 % fetal bovine serum (FBS) in PBS) and centrifuged at 300 x g for 5 min at 4 °C. To obtain cells from the bone marrow, the left femur was flushed with 1 ml PBS. BM cell suspension and cell pellets from thymus and spleen were resuspended in 5 ml red blood cell lysis buffer (RBC, 0.154 M NH_4Cl, 0.05 mM EDTA, 10 mM $KHCO_3$, pH 7.25) and incubated for 5 min at room temperature to deplete erythrocytes. The reaction was stopped by adding 5 ml PBS and centrifuging for 5 min at 4 °C and 300 x g. Whole blood was also supplemented with 5 ml RBC lysis buffer, incubated for 5 min at RT and was centrifuged for 5 min at 4 °C and 300 x g. After centrifugation, supernatant was removed and blood samples incubated a second time in 5 ml RBC for 5 min on ice. Cell pellets from blood, thymus, bone marrow, spleen and inguinal lymph nodes were resuspended in 1 ml PEB. 100 µl from thymus, bone marrow and spleen cell suspension as well as 950 µl of lymph node cell suspension and 1 ml of blood cell suspension were transferred to FACS tubes, topped up to 2 ml volume using PEB to wash and centrifuged again to obtain a cell pellet. For cell counting, cell suspensions were used in dilutions of 1:1000 for BM, 1:10 000 for spleen and thymus and 1:400 for lymph nodes at a cell counter (Coulter Z2) or supplemented with 15 µl CountBright™ absolute counting beads right before the run at the flow cytometer.

2.3.2. Antibody staining and analysis

Antigen	Fluorochrome	Dilution	Clone	Company
CD115	PE	1:100	AFS98	Biolegend (London, UK)
CD3	PE/DZL	1:100	17A2	Biolegend (London, UK)
Gr-1	PerCP/Cy5.5	1:100	RB6-8C5	Biolegend (London, UK)
B220	PE/Cy7	1:100	RA3-6B2	Biolegend (London, UK)
SiglecF	Alexa647	1:100	E50-2440 RUO	Becton Dickinson GmbH (Heidelberg, Germany)
NK1.1	Alexa700	1:100	PK136	Life Technologies (Darmstadt, Germany)
CD8a	APC/Cy7	1:100	53-6.7	Biolegend (London, UK)
CD4	BV570	1:100	RM4-5	Biolegend (London, UK)

Table 2-3: Antibodies for flow cytometry. Listed are targeted antigen, labeled Fluorochrome, dilution, clone and origin.

Cells were resuspended in 100 µl PEB containing an antibody mixture as indicated in **Table 2-3**. Staining was performed while incubating on ice for 30 min and in

darkness. Afterwards, 2 ml PEB were added and cells were pelleted by centrifugation at 300 x g for 5 min at 4 °C. Supernatant was discarded and cells were resuspended in 150 µl 4',6-diamidino-2-phenylindole buffer (DAPI, PEB containing 3 µM DAPI) to exclude dead cells. Samples were immediately run at the Gallios flow cytometer and data was analysed using FlowJo V10 software.

2.4. Leukocyte subset isolation

CD4+, CD8+ T cells and B cells were isolated from spleen and neutrophils were enriched from bone marrow. Organs were processed as described above and after RBC lysis, single cell suspensions were processed using StemCell negative isolation kits according to the manufacturer's instructions. Purity was determined by flow cytometry using the described antibody panel and was more than 91 % for CD4+, CD8+ T cells and B cells and about 70 % for neutrophils. After isolation, RNA was extracted directly as described below.

2.5. Quantitative polymerase chain reaction

2.5.1. RNA extraction

For RNA extraction from whole tissues, organs were immediately frozen after harvest in liquid nitrogen and stored at -80 °C until usage. At the day of RNA extraction, 1 ml QIAzol solution was directly added to frozen organs and transferred to lysis tubes A. Tissue was homogenized using SpeedMill PLUS homogenizer and afterwards, liquid was transferred to a new tube and centrifuged for 10 min at 18 000 x g and 4 °C. Clear supernatant was pipetted to a fresh tube and allowed full dissociation at RT for 5 min. Afterwards, 200 µl chloroform were added, samples were shaken for 15 sec and incubated at RT for 3 min. Solution was centrifuged for 15 min at 18 000 x g and 4 °C and aqueous solution was carefully transferred to a new tube. 500 µl isopropanol were added and RNA precipitation was allowed for at least 1 h at -20 °C. RNA was pelleted while centrifuging for 30 min at 4 °C and 18 000 x g. RNA pellet was washed with 1 ml 70 % ethanol and subsequently resuspended in DNA digestion buffer, containing 1 µl DNase I, 5 µl 10 x DNase I buffer and 44 µl nuclease-free H_2O. DNA was digested at 37 °C for 30 min and 50

µl H_2O as well as 250 µl 70 % ethanol were added afterwards. Whole volume was immediately transferred onto RNeasy Plus Mini Kit columns and RNA was purified according to manufacturer's protocol.
For RNA extraction from cells, frozen cell suspension was resuspended in RLT plus buffer, provided by RNeasy Plus Mini Kit, complemented with □-mercaptoethanol to a final dilution of 1:100. To break cell membranes and obtain RNA, cell suspension in RLT buffer was applied on QIAshredder columns and centrifuged for 30 sec at RT and 18 000 x g. Subsequently, flow-through was transferred onto gDNA elimination columns provided by RNeasy Plus Mini Kit to remove DNA and RNA was purified according to the manufacturer's instructions.
Finally, RNA was diluted into 50 µl RNase-free H_2O and concentration as well as the A260/280 ratio was determined using a NanoDrop™ 2000 spectrometer. Only RNA with an A260/280 ratio higher than 2.0 was used for further analysis and storage was at -80 °C.

2.5.2. Reverse transcription

To obtain cDNA for quantitative real-time PCR, reverse transcription (RT) of up to 2.5 µg RNA was performed using the High Capacity cDNA Reverse Transcription Kit. The master mix contained 2 µl of 10 x RT buffer, 0.8 µl of 25x dNTP mix (100mM), 2 µl of random primers and 1 µl of RT polymerase in a total volume of 20 µl, filled up with nuclease-free H_2O. The PCR was performed for 10 min at 25 °C (annealing), followed by 2 h at 37 °C for reverse transcription and a final denaturation step at 85 °C. After the run, cDNA was diluted to a final concentration of 1 ng/ml and stored at -20 °C.

2.5.3. Quantitative real-time PCR (qPCR)

To quantify expression levels of mRNA, cDNA was used for qPCR analysis. 1 ng cDNA was mixed with 5 µM of respective forward and reverse primers (**Table 2-4**) and 5 µl of SYBR green PCR master mix in a total volume of 10 µl. Samples were applied to a 96-well plate and the run was performed using a StepOnePlus System according to the protocol in **Table 2-5**. The results were analysed with StepOne Software v2.3 and relative mRNA expression was calculated using the ΔΔCT

method, normalized to the housekeeping gene Glyceraldehyde-3-phosphate dehydrogenase (GAPDH).

Primer	Sequence (5' → 3')
Psgl-1 FW	ATC TCA TCC CGG TGA AGC AA
Psgl-1 RV	TTC CGC ACT GGG TAC ATG TG
Cd49d FW	GAA TCC AAA CCA GAC CTG CGA
Cd49d RV	TGA CGT AGC AAA TGC CAG TGG
Cd11a FW	CCA GAC TTT TGC TAC TGG GAC
Cd11a RV	GCT TGT TCG GCA GTG ATA GAG
Cd11b FW	ATG GAC GCT GAT GGC AAT ACC
Cd11b RV	TCC CCA TTC ACG TCT CCC A
Icam-1 FW	GGA CCA CGG AGC CAA TTT C
Icam-1 RV	CTC GGA GAC ATT AGA GAA CAA TGC
L-selectin FW	GAC GCC TGT CAC AAA CGA AA
L-selectin RV	GCC CGT AAT ACC CTG CAT CA
Cxcr2 FW	ATG CCC TCT ATT CTG CCA GAT
Cxcr2 RV	GTG CTC CGG TTG TAT AAG ATG AC
Cxcr4 FW	TCA GTG GCT GAC CTC CTC TT
Cxcr4 RV	CTT GGC CTT TGA CTG TTG GT
Dbp1 FW	AAT GAC CTT TGA ACC TGA TCC CGC
Dbp1 RV	GCT CCA GTA CTT CTC ATC CTT CTG T
Nr1d1 FW	GAT AGC TCC CCT TCT TCT GCA TCA TC
Nr1d1 RV	TTC CAT GGC CAC TTG TAG ACT TC
Per2 FW	GTC CAC CTC CCT GCA GAC AA
Per2 RV	TCA TTA GCC TTC ACC TGC TTC AC
Cry1 FW	CTC GGG TGA GGA GGT TTT CTT
Cry1 RV	GAC TTC CTC TAC CGA GAG CTT CAA
Bmal1 FW	AGA GGT GCC ACC AAC CCA TA
Bmal1 RV	TGA GAA TTA GGT GTT TCA GTT CGT CAT

Table 2-4: Primer sequences for qPCR. FW indicates forward, RV reverse.

Step	Temperature	Time	Cycles
Initial denaturation	95 °C	10 min	1x
Denaturation	95 °C	15 sec	40x
Annealing	60 °C	1 min	
Melt curve	95 °C	15 sec	1x
	60 °C	1 min	
	95 °C	+ 0.7 °C/min	

Table 2-5: Protocol for quantitative real-time PCR.

2.6. Animal treatment

2.6.1. Mobilization assays

C57BL6/N wild-type animals were injected i.p. with 200 mg Bromodeoxyuridine (BrdU) at ZT 7 72 h before tissue harvest at ZT 1, 5, 9, and 13. Tissue harvest and processing was performed as described before, but PBS was used instead of PEB

to avoid interference with Zombie Violet™ Fixable Viability Kit-staining. Indicated volumes of single cell suspensions from different organs were resuspended in a 1:400 Zombie dilution in PBS and incubated 15 min at RT and in darkness. Cells were washed with 2 ml PEB and surface antigen staining was performed as described before. After washing with 2 ml PEB, cells were fixed, permeabilized and stained for BrdU content using FITC BrdU Flow Kit according to the manufacturer's protocol. Finally, cells were resuspended in 135 µl in 1 x Perm/Wash buffer, 15 µl counting beads were added and data was collected at on a Gallios flow cytometer.

2.6.2. Serum transfer

Blood was harvested from wild-type donor animals at the indicated time points using microhematocrit capillaries into tubes without any anti-coagulant. Blood was allowed to clot for 30 min at RT and subsequently centrifuged at 1500 x g for 10 min at 4 °C. Serum was carefully removed, pooled and distributed onto new tubes to avoid individual influences. Until i.p. injection into recipients, serum was stored at 4 °C. 300 – 350 µl serum were injected per recipient mouse and one hour later, recipients were euthanized and blood and tissue was harvested.
For heat-inactivation, isolated serum was incubated at 56 °C for 30 min before storage at 4 °C and subsequent injections at indicated time points.

2.6.3. Low-dose LPS injections

20 ng of LPS in 200 µl PBS or 200 µl PBS only for control animals were injected i.p. into WT animals 4 h prior to blood harvest. Blood was harvested at the indicated time points and processed and analysed as described before.

2.6.4. LPS feeding

WT mice were gavaged with either 300 µg or 1 mg LPS in a total volume of 200 µl PBS 26 h prior to blood harvest. As control, 200 µl PBS only were applied to the animals. Blood was harvested at the indicated time points and processed and analysed as described before.

2.6.5. TNF injections

4 pg TNFα in a total volume of 200 µl PBS or 200 µl PBS only were injected i.v. into WT animals either 1 or 2 h prior to blood harvest at the indicated time points.

2.7. Blocking experiments

2.7.1. Blocking of TLR4/MD-2

Either 30 µg anti-TLR4/MD-2 (**Table 2-6**) antibody or 30 µg isotype (**Table 2-6**), diluted in 200 µl PBS, were injected i.p. at ZT 5 one day prior to blood harvest at ZT 5 and ZT 13. Blood was harvested, processed and analysed as described before.

Antigen	Clone	Company	Resp. control	Clone	Company
TLR4/MD2	MTS510	Becton Dickinson GmbH (Heidelberg, Germany)	Rat IgG2a	2A3	Hölzel (Cologne, Germany)
TNFα	MP6-XT22	Life Technologies (Darmstadt, Germany)	Rat IgG1	TNP6A7	Hölzel (Cologne, Germany)
IL-6	MP5-20F3	Hölzel (Cologne, Germany)	Rat IgG1	TNP6A7	Hölzel (Cologne, Germany)
IL-1β	B122	Hölzel (Cologne, Germany)	Armenian hamster IgG	polyclonal	Hölzel (Cologne, Germany)

Table 2-6: Neutralizing antibodies. Listed are blocking antibodies for targeted molecules, clones, origin and respective isotypes.

2.7.2. Blocking of MyD88 and TRIF

WT animals were injected i.p. with either 100 µg Pepinh-MYD and 100 µg Pepinh-TRIF or with 200 µg Pepinh-Ctrl, diluted in 200 µl PBS. Injection was performed at ZT 5 one day prior to blood harvest at ZT 5 and ZT 13. Blood was harvested, processed and analysed as described before.

2.7.3. Blocking of pro-inflammatory cytokines

100 µg of blocking antibodies against IL-1β, IL-6 and TNFα (**Table 2-6**), diluted in a total volume of 200 µl with PBS, were i.p. injected into WT animals at ZT 5 one day

prior to blood harvest at ZT 5 and ZT 13. Antibodies were either mixed and injected together as antibody cocktail or applied separately. As control, 200 µg rat IgG1 and 100 µg Armenian hamster IgG isotypes (**Table 2-6**) diluted in 200µl PBS were injected i.p. Blood was harvested, processed and analysed as described before.

2.8. Cytokine bead array (CBA)

Blood was harvested from WT animals at indicated time points into tubes substituted with 1:100 0.5 M EDTA. Plasma was isolated by centrifugation at 1500 x g for 10 min at 4 °C, transferred to new tubes and stored at -20 °C until usage. For determining TNFα concentration in plasma, undiluted and 1:2 dilutions of isolated samples were used and processed using the Mouse TNF Enhanced Sensitivity Flex Set according to the manufacturer's instructions.

2.9. Statistical analysis

Statistical analyses were performed using GraphPad Prism 7 software. All data are represented as mean ± SEM. An unpaired student's t-test was used for comparisons between two groups. For comparing three or more groups with one variable, one-way ANOVA followed by Tukey's post hoc test was performed. Two-way ANOVA followed by Bonferroni's post hoc test was used for comparing groups with more than one variable. To analyse significance in oscillations over a time period of 24 h, cosinor analysis was performed. Statistical significance was assessed as *$p<0.05$, **$p<0.01$, ***$p<0.001$ and ****$p<0.0001$.

Chemical	Company	Location
Agarose	Biozym Scientific	Oldendorf, Germany
Ampicillin-t	bela-pharm GmbH & Co. KG	Vechta, Germany
Chloroform	Sigma-Aldrich	Darmstadt, Germany
CountBright™ absolute counting beads	Life Technologies	Darmstadt, Germany
DAPI	Biolegend	London, UK
DNase I Ambion™	Life Technologies	Darmstadt, Germany
DNase I Buffer (10X)	Life Technologies	Darmstadt, Germany
EDTA	Life Technologies	Darmstadt, Germany
Ethanol absolut für Molekularbiologie	AppliChem	Darmstadt, Germany
FastGene 100bp DNA Marker	Nippon Genetics	Düren, Germany
FastGene Optima PCR HotStart	Nippon Genetics	Düren, Germany
FBS	Life Technologies	Darmstadt, Germany
HyPure™ Molecular Biology Grad Water (nuclease-free)	GE Healthcare LifeSciences	South Logan, Utah, USA
Isoflurane	CP-Pharma	Burgdorf, Germany
Isopropanol (Propan-2-ol)	AppliChem	Darmstadt, Germany
$KHCO_3$ (potassium hydrogen carbonate)	Merck	Darmstadt, Germany
Lipopolysaccharide (LPS) from Escherichia coli	Sigma-Aldrich	Taufkirchen, Germany
Liquid sweetener	Rewe	Cologne, Gemany
Metronidazol	Caelo	Hilden, Germany
Midori Green Advance	Nippon Genetics	Düren, Germany
NaCl	Sigma-Aldrich	Taufkirchen, Germany
Neomycinsulfat	bela-pharm GmbH & Co. KG	Vechta, Germany
NH_4Cl (ammonium chloride)	Merck	Darmstadt, Germany
PBS	Apotheke Klinikum Universität München	Munich, Germany
Pepinh-MYD	Invivogen	Toulouse, France
Pepinh-TRIF	Invivogen	Toulouse, France
Proteinase K	Life Technologies	Darmstadt, Germany
QIAzol lysis reagent	QIAGEN	Hilden, Germany
SDS		
SYBR green PCR master mix	Applied Biosystems	Warrington, UK
Tamoxifen	Sigma-Aldrich	Taufkirchen, Germany
TNFα (recombinant, murine)	BioTechne GmbH	Wiesbaden, Germany

Chemical	Company	Location
Tris	AppliChem	Darmstadt, Germany
Vancomycin	Dr Friedrich Eberth Arzneimittel GmbH	Ursensollen, Germany
β-mercaptoethanol	Sigma-Aldrich	Taufkirchen, Germany

Table 2-7: Utilized chemicals and reagents.

Machine	Company	Location
Coulter Z2	Beckman Coulter	Krefeld, Germany
Gallios flow cytometer	Beckman Coulter	Krefeld, Germany
UV Transilluminator	Intas Science Imaging Instruments GmbH	Göttingen, Germany
Light cycler		
Mastercycler Epgradient S	Eppendorf	Munich, Germany
NanoDrop™ 2000	Life Technologies	Darmstadt, Germany
ProCyte Dx™	IDEXX Laboratories	Hoofddorp, Netherlands
SpeedMill PLUS	Analytik Jena AG	Jena, Germany
Thermomixer F1.5	Eppendorf	Munich, Germany

Table 2-8: Utilized machines.

Kit	Company	Location
CBA Mouse TNF Enhanced Sensitivity Flex Set	Becton Dickinson GmbH	Heidelberg, Germany
EasySep™ Mouse B Cell Isolation Kit	StemCell Technologies	Cologne, Germany
EasySep™ Mouse CD4+ T Cell Isolation Kit	StemCell Technologies	Cologne, Germany
EasySep™ Mouse CD8+ T Cell Isolation Kit	StemCell Technologies	Cologne, Germany
EasySep™ Mouse Neutrophil Enrichment Kit	StemCell Technologies	Cologne, Germany
FITC BrdU Flow Kit	Becton Dickinson GmbH	Heidelberg, Germany
High Capacity cDNA Reverse Transcription Kit	Life Technologies	Darmstadt, Germany
RNeasy Plus Mini Kit	QIAGEN	Hilden, Germany
Zombie Violet™ Fixable Viability Kit	Biolegend	London, UK

Table 2-9: Utilized kits.

Software	Company	Location
FlowJo™ V10	Becton Dickinson GmbH	Heidelberg, Germany
GraphPad Prism 7	GraphPad Software	La Jolla, CA, USA
StepOne Software v2.3	Life Technologies	Darmstadt, Germany

Table 2-10: Utilized software.

Material	Company	Location
Lysis tube A	Analytik Jena AG	Jena, Germany
Microhematocrit tubes	VWR	Darmstadt, Germany
QIAshredder	QIAGEN	Hilden, Germany

Table 2-11: Utilized materials.

3. Results

3.1. Effect of light on leukocyte oscillations in blood

Light is the main environmental entrainment factor for the central clock. It synchronizes all peripheral organ clocks via the SNS and glucocorticoids, which is mediated by the SCN in the hypothalamus. However, for peripheral clocks other Zeitgebers such as food uptake are an additional important synchronizing means. Hence, we wondered whether light input controls the rhythmic leukocyte oscillation in blood. For this, mice were kept under either constant light or constant darkness conditions to exclude oscillatory input vie this means and blood, bone marrow and spleen were harvested every 6 h for 24 h from different cohorts of mice (**Figure 3-1A**). For the overall leukocyte counts, we observed an oscillation under normal 12 h light and 12 h darkness conditions (DD) with a peak at circadian time (CT) 7 and a trough at CT13. The term *circadian time* instead of *Zeitgeber time* is used upon the lack of entrainment and thus referring to self-autonomous, free-running oscillations, as it is the case during constant darkness. The counts at CT7 were highly significant compared to the numbers at CT1, CT13 and CT19 (**Figure 3-1B, C**). When mice were kept in complete darkness (DD) for 24 h, the general white blood cell (WBC) numbers still showed a significant peak at CT7 compared to CT1 and CT13 and a nadir at CT13. The data collected after 24 h constant light (LL) input still showed significantly lower leukocyte numbers at ZT19 compared to ZT1 and ZT7. Both DD and LL conditions lowered the WBC count at CT7 and ZT7, respectively, however, only constant light clearly increased the leukocyte numbers at ZT13 (**Figure 3-1B**). To analyse circadian rhythmicity, we used a cosinor analysis to fit our data to a rhythmic curve with a period of 24 h. This was significant for control animals with an acrophase at ZT5.69, as expected (Scheiermann et al., 2012). In mice in complete darkness, there was no significant oscillation observed as stated by cosinor analysis, although it was close to significance with a p-value of 0.09 and the spline through all data points reveals a clear daily tendency. After 24 h of constant light, cosinor analysis showed significant rhythms over 24 h, although the acrophase was slightly shifted towards the activity phase (ZT7.75), resulting in an altered spline (**Figure 3-1C**).

We also analysed the main leukocyte subsets in blood to assess whether specific subtypes were affected. Basically all subsets, namely neutrophils, inflammatory and non-inflammatory monocytes, natural killer cells, CD4+ and CD8+ T cells, B cells, and eosinophils exhibited rhythmic abundancies over 24h with a peak at ZT7 and a trough during the active phase (ZT13 or ZT19, **Figure 3-1D**). When analysing the differences of the two treatment groups to the LD conditions, the drop in leukocyte numbers at ZT7 under both conditions was mainly due to a decrease in lymphocytes, but also eosinophils. Lymphocytes were also overall increased at ZT13 compared to LD conditions, resulting in the significant expansion of WBC counts at this time point. The myeloid cell populations did not show big differences upon exposure to either constant light or constant darkness except for NIM, which were increased at ZT13 in LL conditions (**Figure 3-1D**).

Since bone marrow is the most important organ for haematopoiesis, we also investigated the overall cell counts and leukocyte subsets in bone marrow samples of these mice. WBC abundancies were almost the same independently of either harvest time point or treatment. Solely counts at CT13 after 24 h in constant darkness were slightly elevated compared to the respective numbers at CT1. This effect was the same for the tested populations: neutrophils, IMs, NIMs, NK cells, CD4+ and CD8+ T cells, B cells and also eosinophils. The lymphocytes, especially CD8+ T cells, seemed to express a more pronounced oscillation in their abundancies in the bone marrow compared to the counts of myeloid cells (**Figure 3-1E**).

In the spleen, overall counts neither showed any oscillation nor differences between the two different treatment groups compared with control animals. This effect was also represented by mostly all investigated leukocyte subsets, only IMs and NK cells exhibited a minor peak at CT1 and CT13, respectively (**Figure 3-1F**).

Taken together, constant darkness was not able to severely influence circadian leukocyte oscillation in the circulation while constant light clearly altered the rhythmicity. WBC counts in bone marrow and spleen were not affected by these two different conditions compared to normal light conditions.

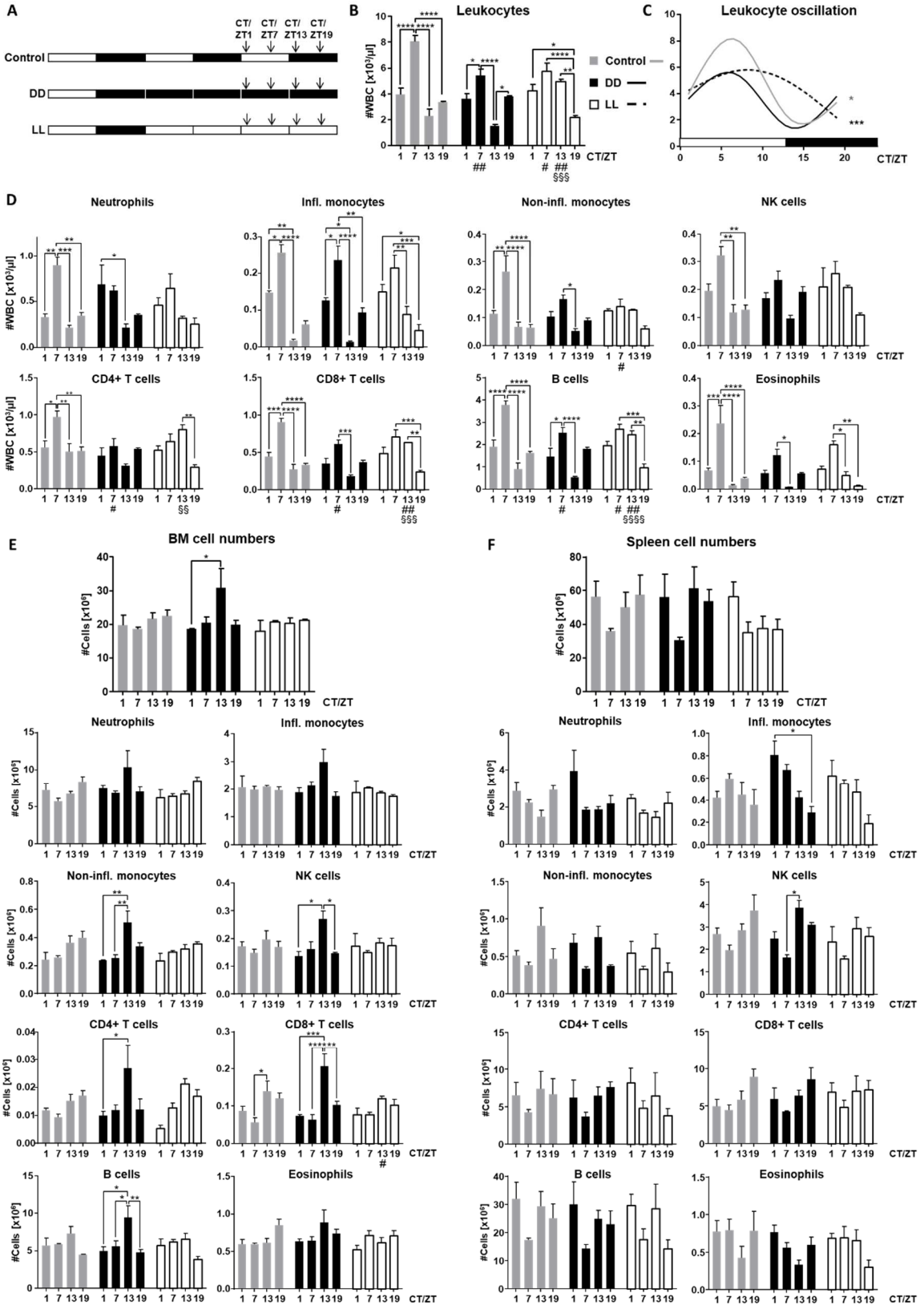
A
CT/ ZT1
CT/ ZT7
CT/ ZT13
CT/ ZT19
Control
DD
LL
B
Leukocytes
#WBC [x10³/µl]
Control
DD
LL
CT/ZT
C
Leukocyte oscillation
CT/ZT
D
Neutrophils
Infl. monocytes
Non-infl. monocytes
NK cells
CD4+ T cells
CD8+ T cells
B cells
Eosinophils
#WBC [x10³/µl]
CT/ZT
E
BM cell numbers
#Cells [x10⁶]
Neutrophils
Infl. monocytes
Non-infl. monocytes
NK cells
CD4+ T cells
CD8+ T cells
B cells
Eosinophils
CT/ZT
F
Spleen cell numbers
#Cells [x10⁶]
Neutrophils
Infl. monocytes
Non-infl. monocytes
NK cells
CD4+ T cells
CD8+ T cells
B cells
Eosinophils
CT/ZT

Figure 3-1: Constant light or constant darkness has little impact on total leukocyte and leukocyte subset oscillation in blood, bone marrow and spleen. (A) Experimental setup for control, constant darkness (DD) and constant light (LL) conditions. Blood, bone marrow and spleen were harvested every 6 h at Zeitgeber time (ZT) and Circadian time (CT) 1, 7, 13 and 19 24 h after onset of respective light conditions, as indicated by arrows. ZT accounts for control and LL experiments, while CT accounts for DD conditions. (B) Leukocyte counts in blood under control (grey), DD (black) and LL (white) conditions. (C) Spline for leukocyte counts from control, DD and LL conditions. (D) Numbers of leukocyte subsets neutrophils, inflammatory and non-inflammatory monocytes, NK cells, CD4+ and CD8+ T cells, B cells and Eosinophils 24 h after onset of light changes. (E, F) Overall cell numbers and leukocyte subset counts in bone marrow (E) and spleen (F). (B, D-F: n=3, two-way ANOVA. C: n=3, cosinor analysis). *p<0.05, **p<0.01, ***p<0.001, ****p<0.0001. # equivalent to *, in comparison to respective time point under control conditions. § equivalent to *, in comparison with respective time point under DD conditions.

3.2. Effect of jetlag on leukocyte oscillations in blood

Since we did not observe disruption of the circadian leukocyte oscillation under these conditions, we aimed to disturb the rhythmic WBC counts using an acute jetlag model. Mice were exposed to light for 24 h that was followed by a 12 h dark period, hence inducing a 12 h jetlag. Sampling started at the beginning of the shifted dark period and took place every 6 h for 24 h (**Figure 3-2A**). The general white blood cell counts in the control animals showed a daily rhythm with significant differences between ZT13 and ZT1 and ZT7. After a 12 h jetlag induction, leukocyte numbers at ZT13 presented significantly higher numbers compared to the control group while maintaining an oscillation over 24 h (**Figure 3-2B**). Cosinor analyses revealed a shifted acrophase from ZT3.28 in control animals to ZT7.38 in animals after jetlag and the spline was clearly altered (**Figure 3-2C**). In most leukocyte subsets, daily rhythms between the four different time points were less significant after jetlag than in the control group, especially for IMs, NK cells, CD8+ cells, B cells and also slightly for neutrophils (**Figure 3-2D**). These data indicate a shift of the WBC trough in the circulation towards the middle of the dark phase with significant differences between jetlag and control group at ZT13 and ZT19 for NIM and NK cells, and eosinophils, respectively. In the bone marrow, we did not observe any differences between either the time points or the jetlag and control group concerning the overall cell counts. Also, leukocyte subsets did not exhibit any of these variances except for CD4+ T cells that had significantly higher abundancies at ZT1 compared to ZT7 and ZT13 (**Figure 3-2E**). However, these dissimilarities were also present after jetlag induction and they also displayed very low cell numbers in bone marrow in general. A similar

phenotype was observed in splenic leukocytes with no oscillatory cell counts and no significant changes after jetlag induction compared to control animals. However, neutrophils and IMs showed daily rhythms in the control group with highest

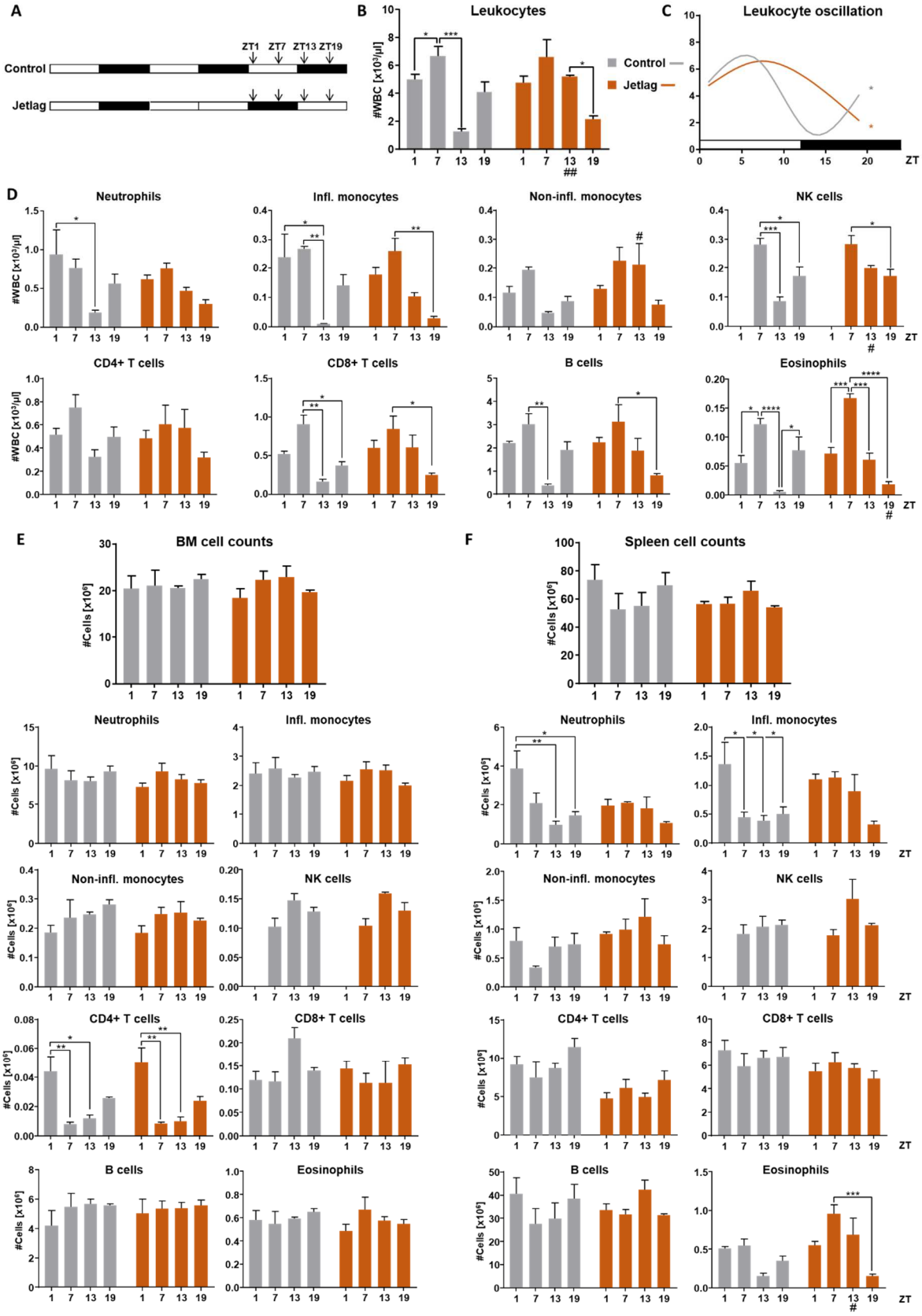

Figure 3-2: Jetlag induction alters leukocyte numbers in blood but has no impact on cell numbers in bone marrow and spleen. (A) Experimental setup for control and jetlag conditions. Blood, bone marrow and spleen were harvested every 6 h at ZT1, 7, 13, and 19 24 h after onset of jetlag conditions, as indicated by arrows. (B) Leukocyte counts in blood after control (grey) and jetlag (orange) conditions. (C) Spline for leukocyte counts from control and jetlag conditions. (D) Numbers of leukocyte subsets neutrophils, inflammatory and non-inflammatory monocytes, natural killer (NK) cells, CD4+ and CD8+ T cells, B cells and eosinophils 24 h after onset of light changes. (E, F) Overall cell numbers and leukocyte subset counts in bone marrow (E) and spleen (F). (B, D-F: n=3, two-way ANOVA. C: n=3, cosinor analysis). *p<0.05, **p<0.01, ***p<0.001, ****p<0.0001. # equivalent to *, in comparison to respective time point under control conditions. § equivalent to *, in comparison with respective time point under DD conditions.

abundancies at ZT1. These differences were abolished after jetlag treatment (**Figure 3-2F**).

To conclude, acute jetlag shifted circadian leukocyte oscillation in blood about 4 h towards the active phase while WBC counts in bone marrow and spleen were not affected by the 12 h light shift.

3.3. BrdU staining does not show significant leukocyte mobilization into the blood stream

On a mechanistic level, we wondered whether the rhythmic leukocyte oscillation in the circulation is a consequence of circadian WBC mobilization from hematopoietic organs into the blood stream, in addition to the recently published rhythmic emigration into organs (He et al., 2018). To address this question, mice were injected with BrdU 72 h before blood and organ harvest (**Figure 3-3A**). BrdU is a component that only labels cells that have proliferated and since there is no proliferation supposed to take place in the circulation, all BrdU positive cells harvested from blood must hence be mobilized from tissues. Using such a short BrdU pulse allows the investigation of young cells that have recently entered the circulation (Balmer et al., 2014; Casanova-Acebes et al., 2013). With a blood harvest every 4 h over 12 h after BrdU injection, we therefore investigated differences in BrdU-labeled cell numbers and proportions over the course of a day. While leukocyte numbers in blood exhibited daily differences with a significant peak at the middle of the day and a trough at ZT13 (**Figure 3-3B**), the fraction of BrdU+ leukocyte subset numbers in the circulation was mostly not rhythmic (**Figure 3-3C**). However, there was a tendency towards increased BrdU+ cells, mostly innate immune cells, during the light phase with a significant peak at ZT9 for NIMs.

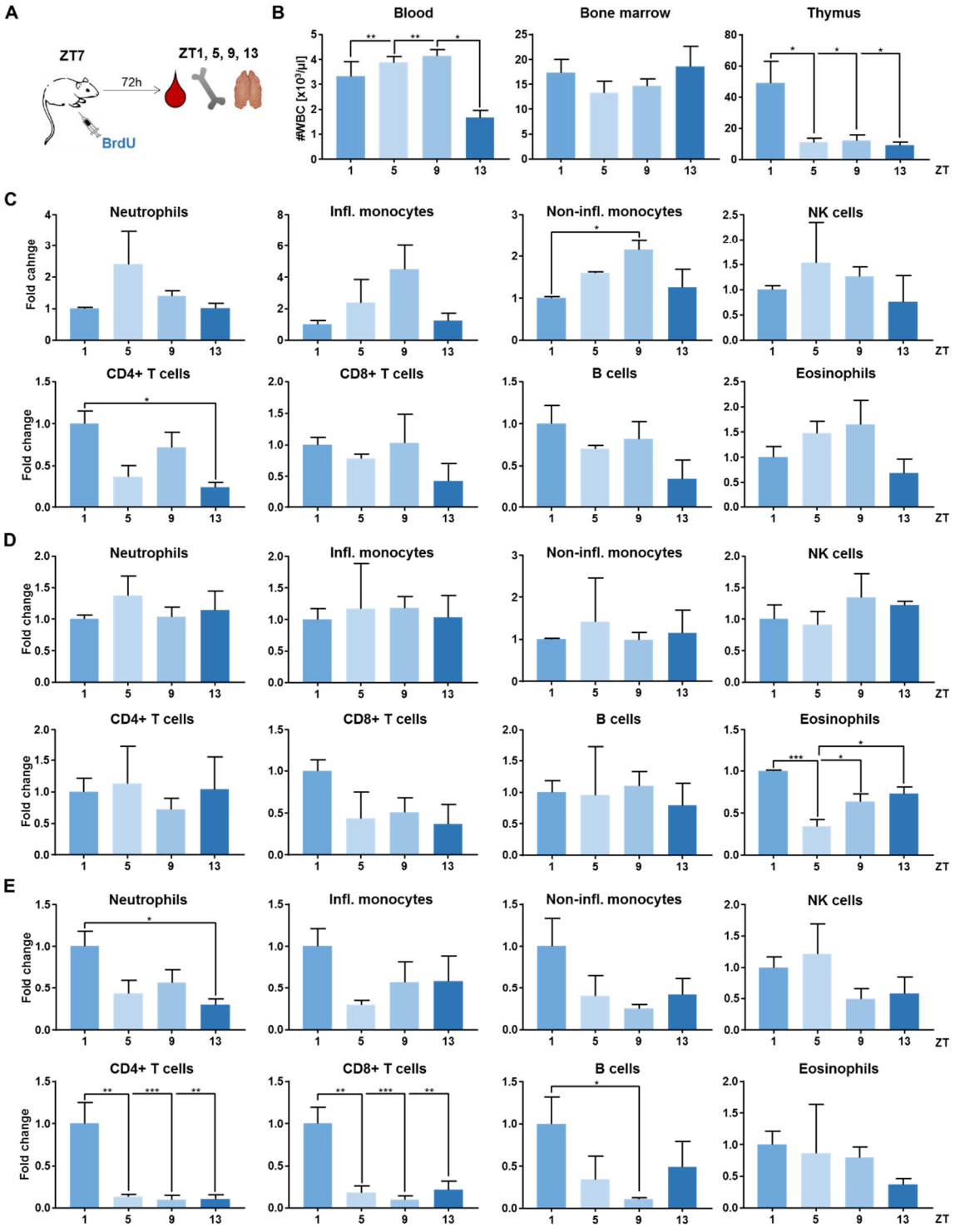

Figure 3-3: BrdU staining does not reveal a rhythmic leukocyte mobilization into the circulation. (A) Mice were injected i.p. with 200 mg of BrdU at ZT7, about 72 h before harvest. Blood, bone marrow and thymus were harvested every 4 h at ZT1, 5, 9 and 13 for 12 h 72 h after BrdU pulse. (B) Overall cell counts in blood, bone marrow and thymus at indicated harvest times. (C-E) Total BrdU+ counts normalized to ZT1 levels in blood (C), bone marrow (D) and thymus (E) for neutrophils, inflammatory and non-inflammatory monocytes, NK cells, CD4+ and CD8+ T cells, B cells and eosinophils (n=2-7, one-way ANOVA). *p<0.05, **p<0.01.

We also analysed the fraction of BrdU+ cell numbers in bone marrow (**Figure 3-3D**) and thymus (**Figure 3-3E**), the two major leukocyte producing organs. Similar to our results obtained from blood, we could not find daily differences in BrdU labelling in bone marrow, except for lower BrdU+ eosinophil numbers at ZT5 compared to ZT1 (**Figure 3-3D**). In the thymus, overall cell numbers were elevated at ZT1 in thymus compared to ZT5, 9 and 13 (**Figure 3-3B**), which was also represented by increased amounts of BrdU+ lymphocytes at ZT1 (**Figure 3-3E**).

Taken together, the proliferation process itself seems not to be rhythmic in bone marrow, while lymphocytes in the thymus show daily BrdU labelling over the course of the day. The mobilization process of especially innate immune cells might be under rhythmic control.

3.4. Light-restricted feeding for 6 h shifts leukocyte oscillation in circulation

Since leukocyte oscillations in blood still persisted without the major entrainment factor light but exhibited altered numbers in constant light conditions and after jetlag, we investigated another key Zeitgeber: food. For this purpose, mice were allowed restricted 12 h food access during either the light or dark phase while the control group had *ad libitum* food supply (**Figure 3-4A**). Actograms of individual mouse behaviour were recorded to study the influence of this experimental setup on locomotor activity of the animals. These experiments were performed in collaboration with Dr. Roee Gutman at the Tel-Hai College in Tel Aviv, Israel. Mice that had food access during the dark and hence their active phase did not show any behavioural changes compared to the *ad libitum* fed group. In contrast, animals that had to take up food during their resting phase displayed an altered activity rhythm with increased activity at the beginning of the light period (**Figure 3-4B**).

Blood was harvested after two weeks of time-restricted feeding (TRF) and after two weeks being back at *ad libitum* feeding at four different time points. All three treatment groups exhibited clear daily leukocyte rhythms after TRF (**Figure 3-4C**) as well as after being back on an *ad libitum* feeding (**Figure 3-4E**) with a peak at ZT7 and a trough at ZT13. Although cosinor analysis did not show significant oscillation after two weeks of dark-restricted feeding (DRF), the counts did not show significant differences to *ad libitum*-fed mice and the spline was similar to the one of

control-fed animals (**Figures 3-4C, D**). Remarkably, leukocyte counts were still oscillatory after two weeks of light-restricted feeding although this setup clearly changed behavioural rhythms of the mice (**Figure 3-4D**). Two weeks after transferring mice back to constant food access, rhythms in leukocyte numbers in blood were oscillatory as shown by cosinor analysis (**Figure 3-4F**).

We speculated that the duration of time-restricted feeding per day might have been too long. Therefore, we repeated the experiment with a more restricted time window

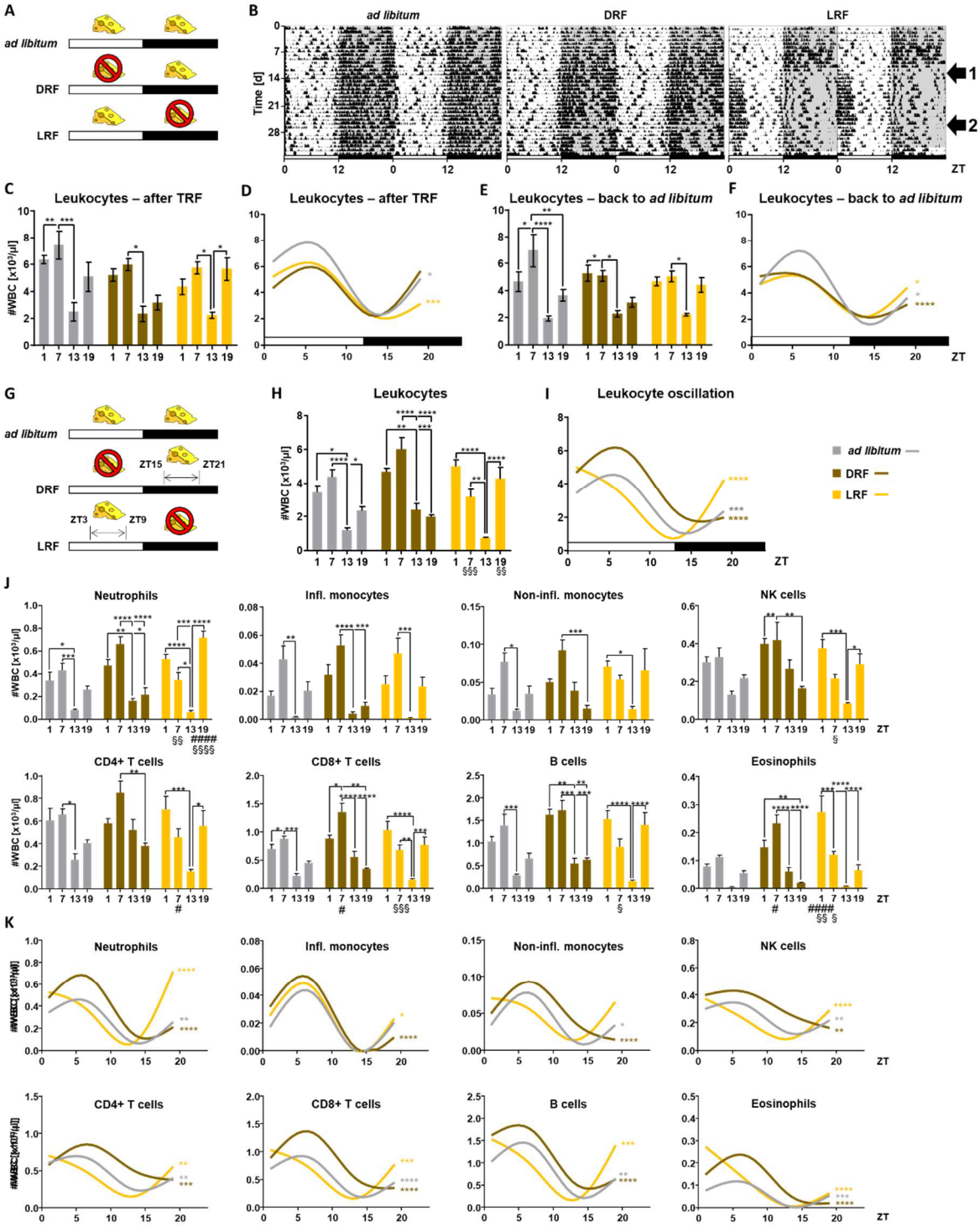

Figure 3-4: Light-restricted feeding for 6 h shifts leukocyte oscillations in blood. (A) Mice had food access either *ad libitum*, or for 12 h only during the dark phase (DRF) or only during the light phase (LRF) for two weeks. (B) Activity of individual animals was recorded before, at the start of TRF (arrow 1) and after the end of TRF (arrow 2). White bars indicate light phase, black bars dark phase. Each black peak represents active behaviour of the animal. (C, E) Blood was harvested after two weeks of TRF (C) and after two weeks back to *ad libitum* feeding (E) and leukocyte counts were measured. (D, F) Splines of leukocyte counts after two weeks of TRF (D) and after two weeks back to *ad libitum* feeding (F). (G) Mice had food access either *ad libitum*, or for 6h from ZT15 to ZT21 and ZT3 to ZT9 during dark and light phase, respectively, for two weeks. (H) Blood was harvested after two weeks of 6 h-restricted feeding (RF) and leukocyte counts were measured. (I) Spline of leukocyte counts after two weeks of 6 h-RF. (J) Leukocyte subsets in *ad libitum*-fed, DRF and LRF mice were analysed using flow cytometry. (K) Splines of leukocyte subsets after two weeks of 6 h-RF. (C, E: n=4, two-way ANOVA. D, F: n=4, cosinor analysis. H, J: n=5, two-way ANOVA. I, K: n=5, cosinor analysis) *p<0.05, **p<0.01, ***p<0.001, ****p<0.0001. # equivalent to *, in comparison to respective time point under *ad libitum* conditions. § equivalent to *, in comparison with respective time point under DRF conditions.

of food access of only 6 h during the middle of either the dark or the light phase (**Figure 3-4G**). In overall blood counts, we saw a clear peak at ZT7 for ad libitum and dark-restricted fed mice. Upon light-restricted feeding, however, the peak was shifted to the earlier time point ZT1. Also, these animals had significantly higher leukocyte counts at ZT19 compared to mice with food access during the dark phase and a clear tendency towards higher counts compared with control animals. While ad libitum and dark-fed mice did not show any significance between ZT13 and ZT19, light-fed mice had significantly higher counts at the later time point (**Figure 3-4H**). To gain more inside into the underlying circadian rhythmicity, we analysed our data using a cosinor analysis. This demonstrated a significant underlying oscillation over 24h for all three conditions. However, while the acrophase for ad libitum and dark restricted feeding was during the early resting phase (ZT3.77 and ZT5.04 for ad libitum and dark-restricted feeding, respectively), mice fed restricted to the light phase showed a clearly shifted peak towards the onset of the rest phase (ZT0.05) (**Figure 3-4I**). This shift seemed to be mainly due to higher counts at ZT19, specifically increased neutrophil and B cell numbers. Almost all cell types except monocytes were significantly reduced at ZT7 under light-feeding compared to animals from dark-restricted feeding, however, NIMs displayed slightly reduced counts at this time point compared with control mice. Eosinophils exhibited significantly higher numbers at ZT1 after light-feeding in comparison to both other treatments (**Figure 3-4J**). Comparing splines of leukocyte subsets, we were able to find a clear shift in neutrophil oscillation after LRF as well as slight shifts in the

rhythms of NK cells, T cells, B cells and Eosinophils. IMs on the other side did not show significant oscillation in control animals (**Figure 3-4K**).

Taken together, food restriction to 6 h during the light phase was able to shift circadian leukocyte oscillation in blood while altered behavioural activity during 12 h restricted feeding had no impact on rhythmic leukocyte counts.

To further check potential effects on hematopoietic organs, we analysed bone marrow and spleen for their overall and subset specific counts. Bone marrow samples did not show any oscillation over the course of the day in ad libitum and dark-fed mice. However, after light-restricted feeding, cell numbers were increased

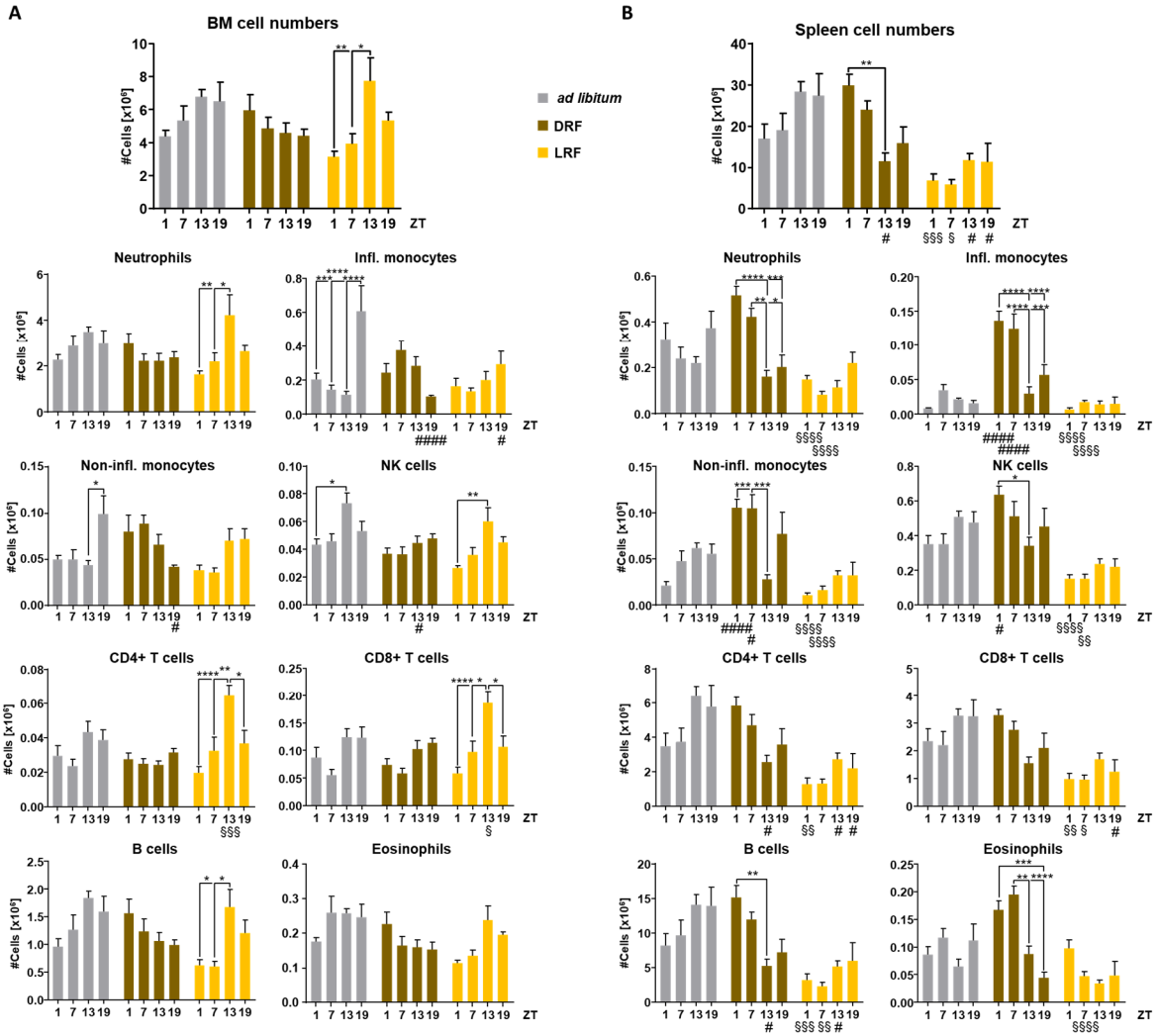

Figure 3-5: TRF slightly alters bone marrow and spleen cell and leukocyte subset numbers. Mice received food either *ad libitum* (grey) or only for 6h during the dark (DRF, brown) or light phase (LRF, yellow). (A, B) Bone marrow (A) and spleen (B) were harvested after two weeks of TRF every 6 h for 24 h at ZT1, 7, 13, and 19. Overall cell numbers were counted and leukocyte subsets were analysed using flow cytometry. (n=5, two-way ANOVA). *p<0.05, **p<0.01, ***p<0.001, ****p<0.0001. # equivalent to *, in comparison to respective time point under ad libitum conditions. § equivalent to *, in comparison with respective time point under DRF conditions.

at the onset of the active phase compared to the time points during rest phase, mostly due to an expansion of neutrophils. Monocytes presented higher numbers at ZT19 under control conditions while lymphocytes were elevated at this time point after food-restriction to the light phase (**Figure 3-5A**). Similar to the bone marrow, splenic counts were not oscillatory over the course of 24h in control conditions. Except for ZT13, counts after dark-restricted feeding did not differ from ad libitum food access. Light restricted feeding however, decreased the cell numbers in spleens of these animals, which was significant for ZT13 and ZT19, and ZT1 and ZT7 in comparison to control and dark-fed mice, respectively. This was mostly a result of reduced numbers in neutrophils, B cells, CD4+ and CD8+ T cells and for ZT7 also for eosinophils. Meanwhile, monocytes were increased at ZT1 and ZT7 after two weeks of dark-restricted feeding (**Figure 3-5B**).
Thus, time-restricted feeding did not alter leukocyte counts in the bone marrow but food restriction to the light phase decreased cell counts in the spleen.

3.5. Light-restricted feeding alters clock gene expression in liver and in mesenteric lymph node

Since we detected a shift in leukocyte rhythms in blood after two weeks of 6 h light-restricted feeding, we wondered whether time-restricted feeding was also able to alter clock gene expression in peripheral organs. We hence analysed mRNA levels for representative clock genes *Nr1d1* and *Per2* that exhibit high amplitudes as well as levels for the clock-controlled gene *Dbp,* a major oscillatory downstream target of the circadian clock, in bone marrow, spleen and liver of *ad libitum*-, dark-restricted- and light-restricted-fed mice at four different time points. There were no significant oscillations in any of these three genes in bone marrow of either *ad libitum*-fed or DRF mice (**Figure 3-6A, B**). Light-restricted feeding induced slight oscillations as indicated by cosinor analysis, although none of these expression levels were significantly different to control or DRF animals (**Figure 3-6A, B**). In spleen, *Nr1d1* expression exhibited a modest oscillatory pattern in *ad libitum* mice and a stronger rhythm in DRF animals (**Figure 3-6D**). This difference was observed by significant alterations at ZT7 in DRF mice compared to control-fed mice (**Figure 3-6C**). For *Dbp*, we did not observe an oscillation after ad libitum feeding while mRNA levels after DRF were rhythmic. On the other side, *Per2* amplitude was lower

in DRF mice and shifted compared to *ad libitum* and LRF animals. LRF did not lead to oscillations in either *Nr1d1* or *Dbp* levels in spleen (**Figure 3-6C, D**).

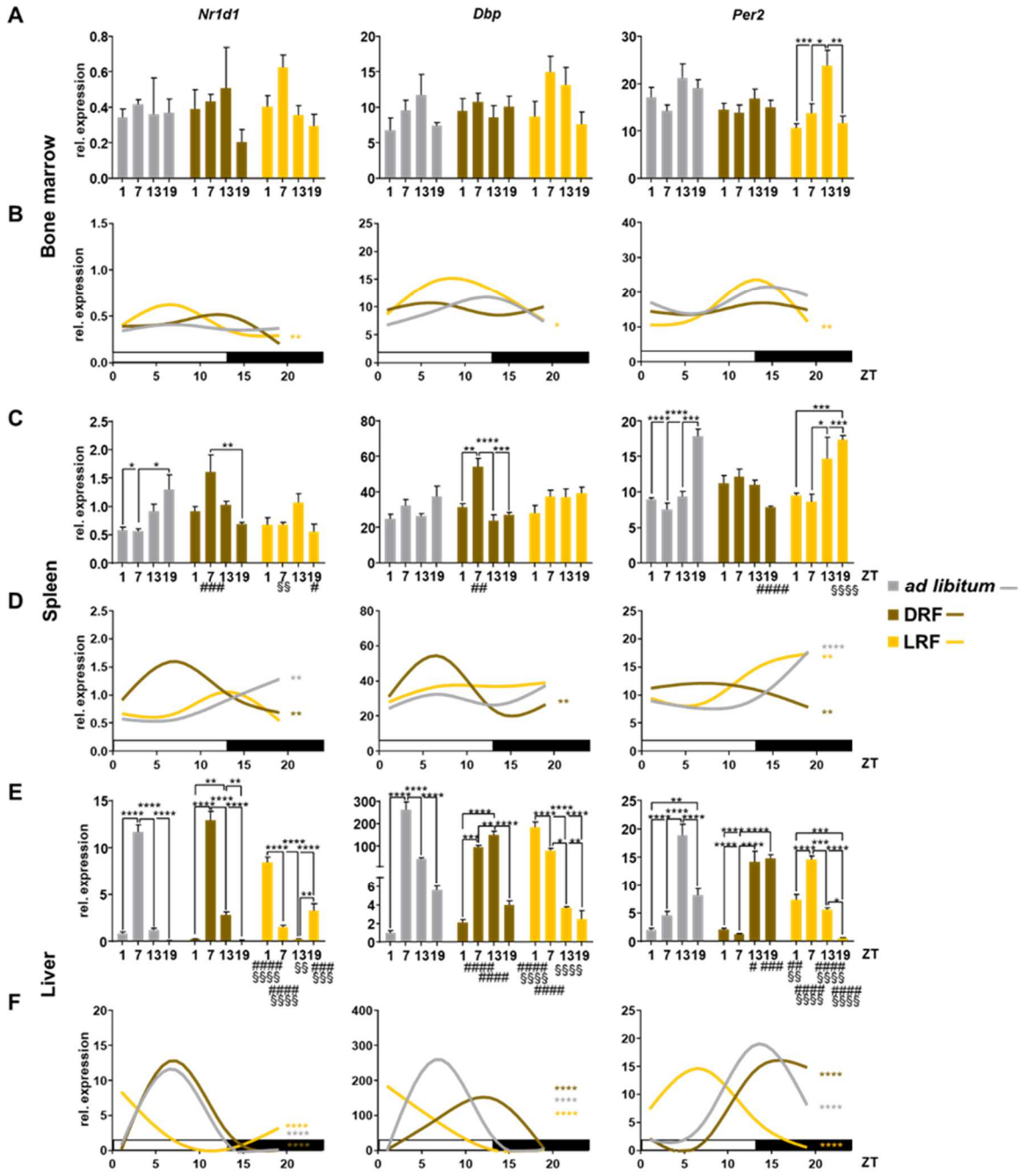

Figure 3-6: Light-restricted feeding shifts clock gene expression in liver. Mice received food either ad libitum (grey) or only for 6h during the dark (DRF, brown) or light phase (LRF, yellow). Bone marrow, spleen and liver were harvested every 6 h for 24 h after two weeks of TRF, RNA was extracted and qPCR analysis for *Nr1d1*, *Dbp* and *Per2* mRNA levels was performed. (A, C, E) Relative expression levels of *Nr1d1*, *Dbp* and *Per2* in RNA isolated from bone marrow (A), spleen (C) and liver (E). (B, D, F) Cosinor analysis for relative expression levels of *Nr1d1*, *Dbp* and *Per2* in bone marrow (B), spleen (D) and liver (E). (n=5. A, C, E two-way ANOVA, B, D, F cosinor analysis) *p<0.05, **p<0.01, ***p<0.001, ****p<0.0001. # equivalent to *, in comparison to respective time point under ad libitum conditions. § equivalent to *, in comparison with respective time point under DRF conditions.

Finally, we analysed clock gene expression in the liver since this organ is closely influenced by metabolites, gut physiology and thus feeding rhythms. We detected very strong rhythms in the expression of all three genes, aligning with published observations (**Figure 3-6E, F**) (Hara et al., 2001). Here, *ad libitum* and DRF animals showed similar oscillatory patterns while, interestingly, LRF animals expressed a clear shift in their daily expression rhythm of *Nr1d1*, *Dbp* and *Per2*. While the peak in *Nr1d1* mRNA levels was detected around ZT7 (ZT 7.13 for *ad libitum* and ZT 7.76 for DRF), the acrophase in LRF animals was shifted to ZT 0.197. *Dbp* exhibited its peak during the middle of the rest phase (ZT 7.61 for *ad libitum* and ZT 10.9 for DRF) and LRF shifted this peak towards the onset of the rest phase at ZT 2.53. *Per2*, on the other hand, peaked at the onset of the active phase (ZT 13.79 for *ad libitum* and ZT 16.22 for DRF), but after LRF, this acrophase was clearly shifted to ZT 6.52 (**Figure 3-6F**).

Additionally, clock gene expression levels were also analyzed in lymph nodes (LN) harvested from two different anatomical sites. In the inguinal LN, mRNA levels of *Nr1d1*, *Dbp* and *Per2* exhibited clear daily expression levels for all three experimental setup conditions (**Figure 3-7A, B**). Similar to the detected acrophases in liver, *Nr1d1* and *Dbp* expression peaked during the middle of the rest phase, while *Per2* demonstrated an acrophase at the beginning of the active phase (**Figure 3-7B**). In mesenteric LN, daily rhythms and peak expression were similar to inguinal LN for *Nr1d1* and *Per2* mRNA peaking during the rest phase and at the beginning of the active phase, respectively, when mice had ad libitum access to food or were only fed during the dark phase (**Figure 3-7C, D**). For *Dbp* expression levels, acrophases were slightly shifted towards the beginning of the active phase under control and DRF conditions when compared to *Dbp* expression levels in inguinal LN or liver. However, light-restricted feeding reduced the amplitude of all three clock genes (*Nr1d1*: from 1.5 in the control group to 0.7 in LRF, *Dbp*: loss of rhythm, *Per2*: from 1.9 in the control group to 1.4 in LRF), resulting in a clearly dampened rhythm (**Figure 3-7C, D**). Also, mRNA expression of *Nr1d1*, *Dbp* and *Per2* at ZT7 and ZT13 was significantly reduced after LRF compared to *ad libitum*- and dark restricted-fed animals (**Figure 3-7C**).

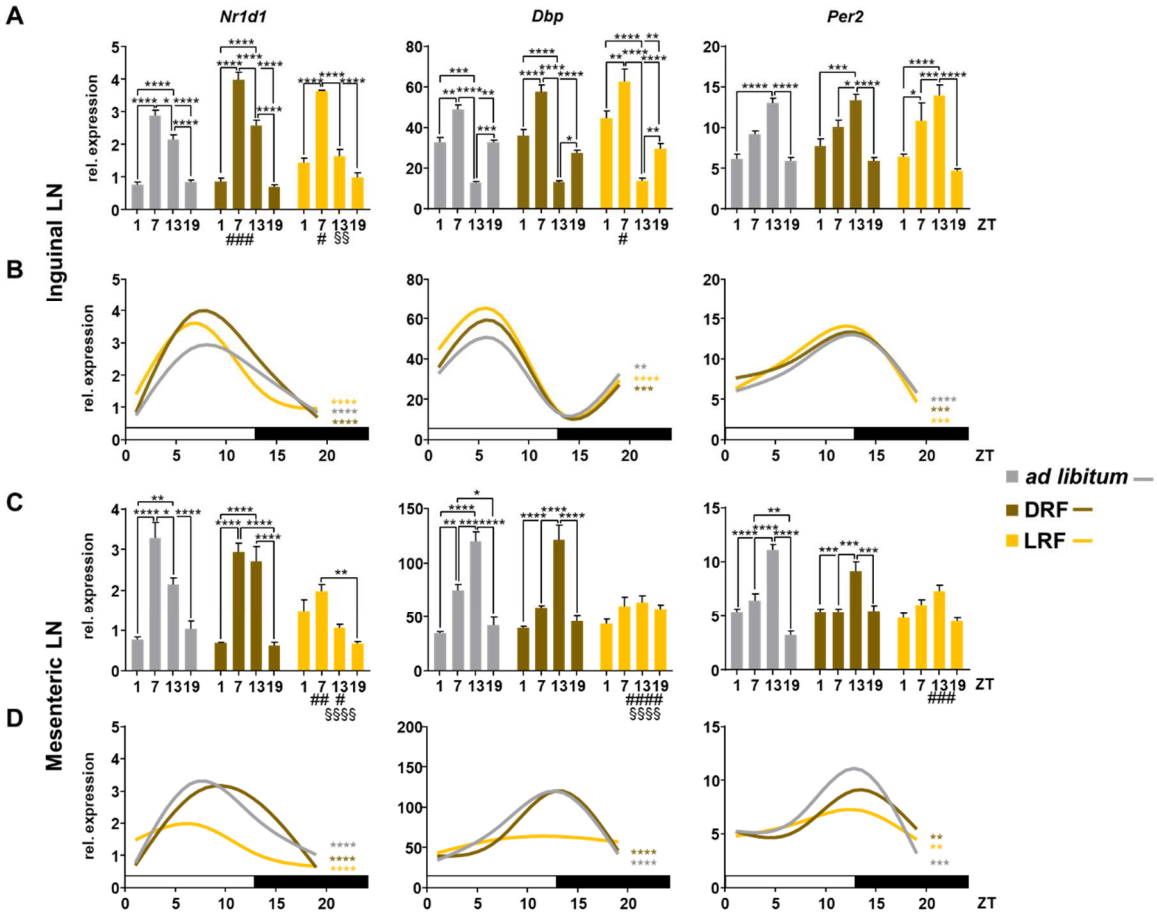

Figure 3-7: Light-restricted feeding shifts clock gene expression in mesenteric LN. Mice received food either ad libitum (grey) or only for 6h during the dark (DRF, brown) or light phase (LRF, yellow). Inguinal and mesenteric LN were harvested every 6 h for 24 h after two weeks of TRF, RNA was extracted and qPCR analyses for *Nr1d1*, *Dbp* and *Per2* mRNA levels were performed. (A, C) Relative expression levels of *Nr1d1*, *Dbp* and *Per2* in RNA isolated from inguinal (A) and mesenteric LN (C). (B, D) Cosinor analysis for relative expression levels of *Nr1d1*, *Dbp* and *Per2* in inguinal (B) and mesenteric LN (D). (n=5. A, C two-way ANOVA, B, D cosinor analysis) *p<0.05, **p<0.01, ***p<0.001, ****p<0.0001. # equivalent to *, in comparison to respective time point under ad libitum conditions. § equivalent to *, in comparison with respective time point under DRF conditions.

To conclude, bone marrow and spleen did not exhibit oscillatory clock gene expression to the same extent as liver or lymph nodes. In liver, light-restricted feeding induced a clear shift in rhythmic expression patterns compared to *ad libitum* and dark-fed animals. Clock gene expression in inguinal LN was not affected by time-restricted feeding while in mesenteric LN, LRF clearly dampened daily oscillation in mRNA expression levels of the investigated clock genes.

3.6. Antibiotics do not alter leukocyte differences in blood

It was recently shown that microbiota themselves exhibit circadian rhythms with respect to their composition and their function and that rhythmic food uptake regulates these oscillations (Liang et al., 2015; Thaiss et al., 2014b; Zarrinpar et al., 2014). Moreover, microbiota were shown to influence the host immune system, which is why we hypothesized that rhythmic microbiota might exert an influence on circadian leukocyte oscillations in blood. For this purpose, we treated wild-type animals with broad-spectrum antibiotics via the drinking water for two weeks to abrogate intestinal commensal bacteria. We harvested blood and lymphoid organs at peak and trough times of circadian leukocyte counts in circulation, namely at ZT5 and ZT13. Comparing total leukocyte counts in blood from antibiotics-depleted (ABX) animals with control mice, we could not detect any differences. Both control and treatment groups displayed significant differences between these two time points (**Figure 3-8A**). For different subsets, we found significance between ZT5 and ZT13 in both treatment groups for NIMs and eosinophils and for control or ABX animals for B cells or IMs and NK cells, respectively. Also, there were no dramatic changes in cell counts in bone marrow after antibiotic-induced microbial depletion. Both groups showed increased cell numbers at ZT13 compared to ZT5 (**Figure 3-8B**). On a subset level, neutrophils displayed slightly decreased counts at ZT13 after antibiotic treatment while lymphocytes, such as NK cells, CD4+ T cells and especially B cells, had significantly increased cell numbers at this time point. We also analysed the thymus as another primary lymphoid organ and detected higher cell counts at ZT13 after two weeks of antibiotics treatment. This was mostly due to increases in CD4+ and CD8+ T cells, the two most abundant cell types in thymus. Neutrophils and NK cells displayed similar increases at ZT13 after antibiotics treatment and NIMs, together with neutrophils, had higher cell counts at ZT5 compared to ZT13 under control conditions while IMs showed this phenotype after ABX (**Figure 3-8C**). However, these cell types are present at very low frequencies in this organ.

In secondary lymphoid organs, splenic cell numbers were not different between either time points or treatments. However, CD4+ and CD8+ T lymphocytes exhibited significantly higher counts at ZT13 compared with ZT5 in ABX animals, which seemed to be compensated by slightly lower myeloid cell numbers at this time point

(**Figure 3-8D**). In inguinal lymph nodes, we detected reduced cell counts at ZT13 after antibiotic treatment, which seemed to be mediated by decreased B cell numbers and also slightly diminished T cell numbers (**Figure 3-8E**).

Hence, antibiotic treatment did not alter circadian leukocyte differences in blood between ZT5 and ZT13 and also showed no effect on leukocyte numbers in bone marrow, thymus, spleen or inguinal lymph nodes.

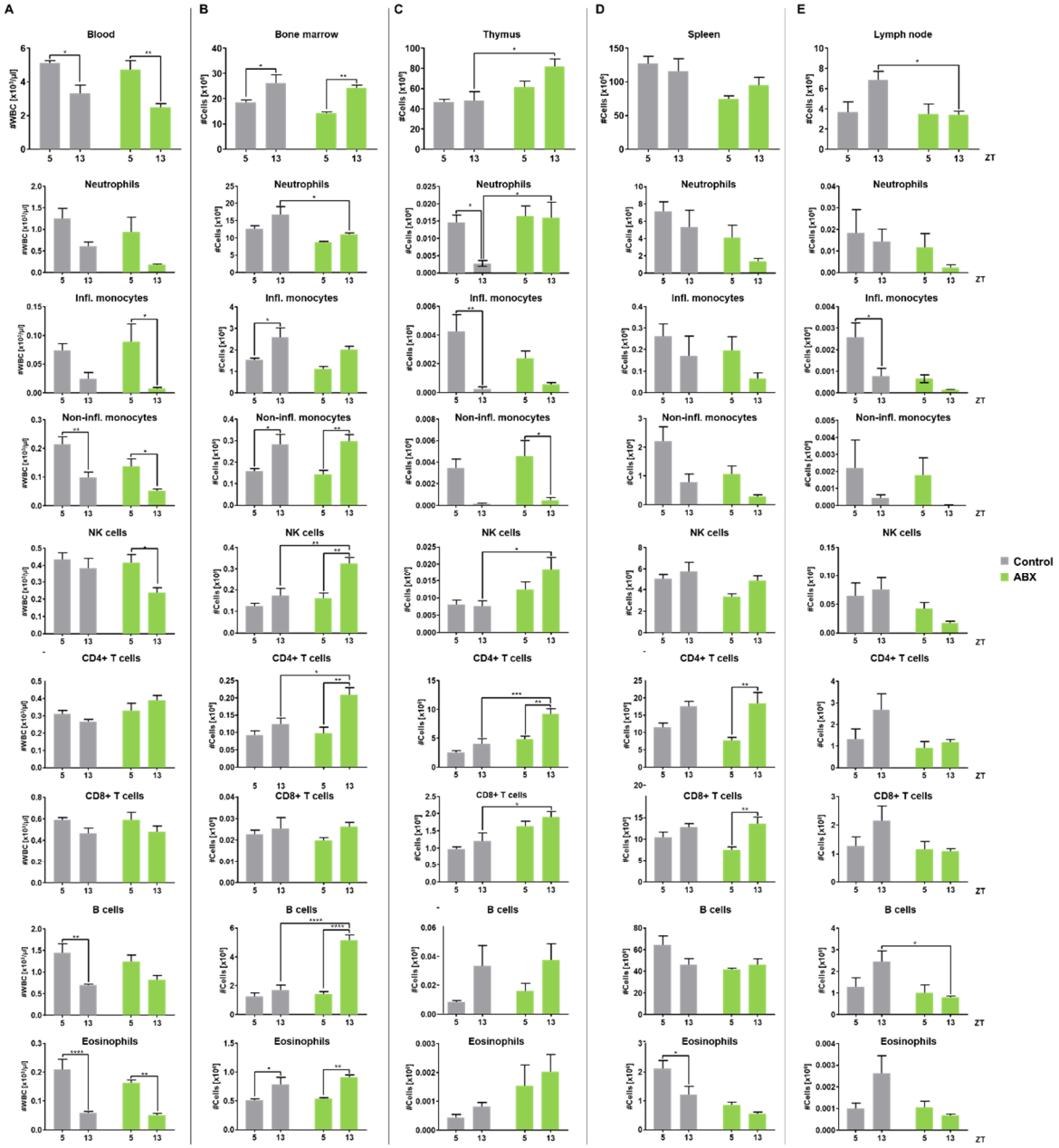

Figure 3-8: Antibiotics-induced microbial depletion does not alter leukocyte numbers in immunological organs. Mice received an antibiotics cocktail to deplete gut microbiota for two weeks. (A-E) Blood (A), bone marrow (B), thymus (C), spleen (D) and inguinal lymph node (E) were harvested after two weeks of antibiotics depletion (ABX) at ZT5 and ZT13. Leukocyte counts were measured and leukocyte subsets were analysed using flow cytometry. (n=5, two-way ANOVA) *p<0.05, **p<0.01, ***p<0.001.

3.7. Germ-free mice show reduced blood leukocyte numbers at peak times

Antibiotic depletion of commensal bacteria did not change circadian leukocyte numbers in the circulation. However, such a depletion is never 100% effective in the depletion of microbiota. We therefore decided to harvest blood as well as primary and secondary lymphoid organs from germ-free mice at peak and trough time points to more thoroughly assess the potential influence of bacteria. This work was done in collaboration with Prof. Dr. Christoph Reinhardt at the Center for Thrombosis and Hemostasis in Mainz, Germany. Indeed, in this setting we detected a significant reduction of leukocyte numbers in germ-free animals at ZT5 compared to specific pathogen free control mice. This decrease was also represented in almost every investigated leukocyte subset, except CD4+ cells, and the effect was stronger in myeloid cells, especially in IM, than in lymphocytes (**Figure 3-9A**). As we analysed cell counts in bone marrow, we could not find any differences between control and germ-free animals, neither for overall cell counts, nor for any investigated subset (**Figure 3-9B**). However, there was a trend for reduced neutrophils and IM counts. This phenotype was similar for the thymus. Again, we could not detect any changes in cell counts and leukocyte subsets between control and germ-free animals (**Figure 3-9C**). Splenic cell counts, on the other side, were significantly increased at ZT13 compared to ZT5 in control animals, which we did not observe in germ-free conditions. This effect was mostly due to higher lymphocyte counts at this time point. However, these cell types did not exhibit any difference in comparison with germ-free animals, while myeloid cells, in their small abundancies, expressed significantly less counts in microbiota-free animals at both investigated time points for neutrophils and IMs and at ZT13 for NIMs (**Figure 3-9D**). In inguinal lymph nodes, we could not detect any changes in overall cell numbers between control and germ-free animals. However, there were significantly less CD4+ T cells at ZT5 after the loss of commensal bacteria. Neutrophils and IM exhibited a trend towards reduced numbers in the germ-free group while the other subsets did not show any alterations (**Figure 3-9E**).

Taken together, germ-free animals exhibited significantly lower leukocyte numbers in blood at ZT5, especially in innate immune cells. These cell types were also

reduced in spleen, while leukocyte numbers in other investigated organs were not affected by the lack of commensal bacteria.

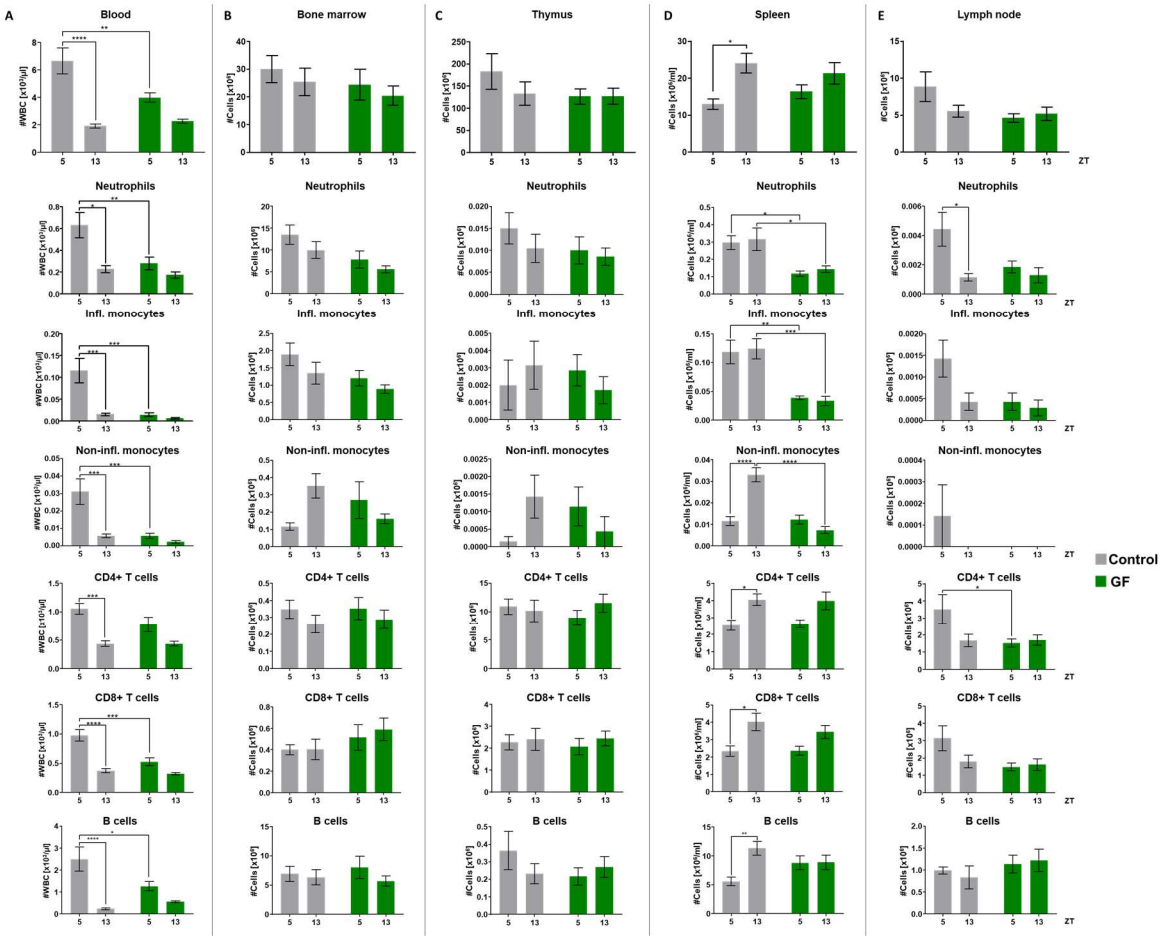

Figure 3-9: Germ-free animals display decreased leukocyte numbers in blood at ZT5. (A-E) Blood (A), bone marrow (B), thymus (C), spleen (D) and inguinal lymph node (E) were harvested from SPF-held control animals (grey) and germ-free (GF) mice (dark green). Leukocyte counts were measured and leukocyte subsets were analysed using flow cytometry. (n=7, two-way ANOVA) *p<0.05, **p<0.01, ***p<0.001, ****p<0.0001.

3.8. Leukocytes harvested from germ-free mice show altered expression of migratory factors

We next focused on the expression of adhesion molecules in isolated leukocyte subsets harvested from the two conditions. We isolated B cells, CD4+ and CD8+ T cells from spleen and neutrophils from the bone marrow from control and germ-free animals and investigated the expression levels of different migratory molecules involved in the leukocyte adhesion cascade.

Investigating the mRNA expression levels of *Selplg* (encoding for PSGL-1) (**Figure 3-10A**), *Itga4* (encoding for CD49d) (**Figure 3-10B**) and *Itgal* (encoding for CD11a)

(**Figure 3-10C**) in isolated CD4+, CD8+ T cells, B cells and neutrophils did not show any alterations between ZT5 and ZT13, neither in control, nor in germ-free animals. Also, no differences between these two animal groups were observed. *Itgam* (encoding for CD11b) revealed higher expression levels at ZT5 compared to ZT13 in specific pathogen free mice in T and B cells. Moreover, this effect was abolished in CD4+ and CD8+ T lymphocytes from germ-free mice with significantly lower mRNA levels at ZT5 (**Figure 3-10D**). For *Icam1*, we detected a significant expression increase in B cells of control animals at ZT13 compared to ZT5. Moreover, germ-free mice showed reduced expression levels for this marker at ZT13 in B and CD4+ T lymphocytes. CD8+ T cells exhibited diminished *Icam1* mRNA levels upon lack of microbiota at ZT5 while neutrophils from these animals displayed the opposite with augmented expression levels at this time point (**Figure 3-10E**). For *Sell* (encoding for L-selectin), neutrophils and CD4+ T cells showed enhanced mRNA expression in germ-free mice at both time points and the expression in CD4+ T lymphocytes exhibited a slight daily effect with higher expression at ZT13 compared to ZT5 in mice without commensal bacteria (**Figure 3-10F**). Additional to these molecules, we also tested for expression of *Cxcr2*, a main mobilization factor for leukocytes, and *Cxcr4* known as a recruitment/retention factor (Addison et al., 2000; Cheng and Qin, 2012). We detected a strong daily effect in T lymphocytes of control mice with high *Cxcr2* expression levels at ZT5 and low ones at ZT13. Interestingly, this effect disappeared in germ-free mice, which exhibited clearly reduced *Cxcr2* at ZT5 and also at ZT13 for CD8+ T cells (**Figure 3-10G**). On the other side, *Cxcr4* exhibited the opposite effect with high mRNA levels at ZT13 in lymphocytes of control animals. Likewise, this difference was abolished in lymphocytes from germ-free mice and expression at ZT5 was significantly increased compared to SPF animals (**Figure 3-10H**).

Taken together, our data show overall a higher expression of pro-migratory factors and retention factors at ZT5 and ZT13, respectively, while germ-free animals lost this rhythm or displayed altered mRNA levels for some of the investigated factors. We therefore next assessed whether circadian clock gene expression was altered in isolated immune cells of these animals. For this purpose, we tested for *Bmal1*, *Clock*, *Per2*, *Cry1* and *Nr1d1* expression levels as key clock genes and also for clock-controlled gene *Dbp*. We found clear daily differences in the expression of *Dbp* (**Figure 3-10I**) and *Nr1d1* (**Figure 3-10J**) in CD4+ T cells and B cells with an

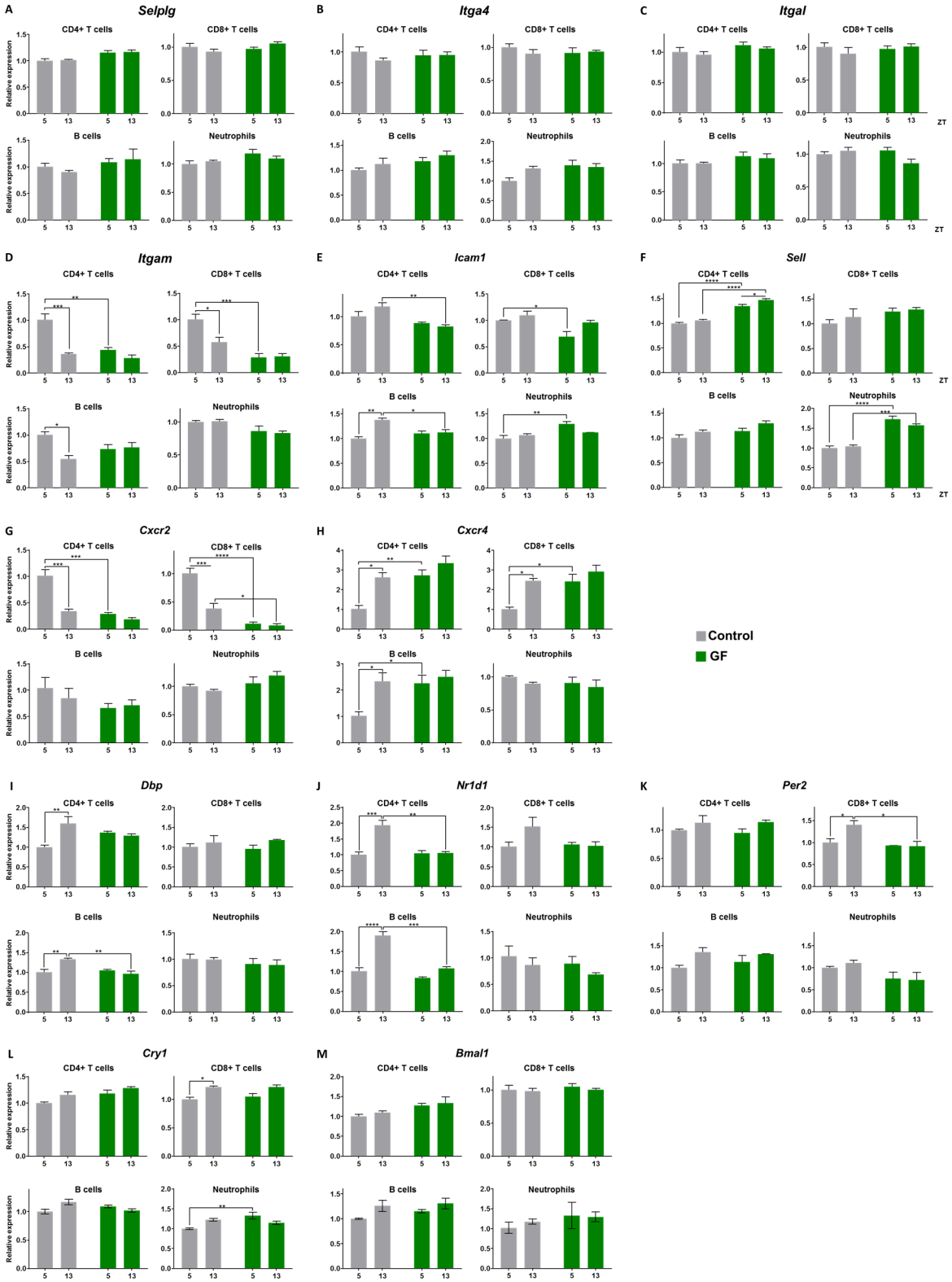

Figure 3-10: Germ-free animals display some altered migratory factors. Lymphocytes and neutrophils were isolated from spleen and bone marrow, respectively, of control and germ-free (GF) animals. RNA was extracted at ZT5 and ZT13 and qPCR analysis was performed for detecting mRNA levels of *Selplg* (A), *Itga4* (B), *Itgal* (C), *Itgam* (D), *Icam1* (E), *Sell* (F), *Cxcr2* (G), *Cxcr4* (H), *Dbp* (I), *Nr1d1* (J), *Per2* (K), *Cry1* (L) and *Bmal1* (M). (n=3, two-way ANOVA). *p<0.05, **p<0.01, ***p<0.001.

increase at ZT13. This difference was lost in the same subsets of germ-free mice

and levels were significantly reduced at the late time point. *Per2* and *Cry1* also displayed higher expression at ZT13 in CD8+ T cells and again, this change was lost in germ-free mice. For *Per2*, there was a significant reduction in CD8+ cells of germ-free mice at ZT13 (**Figure 3-10K**) while *Cry1* was increased in neutrophils of these animals at ZT5 (**Figure 3-10L**). *Bmal1* expression did not show any significant alterations (**Figure 3-10M**).

To conclude, ablation of commensal bacteria altered expression levels in several migratory factors, especially in *Cxcr2* and *Cxcr4* expression of lymphocytes, while clock gene expression remained mostly unchanged.

3.9. Lineage-specific clock disruption does not alter leukocyte counts in blood

We found altered leukocyte numbers in the circulation of microbiota-depleted mice and mice with restricted food access to their resting phase. It had previously been shown that mice lacking circadian clock genes exhibit altered oscillations in their microbiota rhythms due to loss of rhythm in their food uptake (Thaiss et al., 2014b). Also, *Bmal1* global knockout mice present increased leukocyte counts in blood at ZT13 compared to control animals (Scheiermann et al., 2012). We therefore investigated the role of the core clock gene *Bmal1* in local tissues and cells on WBC numbers in the circulation.

Due to our data from the germ-free experiments, we first analysed a *Vil1cre* x *Bmal1*$^{fl/fl}$ mouse model, in which the key clock gene is depleted in intestinal epithelial cells since this is the first contact site between commensal bacteria and the host organism (IEC-*Bmal1*$^{-/-}$). Blood harvest at peak and trough times of leukocyte oscillation did not reveal any differences between control and *Vil1cre* x *Bmal1*$^{fl/fl}$ animals at any time point. Although the differences between ZT5 and ZT13 were not significant, there was a clear tendency towards higher counts at ZT5 in both experimental groups (**Figure 3-11A**). Counts in bone marrow did also not show dissimilarities due to lack of *Bmal1* in IECs (**Figure 3-11B**). In spleen, we detected significant higher cell numbers at ZT5 compared to ZT13 in both *Bmal1*-negative and -positive animals. These observations were mainly due to lymphocyte counts, but also myeloid cells expressed the same tendency. However, there was no change in cell counts between control and *Vil1cre* x *Bmal1*$^{fl/fl}$ mice. In general, all

observed tendencies were not only true for overall cell counts, but also for the different leukocyte subsets (**Figure 3-11C**).

Thus, *Bmal1*-specific ablation in intestinal epithelial cells did not alter leukocyte counts in either blood, bone marrow or spleen.

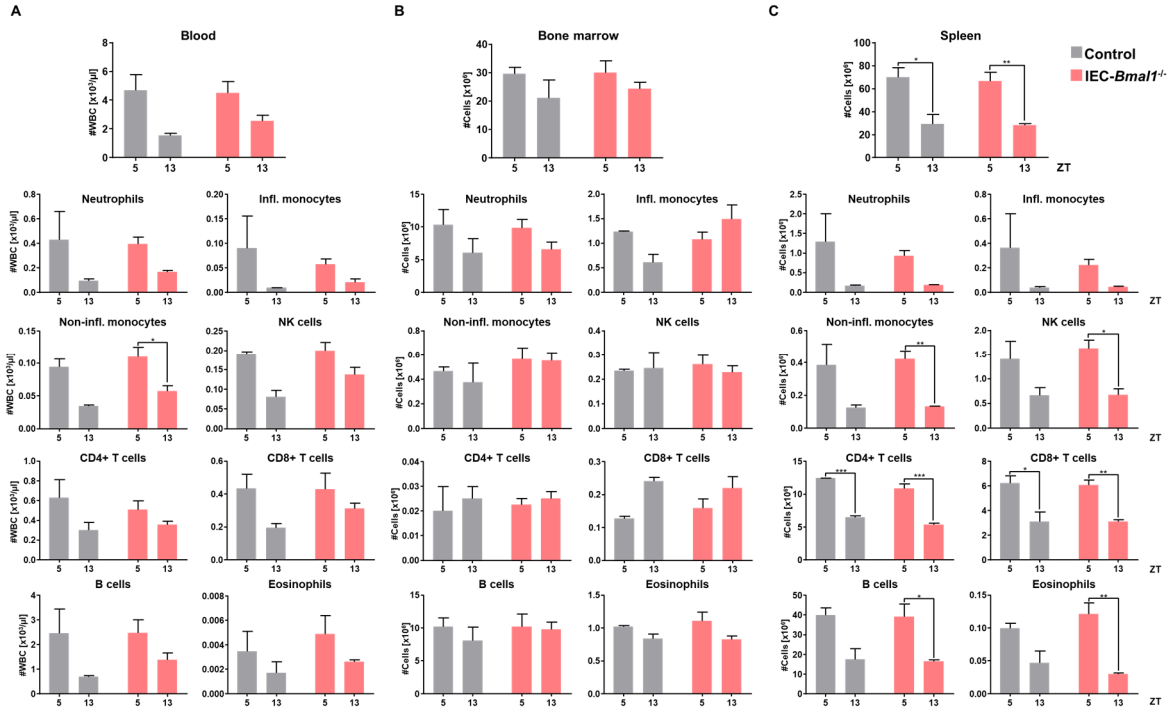

Figure 3-11: IEC-*Bmal1*$^{-/-}$ animals do not have altered leukocyte numbers in blood, bone marrow or spleen. Blood (A), bone marrow (B) and spleen (C) were harvested from *Vil1cre* x *Bmal1*$^{fl/fl}$ (IEC-*Bmal1*$^{-/-}$) and respective control animals at ZT5 and ZT13. Leukocyte counts were measured and leukocyte subsets were analysed using flow cytometry. (n=2-4, two-way ANOVA) *p<0.05, **p<0.01.

Secondly, we used an inducible *Cdh5cre/ERT2* x *Bmal1*$^{fl/fl}$ mouse line to investigate circadian leukocyte numbers at different time points. These animals lack the core clock gene in endothelial cells that are also involved in leukocyte recruitment (EC-*Bmal1*$^{-/-}$). In blood, we detected significant differences between ZT7 and ZT13 in control but not in Cre-positive animals. However, a similar tendency could be observed and there was no significant difference between any tested time point concerning the two mouse lines. Also, different leukocyte subsets in blood did not show dissimilarities comparing *Bmal1*-negative with -positive mice (**Figure 3-12A**). Bone marrow and spleen were only investigated for two time points, close to peak and trough times of WBC counts in the circulation. We were not able to detect any differences between control and knockout animals at these two time points, neither in bone marrow (**Figure 3-12B**), nor in spleen (**Figure 3-12C**). Again, this was not only shown for general cell counts, but also for the investigated subsets. The

abundancy differences in bone marrow were significantly higher at ZT13 compared to ZT7, especially due to higher counts in neutrophils (**Figure 3-12B**). In spleen, there was no significant alteration detectable in either mouse groups (**Figure 3-12C**).

Taken together, *Bmal1* depletion in neither intestinal epithelial cells, nor endothelial cells was sufficient to alter leukocyte counts in blood, bone marrow or spleen.

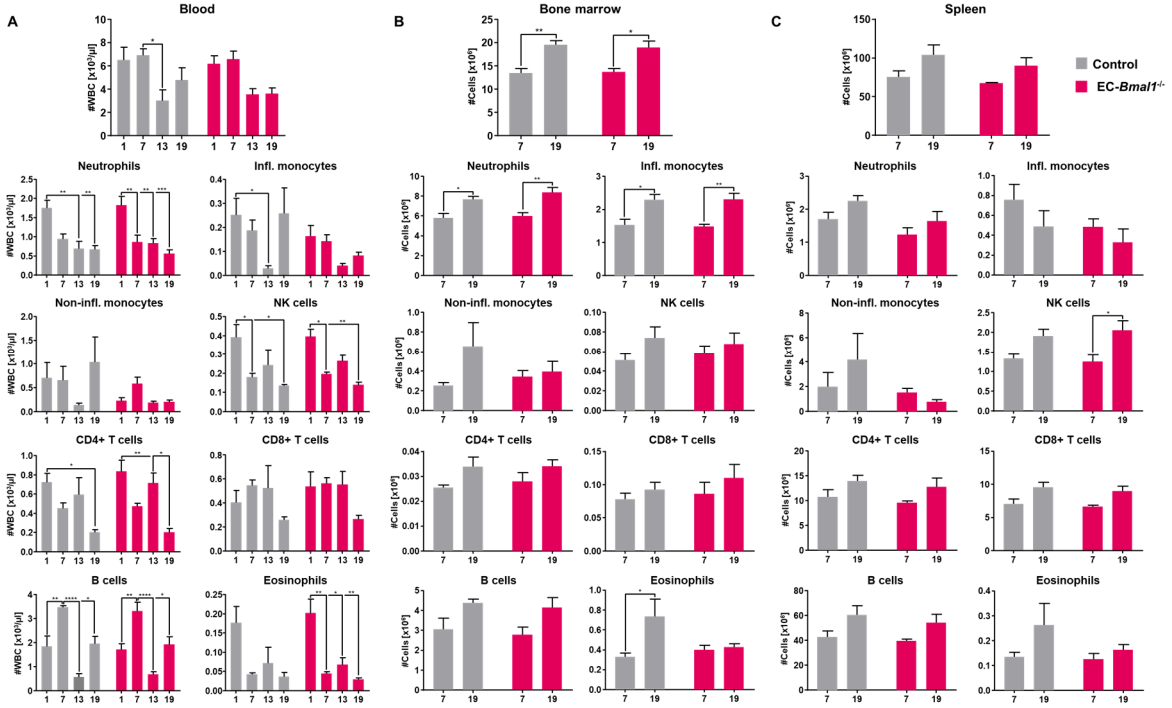

Figure 3-12: EC-*Bmal1*$^{-/-}$ animals do not have altered leukocyte numbers in blood, bone marrow or spleen. (A) Blood was harvested from *Cdh5cre/ERT2* x *Bmal1*$^{fl/fl}$ (EC-*Bmal1*$^{-/-}$) and respective control animals at ZT1, 7, 13 and 19. (B, C) Bone marrow (B) and spleen (C) were harvested from *Cdh5cre/ERT2* x *Bmal1*$^{fl/fl}$ (EC-*Bmal1*$^{-/-}$) and respective control animals at ZT7 and ZT19. (A-C) Leukocyte counts were measured and leukocyte subsets were analysed using flow cytometry. (n=4-8, two-way ANOVA) *p<0.05, **p<0.01, ***p<0.001, ****p<0.0001.

3.10. Transfer of serum harvested in the morning increases neutrophil counts

Due to our observations so far, we hypothesized that factors, potentially microbe-derived, might leak through the intestinal epithelium to influence leukocyte oscillations in blood. This hypothesis is supported by published findings that the permeability of tight junction proteins in the intestine undergoes circadian variations inducing increased leakage during the day and increased expression of occludin and claudin during the night (Kyoko et al., 2014). Since there are many potential

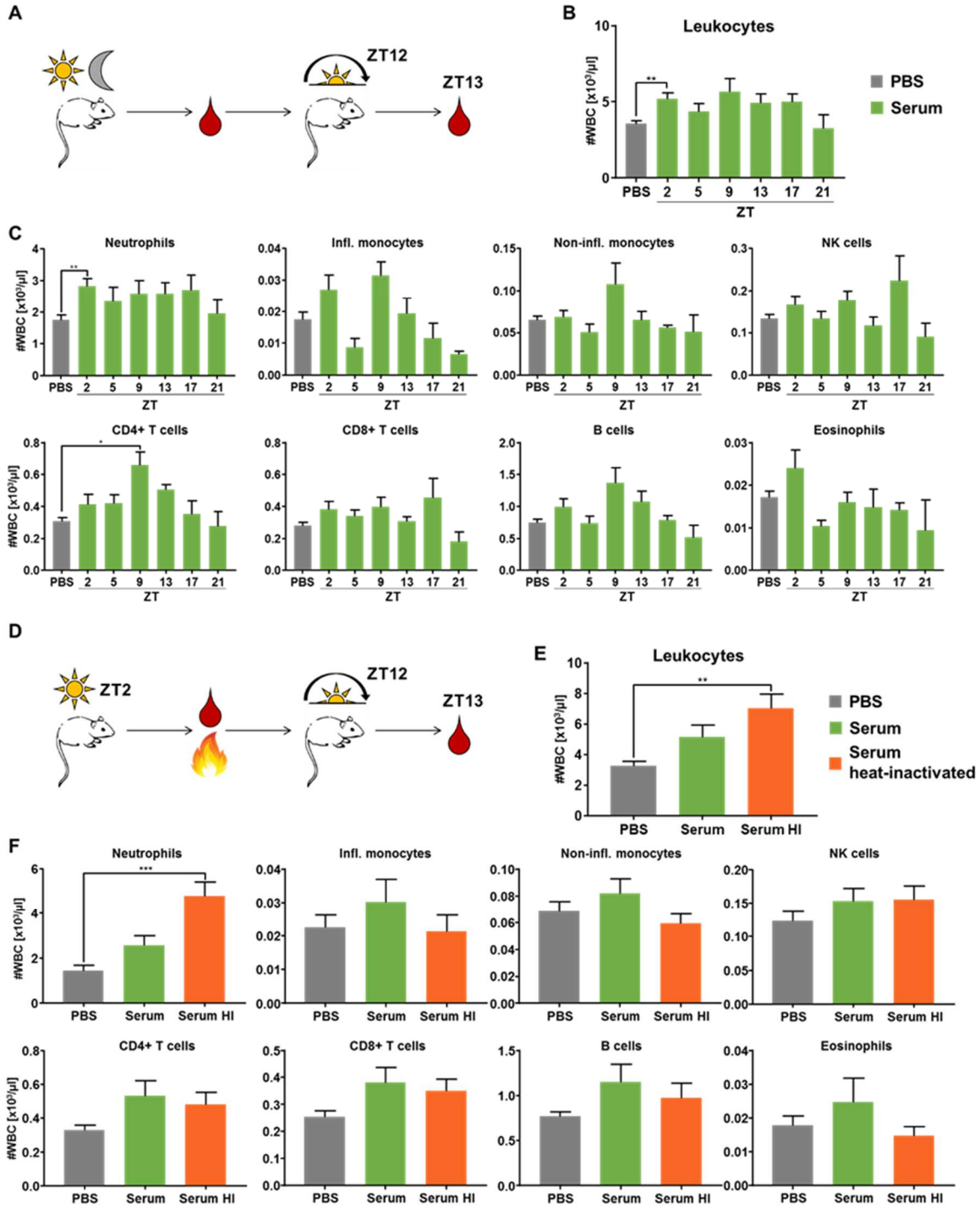

Figure 3-13: Morning serum increases neutrophil numbers, further intensified by transfer of heat-inactivated serum. (A) Blood from donor mice was harvested at ZT2, 5, 9, 13, 17 and 21. Serum was isolated and 200 µl of serum or PBS for control were injected i.p. into recipient mice at ZT12. At ZT13, blood from recipient mice was harvested and analysed. (B) Leukocyte counts were measured and leukocyte subsets (C) were analysed using flow cytometry. (D) Blood was harvested from donor mice at ZT2. Serum was isolated, heat-inactivated and 200 µl of serum or PBS for control were injected into recipient mice at ZT12. At ZT13, blood from recipient mice was harvested and analysed. (E) Leukocyte counts were measured and leukocyte subsets (F) were analysed using flow cytometry. (B, C: n=3-24. E, F: n=6, one-way ANOVA) *p<0.05, **p<0.01, ***p<0.001.

products that could induce this effect, we decided to use a serum transfer model. In

this setup, serum was harvested at different times of the day from donor mice and injected into recipient mice one hour prior to blood harvest at ZT13 (**Figure 3-13A**). Trough time of leukocyte counts was chosen to facilitate the detection of a potential increase in cellularity.

Serum injection led to a slight but significant increase of WBC counts in blood, especially with morning serum or serum harvested during the light phase compared to mice injected with PBS only. After injection of serum from mice at ZT2, leukocyte expansion was significant and this was mostly due to higher neutrophil numbers (**Figure 3-13B, C**). Serum harvested at ZT9 increased counts of CD4+ T cells (**Figure 3-13C**). Hence, we aimed to narrow the broad variability of potential factors by heat-treatment of morning serum, since we observed the biggest effect upon injection of serum from this time point. Using this setup, proteins are heat-inactivated which allows to exclude these as possible influencers (**Figure 3-13D**). Interestingly, we found even higher leukocyte counts in blood after heat inactivation of serum injection harvested at ZT2 (**Figure 3-13E**). Analysing leukocyte subsets, it was neutrophils numbers that were significantly increased after this treatment while other cell types were not affected (**Figure 3-13F**).

Thus, the transfer of serum harvested in the morning increased leukocyte numbers and specifically neutrophil counts. Heat-inactivation of morning serum further increased this effect.

3.11. LPS injection or oral gavage does not alter leukocyte counts

LPS is a strongly negatively charged small molecule. In small amounts in blood, it is mostly bound to positively charges proteins, such as albumin and hence not freely detectable. Heat inactivation of proteins could therefore lead to increased amounts of free LPS (Balmer et al., 2014) and explain the increased effect of expanded neutrophil numbers in the circulation after this treatment. We tried to measure LPS in blood plasma at different times of the day under steady-state conditions, however, the detection limit was not low enough to detect the potentially very low dose amounts of this bacterial product in steady state. We therefore next injected low doses of LPS into mice four hours prior to peak and trough times of WBC counts at ZT5 and ZT13 to mimic a hypothesized daily ‘steady-state inflammation’ (**Figure 3-14A**).

Interestingly, we found a slight reduction of WBC counts in blood at ZT5 after injection of 20ng LPS, which was also represented in numbers of CD4+ T cells. No difference was observed at ZT13 (**Figure 3-14B, C**).

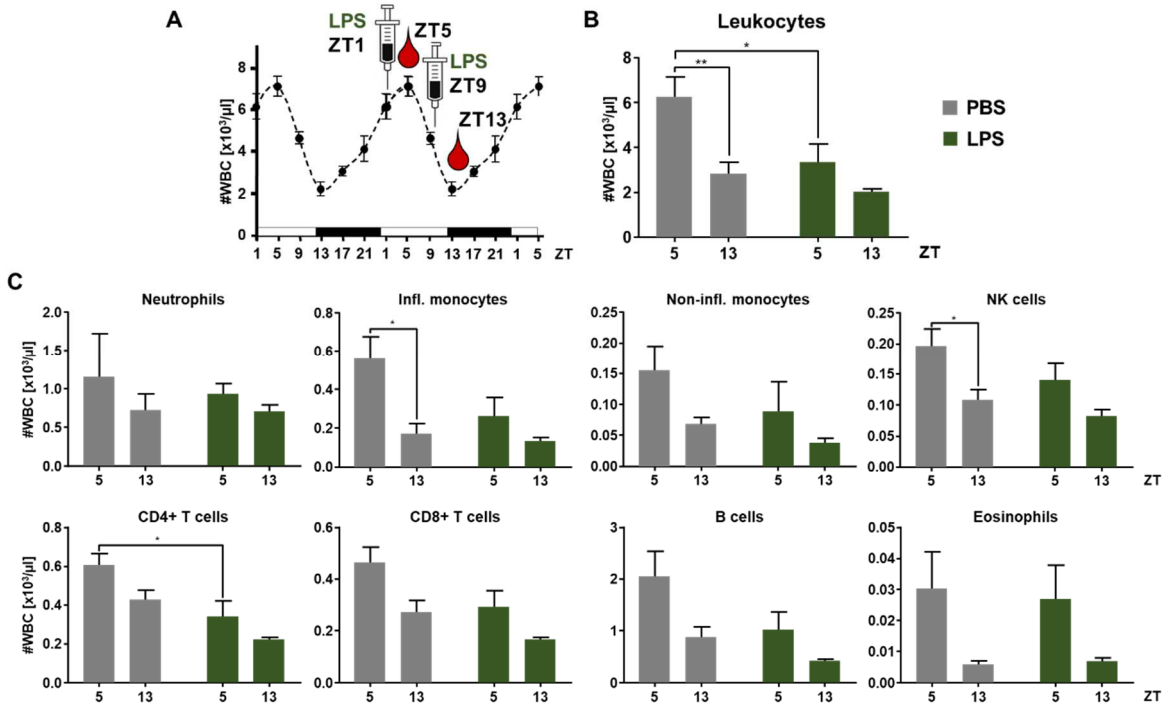

Figure 3-14: Low-dose LPS injections alter leukocyte counts in blood. (A) 20 ng of LPS or 200 µl PBS as control were injected i.p. into mice four hours prior to blood harvest at ZT5 and ZT13, respectively. (B) Leukocyte counts were measured and leukocyte subsets (C) were analysed using flow cytometry. (n=6, two-way ANOVA) *p<0.05, **p<0.01.

Since an intraperitoneal injection does not represent a potential physiological signalling way, we hence administered either high or medium LPS doses per gavage to mimic a potentially more natural uptake of this microbial product. The time points ZT5 and ZT17 were chosen since it was shown that the permeability in the intestinal epithelium was highest and lowest at these times, respectively. Gavage was thus performed 26h prior to these time points at ZT3 and ZT15 to assure sufficient leakage of LPS into host organism (**Figure 3-15A**). Upon feeding 1 mg of LPS, representing the LPS amount of a full microbiome (Zhang et al., 2015), we could not detect any changes in blood leukocyte counts or numbers of leukocyte subsets in comparison to the control group, which was gavaged with PBS (**Figure 3-15B, C**). Also, administering lower LPS levels, did not alter leukocyte counts in blood, bone marrow or spleen. Solely eosinophils were slightly elevated at ZT5 after LPS gavage compared to the control group (**Figure 3-15D-F**).

Taken together, low-dose LPS injections had minor effects on leukocyte numbers in blood at ZT5 while oral administration of high LPS doses did not alter leukocyte counts in blood, bone marrow or spleen.

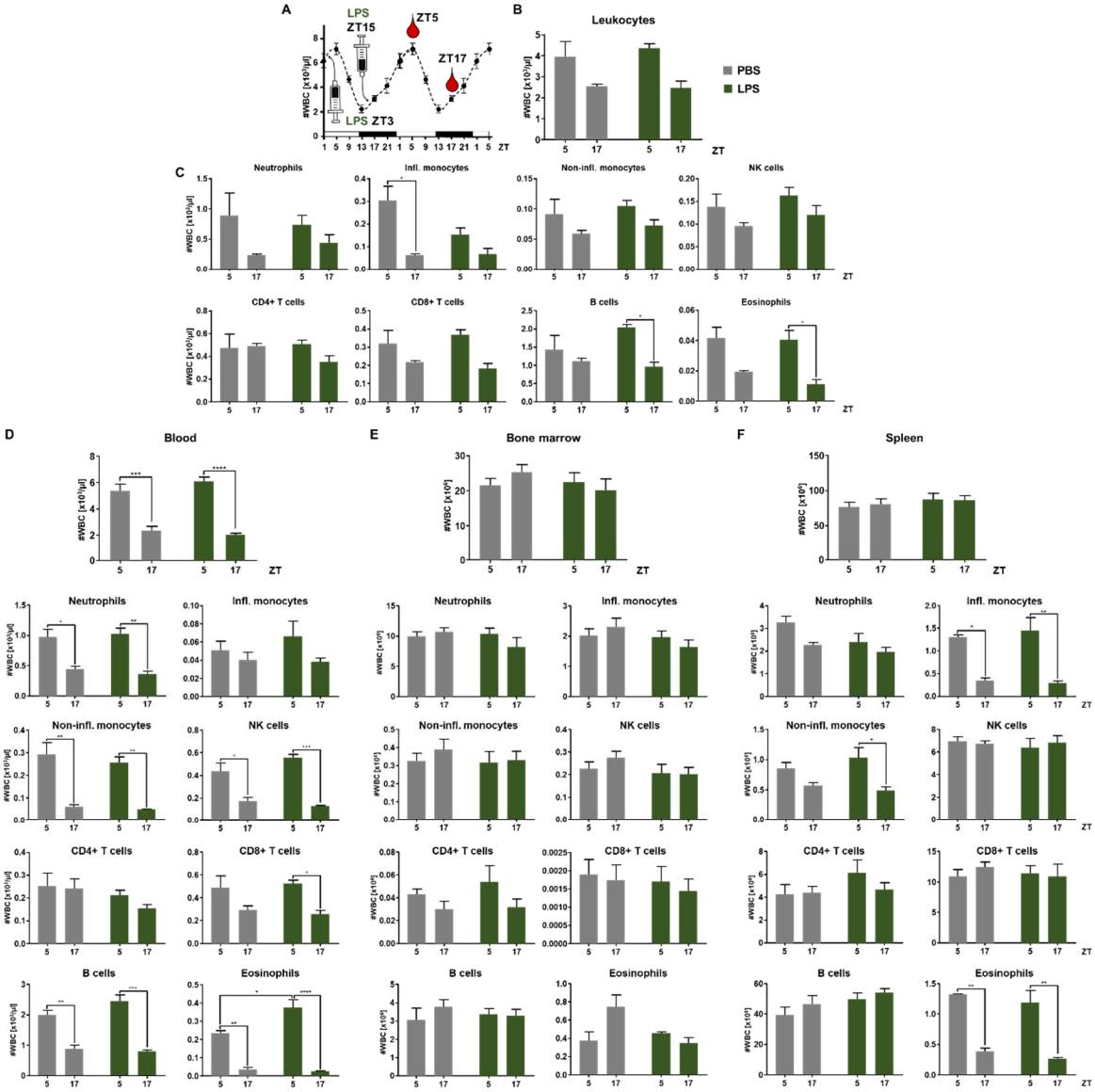

Figure 3-15: Oral LPS administration does not alter leukocyte counts in blood, bone marrow or spleen. (A) 1 mg (B, C) or 300 µg (D-F) of LPS and PBS as control were gavaged into animals at ZT3 and ZT15, 26 h prior to blood and organ harvest at ZT5 and ZT17, respectively. (B, C) Mice were fed with 1mg of LPS or PBS, blood was harvested, leukocyte counts (B) were measured and leukocyte subsets (C) were analysed using flow cytometry. (D-F) Mice were fed with 300 µg of LPS or PBS, blood (D), bone marrow (E) and spleen (F) were harvested, leukcoyte counts were measured and leukocyte subsets were analysed using flow cytometry. (n=3, two-way ANOVA) *p<0.05, **p<0.01, ***p<0.001.

3.12. Pharmacological blocking of TLR4 and TLR-signalling pathway does not alter leukocyte counts

Low-dose LPS administration slightly decreased leukocyte counts in the circulation at ZT5. Since it is possible that we did not titrate the right concentration or appropriate time point for injection and harvest, we performed blocking experiments. Specifically, we targeted downstream signalling pathways involved in the recognition of microbial products.

First, mice were treated with a blocking antibody targeting the TLR4/MD-2 complex at ZT5 one day before harvest at ZT5 and ZT13 (**Figure 3-16A**). TLR4 recognizes LPS and is probably the toll-like receptor that has been studied the most (Lu et al., 2008). Injection of a neutralizing antibody did not alter WBC count in blood at ZT5, nor at ZT13 (**Figure 3-16B**). Also, numbers in leukocyte subsets were not changed after treatment with anti-TLR4/MD2 antibody compared to isotype injected animals (**Figure 3-16C**).

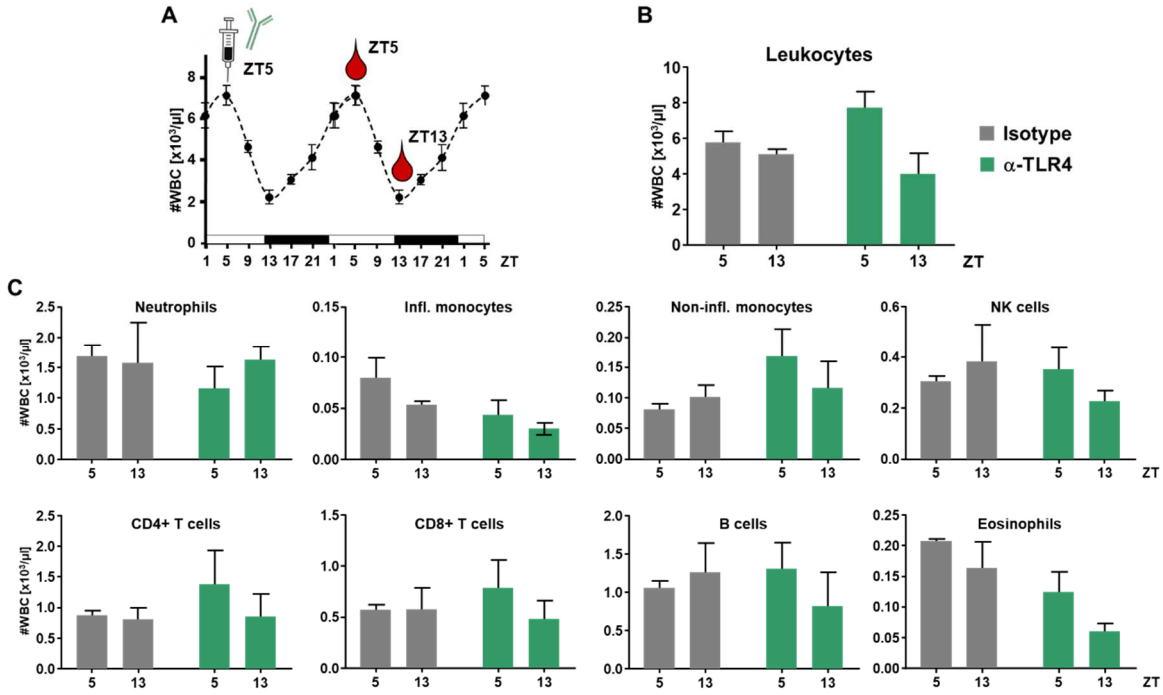

Figure 3-16: Blocking of TLR4 does not alter leukocyte numbers in the circulation. (A) 30 µg of either anti-TLR4/MD2 blocking antibody or respective isotype were injected into animals at ZT5 24 h prior to blood harvest at ZT5 and ZT13. (B) Leukocyte counts were measured and leukocyte subsets (C) were analysed using flow cytometry. (n=3, two-way ANOVA)

Apart from LPS, there are many other microbial products, which are also possible candidates for influencing circadian leukocyte oscillation in blood. We therefore blocked molecules in the pattern recognition pathway. MyD88 and TRIF are

associated with almost every TLR and blocking was shown to immensely impede innate immune response and pathogen recognition (Piras and Selvarajoo, 2014; Yamamoto et al., 2003). We initially injected blocking peptides against these two molecules at ZT5 one day prior to harvest at ZT5 and ZT13 (**Figure 3-17A**). Analysing WBC counts in blood, however, we could not find any differences between overall leukocyte (**Figure 3-17B**) or subset counts (**Figure 3-17C**) in any of both time points.

Thus, neither blocking of TLR4 nor pharmacological inhibition of MyD88 and TRIF altered leukocyte numbers in the circulation.

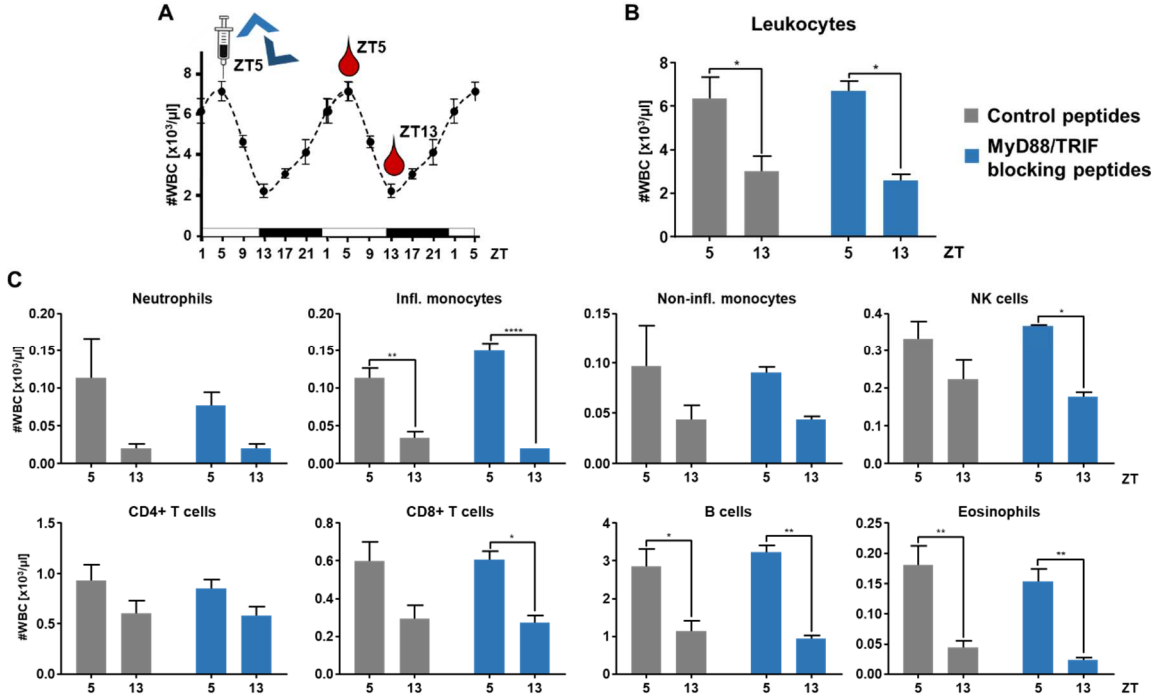

Figure 3-17: Blocking of MyD88 and TRIF does not alter leukocyte numbers in the circulation. (A) 200 µg of either control or MyD88 and TRIF blocking peptides were injected into animals at ZT5 24 h prior to blood harvest at ZT5 and ZT13. (B) Leukocyte counts were measured and leukocyte subsets (C) were analysed using flow cytometry. (n=3, two-way ANOVA) *p<0.05, **p<0.01, ***p<0.001.

3.13. Loss of TLR4 or TLR2 in endothelial cells does not alter leukocyte counts

Although our pharmacological blockade did not show inhibition of TLR4 and MyD88/TRIF using the neutralizing antibody and blocking peptides, respectively, we next investigated leukocyte counts in a conditional knockout mouse models where animals lack another important LPS-recognition receptor TLR2 in endothelial cells (EC-*Tlr2*$^{-/-}$). These experiments were performed in collaboration with Prof. Dr.

Christoph Reinhardt at the Center for Thrombosis and Hemostasis in Mainz, Germany. Besides TLR4, LPS can also bind to TLR2 and induce a pro-inflammatory response. We did not observe any significant differences in overall WBC counts between Cre-negative control and Cre-positive knockout animals at ZT5 or ZT13 (**Figure 3-18A**). There was slight tendency towards higher neutrophil numbers in EC-*Tlr2*$^{-/-}$ mice at ZT13 (**Figure 3-18B**). However, due to limited number of animals, we were not able to investigate these observations in a sufficient amount of mice to gain significant results.

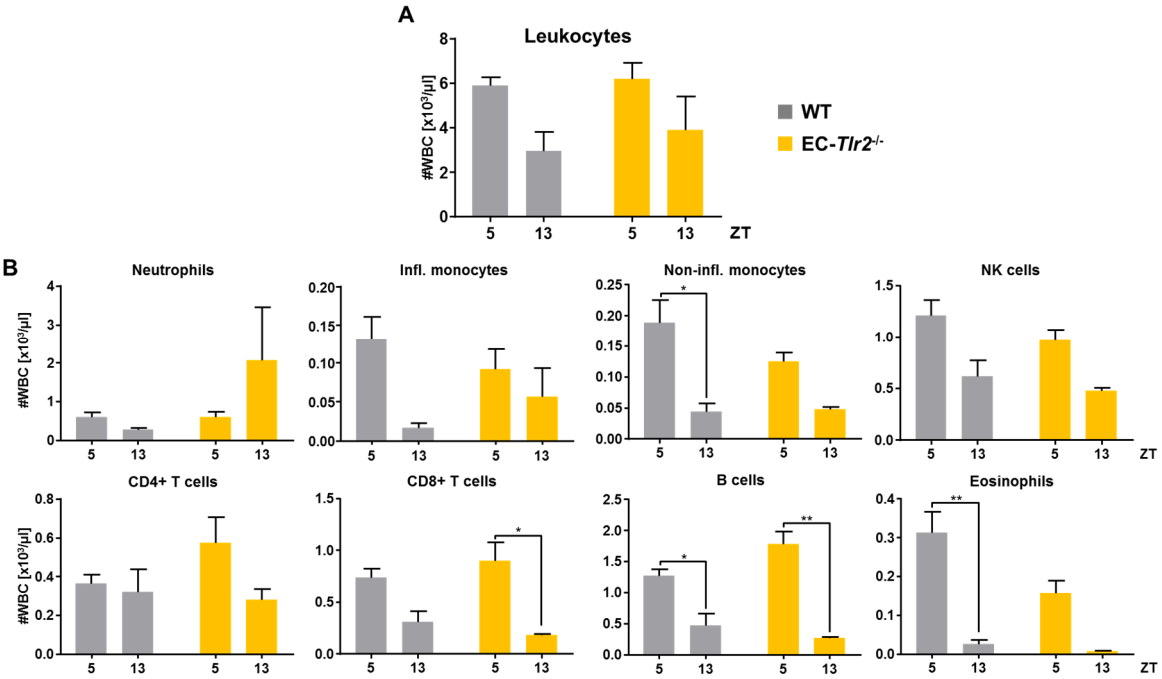

Figure 3-18: EC-*Tlr2*$^{-/-}$ mice do not show significant alterations in blood leukocyte numbers. Blood was harvested from EC-*Tlr2*$^{-/-}$ animals at ZT5 and ZT13. (A) Leukocyte counts were measured and leukocyte subsets (B) were analysed using flow cytometry. (n=1-5, two-way ANOVA) *p<0.05, **p<0.01.

3.14. *Myd88*$^{-/-}$ mice exhibit reduced neutrophil numbers in bone marrow and circulation at ZT5

Since there were no significant alterations upon inhibition of TLR4 and no changes in EC-*Tlr2*$^{-/-}$ animals, we also investigated leukocyte numbers in blood in global *Tlr4*-

KO animals. Additionally, we also tested these counts in global *Myd88*-KO mice to exclude residual activity of these two potentially involved molecules.

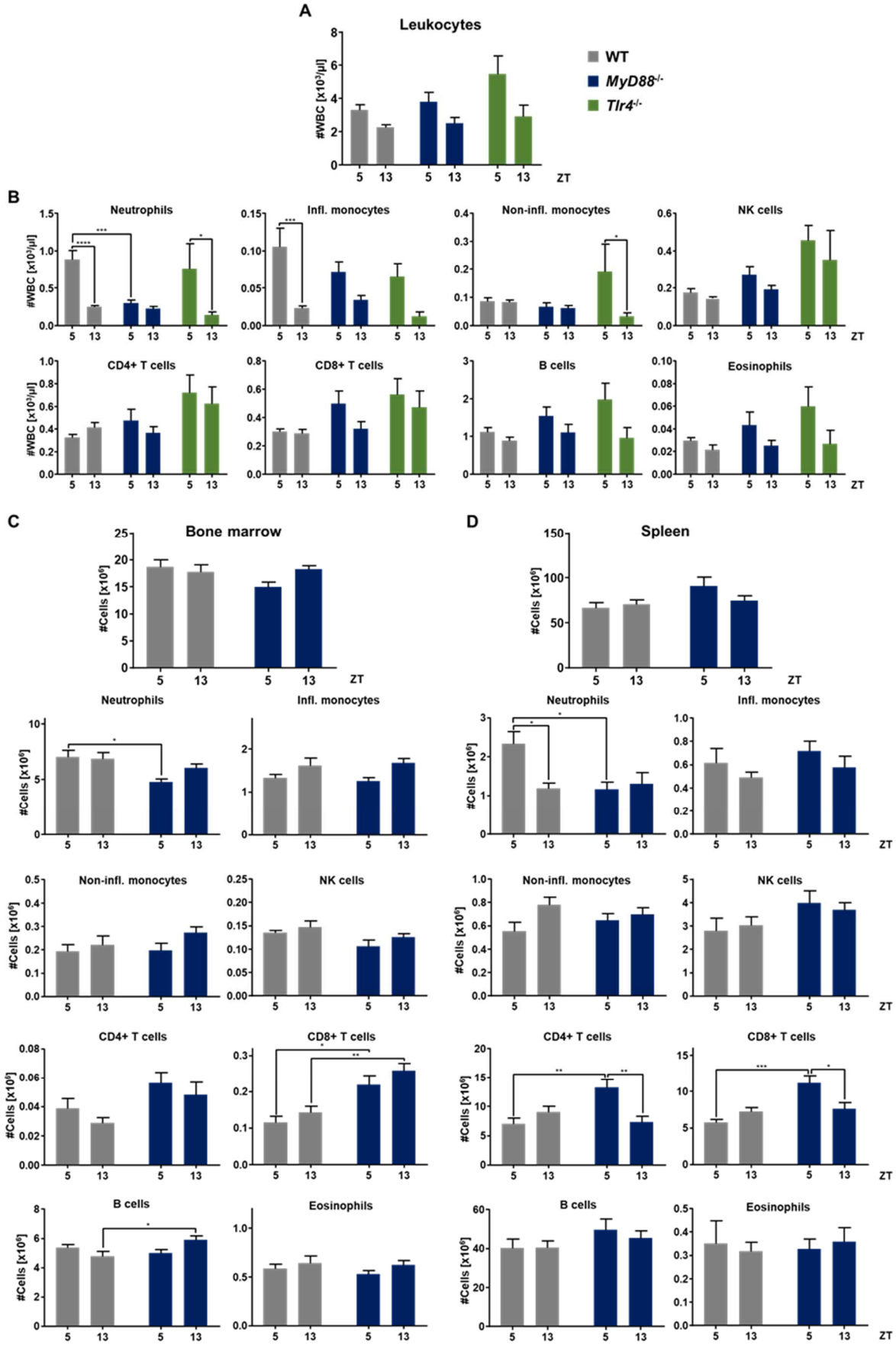

Figure 3-19: *Myd88*$^{-/-}$ animals have reduced neutrophil numbers in blood and bone marrow at ZT5. (A,B) Blood was harvested from WT, *Tlr4*$^{-/-}$ and *Myd88*$^{-/-}$ animals at ZT5 and ZT13. (A) Leukocyte counts were measured and leukocyte subsets (B) were analysed using flow cytometry. (C, D). Bone marrow (C) and spleen (D) were harvested from WT and *Myd88*$^{-/-}$ mice at ZT5 and ZT13. Overall cell counts were measured and leukocyte subsets were analysed using flow cytometry. (n=3-7, two-way ANOVA) *p<0.05, **p<0.01, ***p<0.001, ****p<0.0001.

Overall WBC numbers did not differ between wild-type (WT), *Tlr4*-KO or *Myd88*-KO mice at ZT5 or ZT13 (**Figure 3-19A**). Also, monocytes, lymphocytes and eosinophils showed no significant alterations in their abundance. Neutrophils, however, exhibited significantly less numbers in blood upon lack of MyD88 adaptor molecule at ZT5 compared to WT animals (**Figure 3-19B**). We hence also checked bone marrow and splenic cell numbers in these animals. In bone marrow, there were no changes in global cell numbers between WT and *Myd88*-KO mice. CD8+ T cells showed slightly elevated counts at both time points upon the absence of *MyD88*, while B cells were increased at ZT13 only. On the other side, neutrophils showed a significant decrease in their abundancy at ZT5, in agreement with previous results (**Figure 3-19C**) (Balmer et al., 2014). In spleen, we could detect a similar phenotype. Overall cell counts were not affected in *Myd88* KO mice but CD8+ and also CD4+ T cells were elevated at ZT13 in these animals, while neutrophils again displayed reduced cell numbers. T cells hence exhibited a significantly higher count at ZT5 compared to ZT13 in KO animals while this rhythm was present in neutrophil numbers of WT animals and lost upon *Myd88* depletion (**Figure 3-19D**).
Thus, depletion of *Myd88*, but not of *Tlr4*, diminished neutrophil counts in blood, spleen and bone marrow at ZT5 while other cell types were not affected.

3.15. Blocking of TNFα reduces inflammatory monocytes in blood at ZT5

Activation of pattern recognition receptors and their adaptor molecule MyD88 leads to the expression of pro-inflammatory molecules. Depletion of the major adaptor molecule MyD88 partially phenocopied our results from germ-free animals in neutrophils. To further confirm a potential impact on this signaling pathway, we blocked pro-inflammatory cytokines as downstream modulators and assessed the influence of this inhibition on leukocyte counts in blood at ZT5 and ZT13.

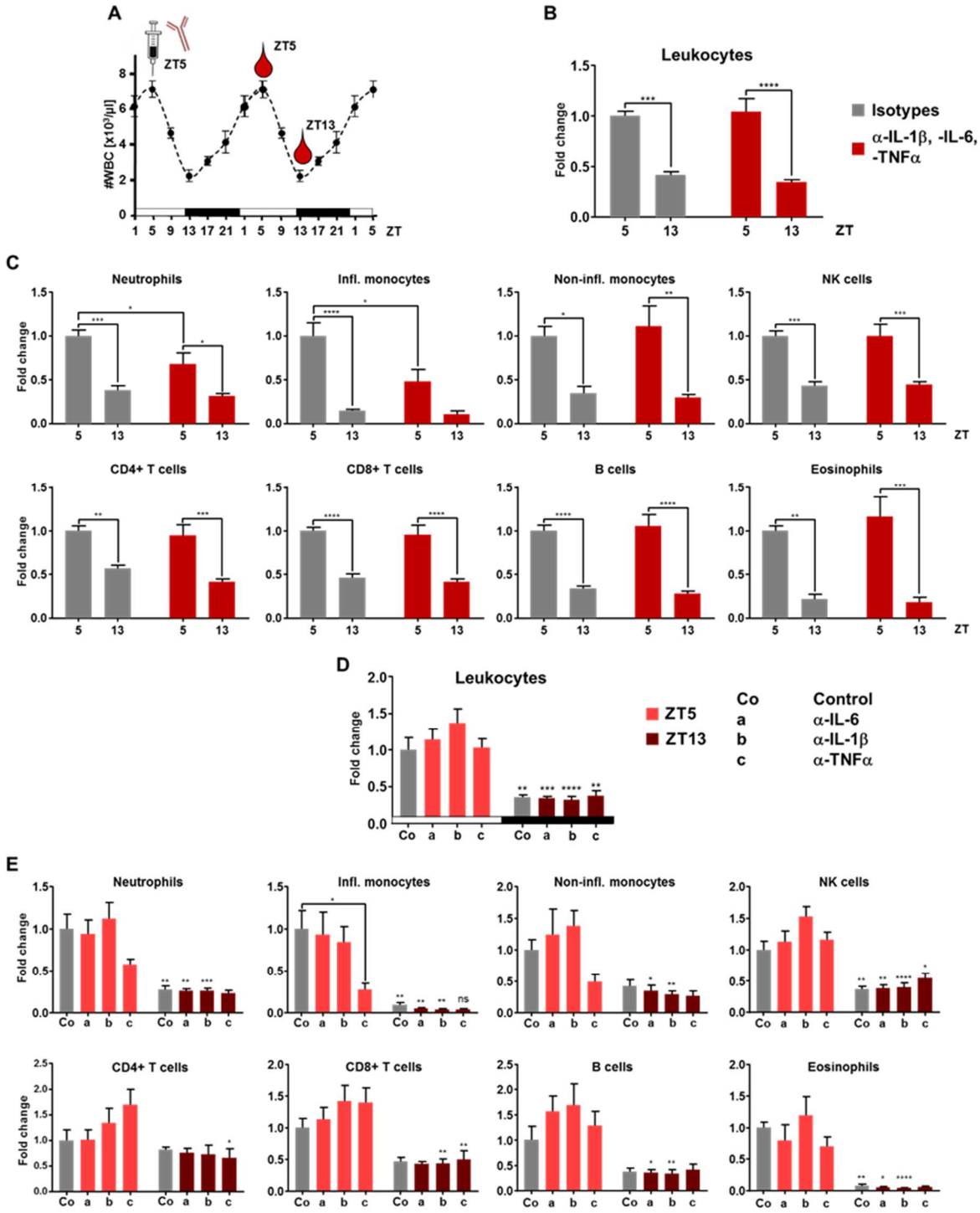

Figure 3-20: Blocking of TNFα reduces neutrophil numbers in blood at ZT5. (A) Blocking antibodies against IL-1β, IL-6 and TNFα were injected at ZT5 24 h prior to blood harvest at ZT5 and ZT13. (B, C) A cocktail of blocking antibodies or a cocktail of respective isotypes was injected, blood was harvested, leukocyte numbers (B) were measured and leukocyte subsets (C) were analysed using flow cytometry. (D, E) Blocking antibodies against either IL-1β (a), IL-6 (b) or TNFα (c) as well as a cocktail of respective isotypes (Co) was injected, blood was harvested, leukocyte counts (D) were measured and leukocyte subsets (E) were analysed using flow cytometry. (B, C: n=6, two-way ANOVA; D, E: n=6, one-way ANOVA) *p<0.05, **p<0.01, ***p<0.001, ****p<0.0001. Stars alone represent significance to respective treatment at ZT5.

Blocking antibodies against the three main pro-inflammatory cytokines IL-1β, IL-6 and TNFα that are activated in the MyD88 pathway were injected at ZT5 one day prior to blood harvest at peak and trough times of leukocyte oscillation (**Figure 3-20A**). There were no differences in blood counts neither at ZT5, nor at ZT13 after treatment with blocking antibodies compared to injection with respective isotype controls (**Figure 3-20B**). However, while lymphoid subsets as well as NIMs, NK cells and eosinophils represented the same phenotype, neutrophil and IM counts were significantly decreased at ZT5 after blocking of pro-inflammatory cytokines (**Figure 3-20C**). Therefore, we aimed to investigate whether this observation is potentially due to one specific cytokine and repeated the experiment with separate injection of neutralizing antibodies against either IL-1β, IL-6 or TNFα. In this setup, overall leukocyte counts in blood again did not show any difference between isotype or blocking antibody-treated group, neither at ZT5, nor at ZT13 (**Figure 3-20D**). Lymphocytes and eosinophils were not altered after the different treatments while NK cells were slightly increased at ZT5 upon inhibition of IL-1β. However, there was a significant decrease in IMs after blockade of TNFα, an effect already observed with the combined inhibition of all three pro-inflammatory molecules. A similar tendency was also seen for neutrophils, although this difference was not significant. These effects could not be observed upon blocking of IL-1β or IL-6 (**Figure 3-20E**).

Thus, blocking of TNFα was sufficient to reduce counts of myeloid cells during the day time, especially IMs, which was not reproducible upon inhibition of other pro-inflammatory cytokines such as IL-1β or IL-6.

3.16. TNFα shows daily oscillation in blood plasma

TNFα can be detected in low doses in blood plasma under steady-state conditions and is among other things responsible for leukocyte mobilization from the bone marrow in the non-inflammatory state (Mizrahi and Askenasy, 2014). Since some publications showed rhythmic TNFα levels in human blood plasma (Petrovsky and Harrison, 1998), we wondered whether this was also true for mice. Hence, we isolated plasma from mice at different times of the day and measured TNFα concentrations using a cytokine bead array. Indeed, we were able to detect a significant oscillation over the course of a day in TNFα levels under steady-state

conditions. The peak occurred at Zeitgeber time 5.9 and the trough at about ZT18 as proven by cosinor analysis (**Figure 3-21**).

Taken together, TNFα exhibited daily oscillations in blood plasma of mice under steady-state conditions, which was of functional relevance.

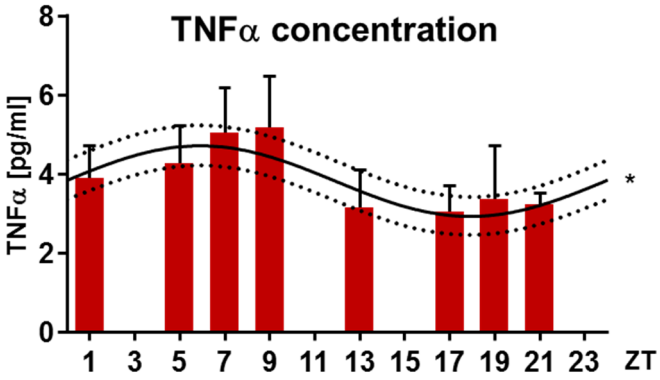

Figure 3-21: TNFα shows daily oscillation in blood plasma. Blood was harvested from mice at ZT1, 5, 7, 9, 13, 17, 19, 21 and 23 and plasma was isolated. Using cytokine bead array, TNFα concentrations were determined. (n=3-8, cosinor analysis) *p<0.05

3.17. Low-dose TNFα injections slightly increase leukocyte numbers in blood

Since the data demonstrate significant differences in TNFα concentrations over the course of a day and additionally, a reduction of myeloid cells in blood after blocking of this pro-inflammatory molecule, the hypothesis was that oscillatory TNFα levels might induce circadian mobilization of leukocytes, especially myeloid cells, into the circulation. Thus, the amount of TNFα that corresponded to the detected physiological TNFα concentration at the acrophase was injected into mice one or two hours prior to blood harvest at the nadir of leukocyte numbers at ZT13, respectively (**Figure 3-22A**). Mice injected at ZT11 did not present any differences in overall leukocyte numbers or subset abundance between injection with either PBS or 4pg of TNFα (**Figure 3-22B, C**). Upon injection at ZT12, however, mice injected with the same TNFα concentration showed significantly higher neutrophil numbers compared to control group (**Figure 3-22B, C**).

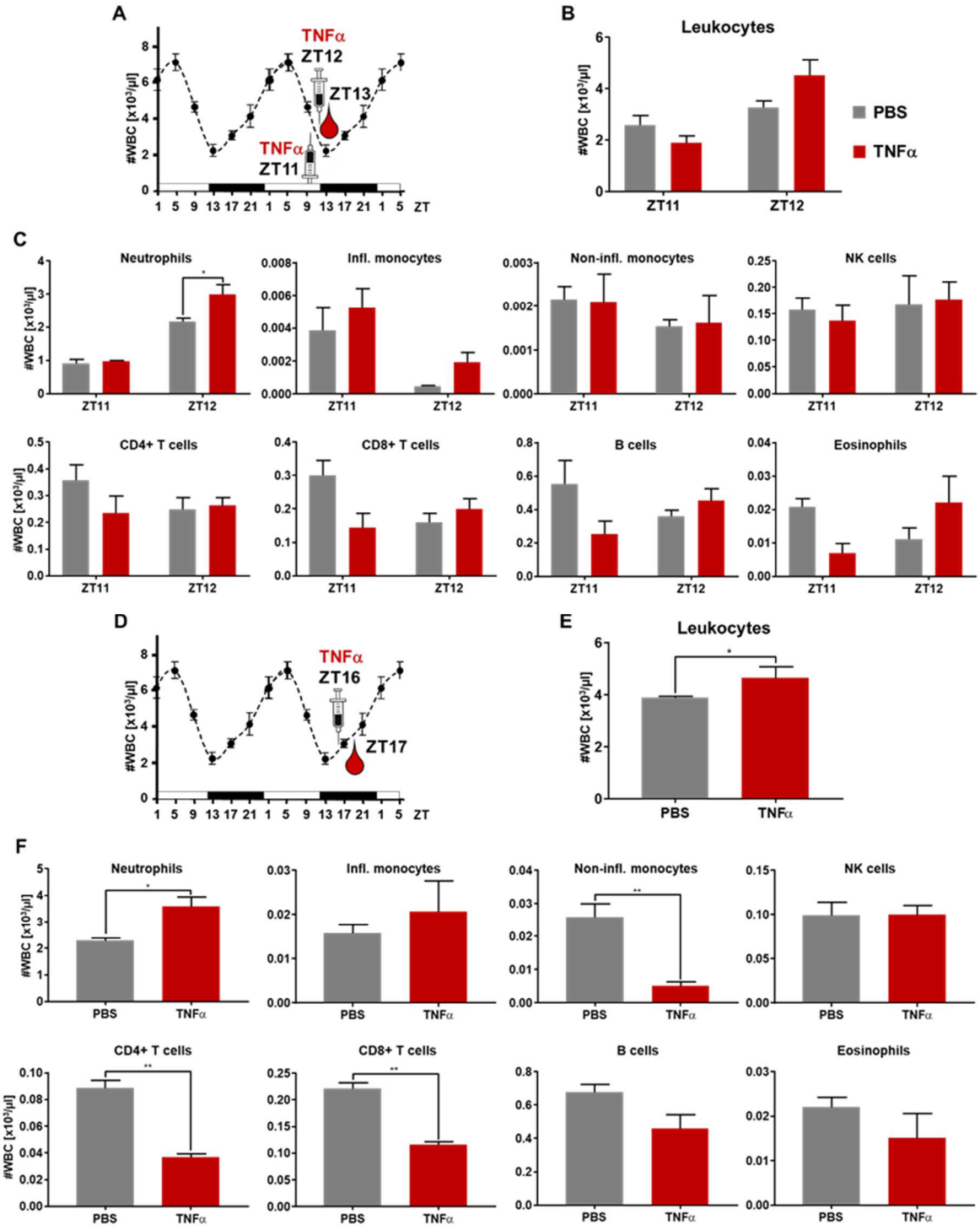

Figure 3-30: Injection of low-dose TNFα slightly increases leukocyte numbers. (A) 4 pg TNFα or PBS were injected i.v. into mice at either ZT11 or ZT12. Blood was harvested from both treatment groups at ZT13. (B) Leukocyte counts were measured and leukocyte subsets (C) were analysed using flow cytometry. (D) 4 pg TNFα or PBS were injected i.v. into mice at ZT16 and blood was harvested at ZT17. (E) Leukocyte counts were measured and leukocyte subsets (F) were analysed using flow cytometry. (n=3, B, C: two-way ANOVA, E, F: unpaired t-test). *p<0.05, **p<0.01

Since the nadir in the TNFα level in plasma was around the middle of the dark phase, we repeated this experiment and injected 4pg TNFα into mice at ZT16 while

blood was harvested at ZT17 (**Figure 3-22D**). In this setup, we observed elevated leukocyte counts after TNFα treatment, which was mainly due to increased neutrophil numbers while other cell types, such as NIMs, CD4+ T cells and also CD8+ T cells were significantly reduced compared to PBS injections (**Figure 3-22E, F**).

To conclude, injections of low-dose TNFα at the beginning of the active phase slightly increased leukocyte numbers, especially neutrophil counts.

3.18. *Tnf*$^{-/-}$ mice do not show altered leukocyte numbers in the circulation

Finally, we investigated leukocyte numbers and subset abundance in mice lacking TNFα in collaboration with Dr. Daniel Lucas at the University of Michigan, USA. Blood was harvested from these animals at peak and trough times of leukocyte counts and overall WBC numbers as well as subset counts were analyzed. In leukocyte counts, there was no significant difference between WT and *Tnf*$^{-/-}$ mice, neither at ZT5, nor at ZT13, and *Tnf*$^{-/-}$ mice exhibited a clear daily difference between

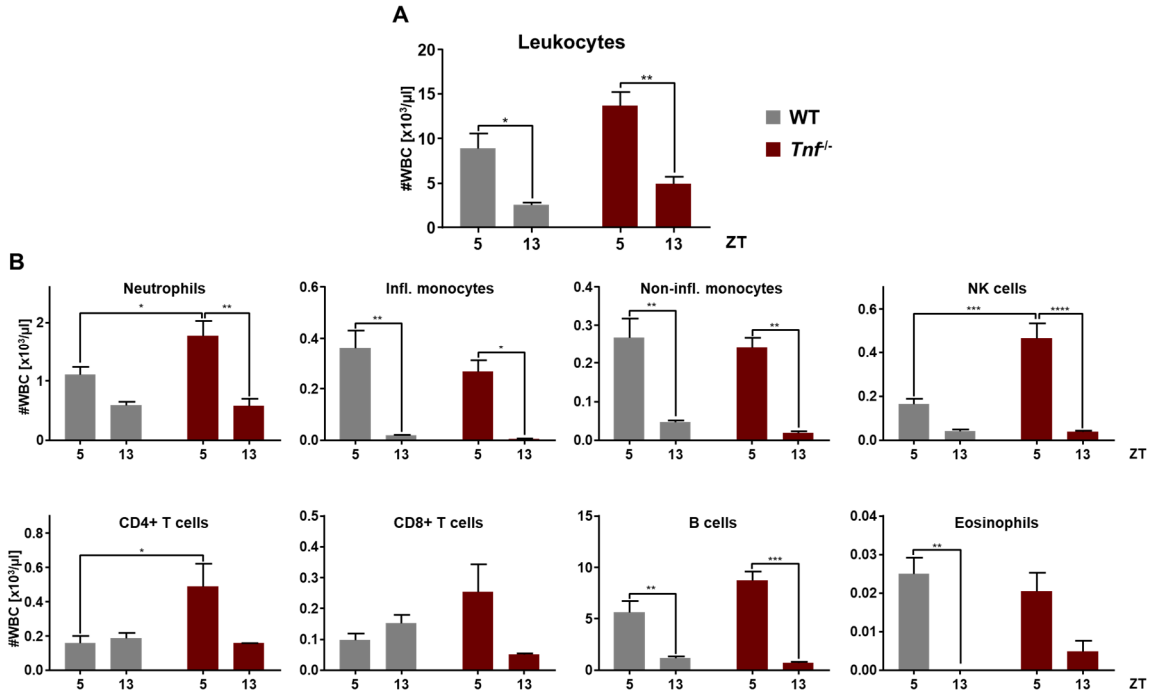

Figure 3-2339: *Tnf*$^{-/-}$ animals do not have altered leukocyte counts in the circulation. (A, B) Blood was harvested from WT and Tnf-/- mice at ZT5 and ZT13. (A) Leukocyte counts were measured and leukocyte subsets (B) were analysed using flow cytometry. (n=4, two-way ANOVA) *p<0.05, **p<0.01, ***p<0.001.

ZT5 and ZT13 (**Figure 3-23A**). Neutrophil, NK cell and CD4+ T cell counts, however, showed a significant increase at ZT5 upon genetic depletion of *Tnf* compared to control littermates while other subsets were not affected (**Figure 3-23B**).
Thus, genetic ablation of TNFα has small effects on leukocyte numbers in blood but not on their counts between ZT5 and ZT13.

3.19. Summary

Of the investigated key entrainment factors, changes in light and feeding times were able to alter leukocyte oscillation in blood. However, these rhythms still persisted during the absence of light while the complete absence of microbiota dampened leukocyte numbers in blood at their peak time. A functional molecular clock in potentially involved peripheral tissues was not necessary for differences between ZT5 and ZT13, but time-restricted feeding altered clock gene expression in organs in close proximity to the gut. Rhythmic mobilization might be an underlying mechanism for the leukocyte oscillation in the circulation and a heat-stable factor in morning serum is possibly inducing this effect. Only full ablation of the TLR adaptor molecule MyD88 could decrease neutrophil numbers in blood at the peak time and this effect is not dependent on either TLR4 ligand LPS or global and endothelial TLR4 and TLR2 expression. TNFα potentially acts downstream of MyD88 as indicated by its daily oscillation in blood plasma at steady-state conditions as well as by decreased neutrophil numbers in blood after blocking.
Taken together, time-restricted feeding is able to influence circadian leukocyte oscillations in blood, probably via mediating a rhythmic release of microbial factors into the blood stream that act via MyD88 and TNFα to induce a rhythmic leukocyte mobilization.

4. Discussion

4.1. Which entrainment factor influences leukocyte oscillation in blood?

4.1.1. The influence of light

Light is the main entrainment factor for many daily physiological functions and our data show that acute disruption of this Zeitgeber is able to alter leukocyte numbers in the circulation (**Figure 3-2**). However, the absence of this entrainment factor does not result in the abolishment of leukocyte rhythms, but in still persistent, if slightly dampened, oscillations of white blood cells, especially in innate immune cells (**Figure 3-1**). Cosinor analysis was not able to prove statistical significance for this rhythm under complete darkness, however, the analysis is designed for oscillations over a course of 24 h and free-running rhythms are often not very well aligned with this requirement (Eckel-Mahan and Sassone-Corsi, 2015). Hence, the comparison between the different time points is of more impact and shows clear alterations with the same peak and trough times as for animals kept under normal light conditions. This is in accordance with previous publications (Scheiermann et al., 2012; Stenzinger et al., 2019), meaning that leukocyte oscillation in blood is *bona fide* circadian, since it is still persisting in a non-rhythmic environment. On the other side, exposure to constant light abolished the significant difference between peak and trough times of leukocyte numbers in blood, although an overall rhythm was maintained over the course of 24 h (**Figure 3-1**). This effect might be due to the fact that constant light leads to an increased inflammatory phenotype in mice (Mizutani et al., 2017), hence explaining increased leukocyte numbers at ZT13.
To conclude, light is able to influence leukocyte oscillations in blood, but does not cause them. Therefore, this entrainment factor probably functions as adjustment and synchronizing factor and acts via the central pacemaker.

4.1.2. The influence of food and behavioural activity

Light is the most prominent entrainment factor since it synchronizes the central clock in the SCN. However, it is not the only one and food, but also behavioural activity

are able to influence peripheral clocks, but also the central pacemaker (Bass and Takahashi, 2010; Tahara and Shibata, 2013).

Time-restricted feeding with limited access to food for 12 h during light or dark phase did not severely influence rhythmic leukocyte abundancies in blood (**Figure 3-4**). However, light-restricted feeding altered behavioural activity of the mice resulting in increased movements at the beginning of their actual resting phase and also reduced motion during their active phase. These results underline the strong internal cue of leukocyte oscillation since not even alterations in another powerful entrainment factor behaviour (Mrosovsky et al., 1989) managed to influence this rhythm.

We speculated that a food restriction to 12 h might not be sufficient to influence changes over the course of a day. This is why we repeated the experimental setup with food restriction to only 6 h during either the middle of the dark or the light phase. These results show a clear shift of about 4 h after light-restricted feeding towards the beginning of the resting phase while maintaining a similar amplitude as during dark-restricted feeding. Compared to mice who had ad libitum access to food, amplitudes of leukocyte oscillation were increased in the restricted-feeding setup. We hence interpret that food restriction to only 6 h during the respective active phase further increases leukocyte rhythm in the circulation. This might also explain why it was the differences at ZT7 and ZT19 between light- and dark-restricted feeding, which showed statistical significance and not LRF in comparison with control feeding patterns (**Figure 3-4**).

In conclusion, time-restricted feeding to only 6 h during the respective rest phase is able to alter leukocyte oscillation although loss of the main entrainment factor light and even changes in the entrainment factor behavioural activity were not. This indicates a crucial role of rhythmic food uptake to impact the immune system in a so far not yet investigated way.

4.2. Is the effect due to rhythmic homing or mobilization?

Since leukocyte rhythms are present in the oscillation, it is consequential to think about oscillatory re-distribution of these cells into different organs. Leukocyte migration broadly consists of two directions: mobilization, e.g. input into blood from production sites, and recruitment or homing into peripheral tissues. Recently, we

were able to publish two studies about circadian homing of leukocyte subsets into tissues (Druzd et al., 2017; He et al., 2018), demonstrating a daily migratory behaviour of leukocytes. Leukocytes are recruited more intensely to peripheral tissues at the beginning of the behavioural active phase (night), due to increased expression of pro-migratory factors on both the white blood cells and endothelial cells. This results in reduced cell numbers in blood at this time of the day, as shown by blocking experiments as well as adoptive transfer setups (He et al., 2018). On the other side, haematopoietic stem and progenitor cells (HSPCs) were shown to be rhythmically mobilized from bone marrow into the blood stream, leading to increased abundancies during the rest phase. This effect is mediated by reduced CXCL12 expression levels in the bone marrow as well as reduced CXCR4 levels on leukocytes (Lucas et al., 2008; Scheiermann et al., 2013). Since rhythmic homing has been extensively studied, it is not yet clear to which extent an oscillatory mobilization might contribute to the circadian leukocyte rhythms in blood.

First, to test for potential differences in re-distribution of cells after altering the two main entrainment factors light and food, leukocyte counts and subsets were also analysed in bone marrow and spleen. Under control conditions (LD and *ad libitum* feeding), abundancies of leukocytes in bone marrow did not show any oscillations between the four different harvest time points except for increased monocyte numbers during the active phase while *ad libitum* feeding (**Figure 3-5A**) and an oscillatory pattern in CD4+ T cells in the control group of acutely jetlagged mice (**Figure 3-2E**). However, CD4+ T cells are not the most prominent leukocyte subset in bone marrow, explaining why maybe already small changes might result in significant differences. Also, there were rhythms in BM cell counts in the control group of antibiotic-treated animals (**Figure 3-8B**) that were different to the ones observed in monocytes of the control group of the TRF-experiment. No other publication has observed these time-dependent differences in BM cell numbers (Druzd et al., 2017; Stenzinger et al., 2019) and we speculate that these alterations might be due to almost daily handling of these animals or by receiving sweetened drinking water, potentially resulting in abnormal leukocyte abundancies.

For leukocyte numbers identified in the spleen, we were also not able to show significant rhythms except for neutrophils and inflammatory monocytes, which were significantly reduced during the end of the resting period and during the active phase in control conditions of the jetlag experiment (**Figure 3-2F**). The spleen is supposed

to represent the leukocyte subset composition of the circulation since it filters the blood for old red blood cells in a high turnover rate. Thus, these elevated numbers might simply reflect the blood composition in that setup. Also interestingly, literature shows conflicting data about circadian leukocyte counts in spleen (Druzd et al., 2017; Stenzinger et al., 2019), indicating weak oscillatory patterns of this organ.

In conclusion, there are none or weak rhythms in cell counts of spleen and bone marrow, which are susceptible to disturbances and do hence not indicate a re-distribution of leukocytes according to the time of the day under steady-state conditions. However, cell numbers in these organs are represented in a different dimension when compared to blood, meaning that minor changes might not be addressed by a counting readout. Additionally, it was shown that adoptively transferred cells home in a circadian manner into these organs, confirming that rhythmic recruitment of leukocytes into peripheral organs plays a role in circadian leukocyte migration (He et al., 2018).

Upon modulating the key entrainment factors, no major alterations were observed in bone marrow and spleen when compared to the group-respective controls except for light-restricted feeding. In this setup, BM cell counts exhibited a rhythmic pattern over the course of the day, which was represented by neutrophils and lymphocytes (**Figure 3-5A**). As already mentioned before, this effect could be explained by sensitive and easily disturbed counts in this organ, potentially induced by daily interruption for restricted food access. Interestingly, splenic leukocyte counts were significantly reduced after two weeks of light-restricted feeding, especially in comparison with dark-fed animals that exhibited oscillatory WBC numbers (**Figure 3-5B**). As observed in leukocyte counts in the circulation, we speculate that 6 h food restriction to the active phase further increased underlying circadian regulations and hence the results in spleen reflect leukocyte numbers from blood.

To conclude, leukocyte counts in bone marrow were not stable enough to speculate about the influences of key entrainment factors while abundancies in spleen seem to reflect the effect in the circulation, although this effect was not consistent across the performed experiments. To gain more information about a circadian re-distribution of leukocytes, it would hence be necessary to first investigate more potential homing organs. Second, performing adoptive transfer experiments at different Zeitgeber times in animals with altered key entrainment factors would

increase understanding about daily homing and potentially exclude influences on the circadian homing zip-code.

To assess a potentially oscillatory influence of leukocyte input into the circulation, we labelled cells with a single BrdU pulse to mark all newly proliferating cells and analysed the number of BrdU-positive cells in the circulation and hematopoietic tissues such as bone marrow and thymus after 72 h. In blood, all leukocytes should be terminally differentiated (post mitotic) and hence, all BrdU-positive cells detected in the circulation must have been mobilized from other organs, probably from their site of production. There was no circadian egress or proliferation observed in BM, while the mobilization into blood seemed to be slightly rhythmic with regard to the amount of BrdU+ leukocyte subsets in the circulation, mostly for innate immune cells (**Figure 3-3**). The observations in bone marrow and thymus are potentially due to a complex interplay between differentiation, proliferation and cell death, aggravating interpretation of these results. Additionally, technical problems with the flow cytometer while analysing leukocyte counts in thymus do not allow any interpretation of these data.

Other publications were able to show decreases in BrdU+ granulocytes and neutrophils in BM while the abundancies increased in blood, hence demonstrating a time-dependent efflux of freshly proliferated cells into the circulation (Balmer et al., 2014; Casanova-Acebes et al., 2013). However, these groups observed a time frame over 72 h while here, only 24 h were investigated to gain information about daily effects. Also, the composition in blood represents a constant influx and efflux of mobilized, recruited and also homing leukocytes, which makes it hard to clarify the results. Moreover, it is possible that timing of the BrdU pulse was not ideal, however, administration by drinking water would not have been able to ensure equal BrdU uptake by individual animals.

Thus, further fine-tuning of this method is necessary to allow investigation of circadian mobilization from leukocyte-producing organs. In addition, blocking of pro-migratory factors that mediate extravasation would elucidate the role of an oscillatory leukocyte influx into the circulation since it would exclude recruitment and homing as additional disturbance factors.

4.3. How is the effect of time-restricted feeding mediated?

It was recently shown that microbiota exhibit daily rhythms in their composition and function (Leone et al., 2015; Liang et al., 2015; Thaiss et al., 2014b; Zarrinpar et al., 2014). Moreover, these rhythms impact host transcriptomes, metabolomes and epigenetic modifications in intestine in liver and this effect is mediated by circadian adherence of commensal bacteria to the intestinal epithelial cell wall (Thaiss et al., 2016a). Strikingly, loss of the two major clock components *Per1* and *Per2* abolished these rhythms but time-restricted feeding was able to rescue them again (Thaiss et al., 2016a; Thaiss et al., 2014b). Taken together, these results indicate that time-restricted food access is probably the driver for daily oscillations in microbiota.

Since it is also well known that microbiota influence the immune system on multiple ways and that this happens not only locally in proximity to the gut, but also systemically (Thaiss et al., 2014a), we hence hypothesized that our findings from TRF-experiments are mediated by the gut microbiome and found reduced counts in every investigated leukocyte subset in blood of germ-free animals at ZT5. Leukocyte numbers in organs remained mostly unaltered, except for CD4+ T cells in inguinal lymph nodes of GF animals at ZT5 and innate immune cell numbers at both time points in spleen. These subsets were significantly reduced in mice lacking commensal bacteria (**Figure 3-9**). However, these animals are described to exhibit a reduced cellularity in immune cells of epithelial tissues and also smaller sizes of e.g. mesenteric lymph nodes (Round and Mazmanian, 2009), hence providing a potential explanation for this observation. WBC counts in spleen showed inverted counts to blood leukocyte numbers in SPF control animals, which we have not observed before. Since these animals were raised in a different animal facility, it is possible that these differences were induced by the different environment.

Interestingly, we were not able to confirm these results in blood leukocyte numbers in antibiotic-induced microbiota depleted mice (**Figure 3-8**). In these animals, differences in leukocyte abundancies between ZT5 and ZT13 in the circulation still persisted after two weeks of antibiotic treatment while thymic and inguinal lymph node counts at ZT13 were slightly increased and decreased, respectively. It is possible that antibiotic treatment affected these cell counts, however, our main readout in blood remained unchanged, leading us to the assumption that broad-spectrum antibiotics were not able to influence circadian leukocyte numbers.

Although we observed a clearly different phenotype in germ-free animals, this result was not completely unexpected. It is known that treatment with broad-spectrum antibiotics does not deplete 100% of commensal bacteria. Mainly *Proteobacteria* are left in the intestine as well as all other commensal organisms, such as fungi or viruses (Kennedy et al., 2018; Zarrinpar et al., 2018). Although there are controversial publications about daily oscillations in *Proteobacteria* (Godinho-Silva et al., 2019; Liang et al., 2015), nothing is yet known about rhythms in other commensal organisms. Moreover, Thaiss et al. found persisting oscillations in microbiota after only one week of antibiotic treatment, indicating that the time of antibiotic supply might not have been long enough to efficiently abolish microbiota daily rhythms (Thaiss et al., 2014b). Antibiotic composition, treatment times and also method of treatment - suggesting gavage of antibiotics instead of supplement in drinking water to ensure full dose uptake - differ a lot between different publications (reviewed in (Kennedy et al., 2018). Taken together, it is possible that low doses of remaining intestinal bacteria kept their daily rhythm and were sufficient to induce oscillatory cues in the host organism.

In conclusion, rhythmic food uptake shapes daily microbiota which in turn influence leukocyte numbers in the circulation. Interestingly, low levels of remaining bacteria or organisms seem to be sufficient to keep daily differences between ZT5 and ZT13, indicating a process that requires very low-dose input signals. Since only two time points were investigated, we cannot conclude whether oscillation was abolished or shifted upon the lack of microbiota. Hence, blood harvest at additional time points over a course of 24 h is necessary to gain more insights about leukocyte oscillation in the circulation of germ-free animals.

To obtain information about the migratory behaviour of leukocytes in these animals, we decided to isolate CD4+ and CD8+ T cells, B cells and neutrophils and analysed mRNA levels of several molecules involved in leukocyte migration. We have published before that several of these factors exhibit daily oscillation in their protein expression on different leukocyte subsets and hence provide a rhythmic zip code of leukocyte migration (He et al., 2018). However, we could not confirm most of these differences at the mRNA level, except for *Cxcr4*, which also presented higher protein levels at ZT13 compared to ZT5 in our recently published data (**Figure 3-10**). Nevertheless, we only tested expression at two different time points in this setup compared to at least four time points before. Also, mRNA and protein levels can

differ immensely since post-translational modifications, mRNA stability as well as protein degradation influence these two readouts in a complex manner. Most interestingly to us were expression patterns of *Cxcr2* and *Cxcr4*, which showed inverted oscillations to each other. Since *Cxcr2* is known to be a recruitment factor for leukocyte homing (Addison et al., 2000) while *Cxcr4* is responsible for retention of leukocytes within an organ (Cheng and Qin, 2012), we conclude that these daily expression patterns might be one responsible mechanism for circadian leukocyte numbers in blood. Even more, these differences between ZT5 and ZT13 were lost in lymphocytes of germ-free animals. Although *Cxcr2* is primarily expressed on myeloid cells, publications have also demonstrated a role of this molecule in lymphocytes (Lippert et al., 2004; Tani et al., 1998). This indicates a potential machinery of how altered leukocyte numbers in the blood of germ-free mice are regulated.

We also analysed clock gene expression in the isolated leukocyte subsets but could hardly detect significant differences between ZT5 and ZT13. As it is possible that these two time points were not the best ones to detect expression differences of *Bmal1* and *Cry1* since these two clock genes exhibit their peak and trough levels at other time points, *Per2* was actually shown to exhibit clear daily differences between ZT5 and ZT13, which we could not confirm. Also, *Dbp* and *Nr1d1* were published to exhibit inverted expression levels with decreased mRNA levels at ZT13 (Druzd et al., 2017). However, these data were obtained from inguinal lymph nodes while lymphocytes and neutrophils were harvested from spleen and bone marrow, respectively. Additionally, the reduced expression of some clock genes in germ-free animals might enlighten further regulation of the microbiota on peripheral and systemic immune modulation.

Taken together, our attempts to describe daily mobilization of leukocytes into the circulation were impeded by insufficient methodological approaches. Additional experiments, such as BrdU labelling or homing assays are necessary to investigate leukocyte migration under the control of time-restricted feeding or commensal bacteria. However, altered daily expression of migratory factors in germ-free animals provided a first insight into potential underlying mechanisms and assume that rhythmic mobilization is a possible explanation for circadian leukocyte oscillation in blood.

4.4. What is the role of clock genes?

4.4.1. Influence of food on clock gene expression

Every nucleated cell type investigated thus far exhibits an autonomous molecular clock machinery. These peripheral clocks are usually entrained by the central conductor in the brain, the SCN. However, since light is not the only external Zeitgeber, other entrainment factors, such as food, are able to synchronize peripheral clocks and, in case of disruption, also able to de-synchronize several peripheral clocks, such as liver, heart, pancreas, kidney and intestine, from the central clock as shown in several time-restricted feeding studies (Damiola et al., 2000; Hara et al., 2001).

We decided to investigate mRNA levels of *Nr1d1* (*Rev-Erbα*) and *Per2* expression as strongly oscillating clock genes with peaks at opposite times of the day. Additionally, the clock-controlled gene *Dbp* was also assessed for its daily rhythm to also investigate the next level of the clock-controlled machinery in bone marrow and spleen, but also in liver as well as in inguinal and mesenteric lymph nodes.

Cosinor analysis was able to reveal significant oscillations after light-restricted feeding in the bone marrow and dark-restricted feeding in the spleen for all three genes (**Figure 3-6A-D**). However, expression levels failed to reach the same extent of expression and the same peak and trough times of oscillation as observed in other organs. Input from various cell types in different developmental stages may cause this diverse effect, since they probably underlie multiple external and internal entrainment factors, additionally to their cell-autonomous clock machinery. Additionally, hematopoietic cells may be less synchronized than other resident cell types since a majority of the former is migratory.

The liver is closely connected to the intestine as all the blood leaving the digestion system passes first through the liver. A strong shift in rhythmic expression patterns after light-restricted feeding of all three investigated clock genes was observed in this organ, resulting in almost completely inverted oscillations (**Figure 3-6E, F**), which is in line with previous publications (Damiola et al., 2000; Hara et al., 2001). This indicates a dramatic impact of the entrainment factor food on peripheral clock gene expression in an organ that is receiving direct input from the gut.

To gain more information about the influence of time-restricted feeding on lymphoid organs, clock gene expression in lymph nodes harvested from two different

anatomical sites was tested. It was already shown that inguinal lymph nodes exhibit strong oscillations in their clock gene expression (Druzd et al., 2017) and this was confirmed by our data. These rhythms were also not perturbed by food access limited to the rest phase of the animals (**Figure 3-7**). However, light-restricted feeding was able to dampen the rhythms in the investigated clock genes in mesenteric lymph node. Although the peak in *Dbp* mRNA level was shifted compared to the inguinal lymph node, it has been published that the highest count in lymph node cellularity is also shifted in comparison to other lymph nodes (Druzd et al., 2017), providing a potential explanation for this observation.
These data hence indicate that food as entrainment factor has a range in which it synchronizes peripheral clock expression. Especially the results from inguinal and mesenteric lymph nodes provide a clear insight into how far food uptake can fine-tune the molecular clock machinery in peripheral organs even impacting very similar organs just due to their proximity to the gut.

4.4.2. Influence of clock genes on rhythmic leukocyte numbers in blood

The relationship between the clock machinery and the immune system as well as the symbiosis between commensal bacteria and the host are bi-directional. For this reason, we aimed to investigate the role of clock genes on daily leukocyte numbers in blood by depleting the core clock gene *Bmal1* in tissues that are important at the microbiota-host interface as well as crucial for leukocyte migration. Endothelial cells were shown to exhibit rhythmic clock gene expression and depletion of *Bmal1* in these cells ablated daily homing of leukocyte subsets to organs (He et al., 2018). However, there were no detectable differences in leukocyte numbers in blood between EC-*Bmal1*$^{-/-}$ or respective control animals (**Figure 3-12**). These distinct observations can be explained since He et al. mainly investigated the amount of adoptively transferred cells while our data only represent the overall cell numbers. Potentially, mobilization is also altered in these animals to balance the consistent leukocyte numbers in blood. To further investigate an impact of *Bmal1* expression in endothelial cells on leukocyte numbers and migration in the circulation, it would thus be necessary to include experiments about homing and mobilization behaviour, such as a homing block or BrdU labelling.

It is known that a functional clock machinery in intestinal epithelial cells is crucial for a functional systemic metabolism by regulating daily MAMP-sensing TLR expression patterns in these cells (Mukherji et al., 2013). This finding made us speculate that circadian microbiota composition and especially biogeography (Thaiss et al., 2014b; Thaiss et al., 2016b) might be able to modulate circadian leukocyte oscillation via influencing clock gene expression in intestinal epithelial cells. Thus, we also analysed blood, bone marrow and spleen from mice lacking *Bmal1* at this interface between commensal organisms and host physiology. Although differences between ZT5 and ZT13 in control animals were not significant, the tendency was clear and there was no change in leukocyte numbers in blood, bone marrow or spleen between control and IEC-*Bmal1*$^{-/-}$ mice (**Figure 3-11**).

To conclude, ablation of clock gene expression at different interfaces between gut microbiota and leukocyte mobilization is probably not sufficient to alter circadian leukocyte numbers in blood. However, the molecular clock machinery in peripheral organs related to the gut is affected by external entrainment factors such as food, indicating a relationship between this external entrainment factor and the molecular clock. Additionally, to maintain bi-directionality in this setup, *Per1/2*-KO animals were shown to lose the circadian rhythms in their microbiota due to continuous food consumption (Thaiss et al., 2014b). In conclusion, the central clock seems to maintain a rhythmic behaviour in food uptake which in turn fine-tunes molecular clocks in several peripheral organs. Upon ablation of the central pacemaker, restricted food uptake manages to restore the rhythms not only in the commensal bacteria, but also the oscillations of the serum metabolome (Thaiss et al., 2016a). In addition, light-restricted feeding was even able to invert the rhythms in microbiota while maintaining normal light-dark cycles (Thaiss et al., 2014b). This indicates the immense impact of food as external entrainment factor and highlights its importance in adjusting a circadian homeostasis, not only in metabolic organs, but also in the mesenteric lymph node.

4.5. What are the molecular mechanisms mediating the effect of timed food uptake?

Multiple studies have focused on how diet, microbiota composition and a restricted food uptake modulate host metabolism (Asher and Sassone-Corsi, 2015; Leone et

al., 2015; Thaiss et al., 2016a). However, there are only few publications to investigate the influence of these factors on the host immune system, especially in a systemic and not local manner, although the awareness of the interplay between commensal bacteria and immunity is constantly increasing (Thaiss et al., 2014a). Several studies have already proposed a systemic influence of commensal bacteria on host immunity and during the last years, some publications were able to detect microbial-derived factors in blood, spleen and bone marrow of the host under steady-state conditions. These factors, such as LPS and peptidoglycan, severely influenced the innate immune system and also primed the immune response to an improved defence against pathogens (Clarke et al., 2010; Zhang et al., 2015). Interestingly, another publication demonstrated circadian expression of tight junction proteins in the colonic epithelium which was associated with daily permeability of this barrier (Kyoko et al., 2014). In conclusion, we assume that daily leakage of microbial factors into the host organism is able to shape circadian leukocyte mobilization in the blood stream. However, not only microbial products, but also microbial-derived metabolites are able to affect host immunity (Levy et al., 2016). This leaves multiple molecules that potentially influence rhythmic leukocyte numbers in the circulation. Thus, we harvested serum from mice at different times of the day and injected it into recipient mice at the nadir of leukocyte numbers to increase the chances of a possible effect. Especially serum that was harvested in the morning increased overall leukocyte and specifically neutrophil numbers when transferred to mice in the evening, while CD4+ T cells were increased after transfer of serum harvested in the afternoon (**Figure 3-13**). This indicates that sterile blood serum contains a factor which increases leukocyte numbers in a daily manner. The time point with the highest response, ZT2, also fits into the observation of peak leukocyte numbers at ZT5, hence anticipating a potential mobilization of leukocytes, most likely from the bone marrow. Differences between neutrophils and CD4+ T cells could be explained by differences in the cell-autonomous clock in these cells, which may lead to slight shifts in their oscillation in blood (Druzd et al., 2017; Ella et al., 2018). To narrow many diverse possible factors, serum from ZT2 was heat-inactivated before being transferred into recipient animals, thereby denaturing proteins and destroying heat-sensitive factors. Interestingly, this treatment further increased the observed effect in leukocytes and specifically neutrophils (**Figure 3-13**). LPS is a heat-stable molecule and was shown to be bound by serum proteins

such as albumin (Komatsu et al., 2016), potentially covering its pathogenic endotoxin lipopolysaccharide A. Heat-inactivation destroys albumin and might lead to increased LPS concentrations in serum, possibly explaining the observed further increased effect after this treatment. However, injections of low-dose LPS four hours before peak and trough times of leukocyte counts in blood were not able to reproduce the effect as seen after serum transfer (**Figure 3-14**). A study has shown that orally applied fluorescently labelled LPS could be detected on neutrophils in blood, spleen and bone marrow (Zhang et al., 2015). Since tight junction molecules in gut also underlie circadian regulation, LPS was gavaged 26 h prior to peak and trough times of daily intestinal permeability (Kyoko et al., 2014) to mimic a more physiological uptake of LPS than i.p. injection. Nevertheless, not even high LPS doses, imitating the amount of a complete microbiome, were able to alter leukocyte numbers in blood, bone marrow or spleen (**Figure 3-15**). It has been shown that neutrophil function is dependent on the microbiota (Clarke et al., 2010). However, it was also demonstrated that this relationship is not dependent on LPS, but rather on peptidoglycan. Additionally, it was published that sufficient myelopoiesis in the bone marrow is dependent on a high variability of commensal bacteria (Balmer et al., 2014), assuming that the observed effect after serum transfer cannot be reduced to a single factor. Specificity on mainly neutrophils can be explained by the fact that this cell type is the first one at a site of infection and also other studies identified microbiota-dependent priming of these cells under steady-state conditions (Clarke et al., 2010; Zhang et al., 2015).

Taken together, one or several heat-stable factors in blood serum increase specifically neutrophil numbers at the beginning of the rest phase. To prove the origin from the microbiota of these molecules, serum transfer of germ-free and conventionally-raised animals, harvested at different times of the day, should be injected into recipient GF and SPF animals, respectively, and leukocyte counts in blood should be analysed in addition to the transfer and analysis of fractionated serum.

4.6. Which pathway is involved in the relationship between timed food and leukocyte oscillation in blood?

4.6.1. Involvement of the TLR pathway

To further exclude several potential microbial products, we blocked and ablated prominent factors of pattern recognition pathways, namely TLR4, TLR2 and more general, TLR adaptor molecules MyD88 and TRIF. Pharmacological inhibition of TLR4 or MyD88 and TRIF did not affect leukocyte numbers in blood at ZT5 and ZT13. However, the control group in the blocking experiment of TLR4 failed to exhibit significant differences between these two time points (**Figure 3-16**). Since the animals are housed in common rooms with many people having access, we cannot exclude that light was turned on during darkness times, providing a potential explanation of this observation. Nonetheless, injection of a TLR4-blocking antibody did not change leukocyte abundancies compared to isotype-treated animals, abrogating a potential effect of this treatment. It is still possible that the incubation period of 24 h was too long to promote changes in leukocyte numbers in blood or, additionally, that application time did not hit the right time point. Also, leukocyte oscillation could still be altered at other time points since we only investigated two Zeitgeber times. However, it is also likely that inhibition was not complete, hence leaving low-dose signals that might still be sufficient to induce circadian leukocyte oscillation. We have already seen that very low levels of commensal bacteria, left after antibiotic treatment, seemed to be enough to not ablate daily differences in leukocyte numbers in blood.

Thus, genetic ablation of these factors involved in pattern recognition signalling was necessary to fully investigate their involvement in this pathway. An endothelial knockout TLR2 did not show significant differences between peak and trough times of leukocytes compared to littermate controls although neutrophils exhibited a trend to a loss of time-dependency between these time points (**Figure 3-18**). However, we only had limited availability of these animals and could hence not use a sufficient number of mice to confirm these effects. Since TLRs are not only crucial in pattern recognition on endothelial cells, we investigated the leukocyte oscillation in blood also in global *Tlr4*$^{-/-}$ animals although the results did not show any alterations compared to wild-type controls. Control animals did neither show significant differences between ZT5 and ZT13 in these experiments, complicating

interpretation of the results since the TLR-depleted animals did neither gain significance between these time points (**Figure 3-19**). Since these animals were analysed in collaboration with other groups and hence kept in different animal facilities, we cannot attest that strict darkness was kept during the active phase. Already short light exposure during that time as well as dim light is able to disturb the circadian machinery and could hence explain dampened rhythms in leukocyte numbers (Fonken et al., 2013; Miyake et al., 2000). However, this is a general problem when working in animal facilities where many people had access and may not be aware of this issue, particularly when performing experiments at locations where chronobiology is usually not considered. Nevertheless, comparison of knockout animals with wild type mice still provides insight into the phenotype upon genetic ablation and there were no differences detectable.

On the other side, *Myd88*$^{-/-}$ mice did not exhibit alterations in their overall WBC count in blood when compared to control animals, however, the number of neutrophils was significantly reduced at ZT5. In this subset, counts also showed significant differences between both time points, indicating that oscillation in this subset was still persisting and hence confirming the reduction in *Myd88*$^{-/-}$ animals. Interestingly, this decrease was also present in bone marrow and spleen while lymphocytes seemed to be increased at ZT5 and ZT13 in spleen and bone marrow, respectively (**Figure 3-19**). It has been published that myelopoiesis requires MyD88/TICAM1-signalling (Balmer et al., 2014), which explains the specific reduction in neutrophils and no other cell types. However, this publication did not find differences in myeloid cell types in peripheral blood, indicating a daily phenotype since we did neither observe differences in neutrophils counts at ZT13. It is thus possible that loss of *Myd88* affects rhythmic leukocyte mobilization or recruitment and depending on the investigation time point, differences can be found or are not present. Additionally, it was shown that neutrophils lacking *Myd88* exhibited a delayed ageing process, which comes along with reduced extravasation and thereby strengthening the observed specificity for this subset (Zhang et al., 2015). Interestingly, these two publications were also able to link these neutrophil-specific *Myd88* dependency to the microbiome, which supports our hypothesis of the influence of daily microbiota on circadian neutrophil rhythm (Balmer et al., 2014; Zhang et al., 2015). The increased lymphocyte numbers might also underlie this altered migration process and publications about the role of MyD88 in the adaptive immune system

demonstrated an impaired accumulation of lymphocytes at the site of infection (Frazer et al., 2013; Loures et al., 2011), indicating a potential retention of these cells at other tissues - such as bone marrow or spleen. In conclusion, TLR4 does not seem to be involved in mediating potentially microbiota-derived oscillating factors to shape leukocyte rhythms in blood, as already indicated by constant oscillations upon LPS injection or gavage. Since only genetic ablation, but not pharmacologic inhibition of MyD88, was able to reduce specifically neutrophil numbers in blood, it is possible that low doses of microbial factors, which are recognized in *Myd88*-associated pathways, are sufficient to shape rhythms in leukocyte numbers in the circulation. The specific effect on neutrophils and no other subsets could be explained by the fact that MyD88 is not the only important adaptor molecule downstream of pattern recognition receptors. For example, TRIF and TICAM1 are equally important and only additional genetic ablation of all of these molecules would block PRR signalling to a greater extent, potentially also affecting other leukocyte subsets. Also, to investigate a potential effect in leukocyte migration, more experiments such as adoptive transfers, homing blocks, mobilization assays and also proliferation and apoptosis assays are necessary to confirm these considerations.

4.6.2. The role of TNFα

The actual mediators of PRR signalling are cytokines that target the migration of leukocytes. Most prominent pro-inflammatory cytokines downstream of PRRs are IL-6, IL-1β and TNFα. Blocking of these molecules specifically reduced counts in innate immune cells at noon, which was mainly due to the inhibition of TNFα (**Figure 3-19**). As crucial part of the immune system, neutrophil and monocytes are usually recruited first to the site of infection and hence more susceptible to pro-inflammatory signals, thereby explaining the specific effect on myeloid and not on adaptive immune cells. Strikingly, TNFα was found to exhibit daily oscillations in blood plasma under steady-state conditions (**Figure 3-21**), indicating that upstream regulation of its expression must receive some oscillatory input. Peak and trough time points of its presence, however, is slightly delayed compared to leukocyte oscillations in blood. This suggests that the TNFα oscillation might also be an output effect of circadian leukocyte numbers in blood and not directly inducing the rhythmic

mobilization of the cells into the circulation. However, injections of physiological TNFα concentrations slightly increased leukocyte and specifically neutrophil numbers in blood when applied at the right time point (**Figure 3-22**). This result indicates that very low TNFα doses might be involved in leukocyte mobilization under steady-state conditions and the detected rhythms could provide a bridge between oscillating microbiota-derived factors, PRR signalling and circadian leukocyte oscillation in blood. Strikingly, it is already known since 1995 that TNFα presents also daily oscillation in human blood plasma over the course of the day (Cermakian et al., 2013; Young et al., 1995). This emphasizes the meaning of these rhythms since it is apparently evolutionary conserved between species. Humans also exhibit circadian leukocyte numbers in blood over the course of the day with inverted peak and trough times, since they are diurnal and not nocturnal organisms such as rodents (He et al., 2018; Scheiermann et al., 2013).

We have seen before that pharmacological blockade was not sufficient to induce an effect on leukocyte counts in the circulation. Interestingly, investigations in *Tnf*$^{/-}$ animals did not mimic our observed results from inhibiting TNFα using neutralizing antibodies. On the contrary, neutrophil counts were even increased at ZT5, as well as abundancies of NK cells and CD4+ T cells (**Figure 3-23**). *Tnf*$^{/-}$ animals were surprisingly shown to exhibit intact cytokine production upon LPS challenge with almost normal immune cell function (Marino et al., 1997). This indicates compensatory mechanisms in these mice, potentially adapted during development. However, they demonstrated increased susceptibility to pathogen infection (Marino et al., 1997; Pasparakis et al., 1996), which might suggest that the adaption is only in response to bacterial products and not in response to full bacterial challenge. This would support the hypothesis that oscillatory leakage of microbial factors induces TNFα oscillations in blood which might be overcompensated by other cytokines in *Tnf*$^{/-}$ animals. The fact that other cytokines potentially also play a role in controlling leukocyte numbers in blood is supported by the finding that combined blocking of IL-6, IL-1β and TNFα also reduced neutrophil numbers while TNFα neutralizing only was restricted on the decrease in inflammatory monocytes (**Figure 3-19**). To prove this, however, investigation of cytokine level in TNF-KO mice are necessary, ideally in combination with additional cytokine blocking experiments, investigations of oscillations in these candidates and assays to study migratory behaviour such as adoptive transfers or homing blocks. Furthermore, it is also possible that unequal

distribution of the blocking antibody within the animal resulted in uneven TNFα concentrations over different compartments, thereby creating a gradient which possibly affected leukocyte distribution and migration.

Taken together, rhythmic TNFα might play a role in mediating circadian leukocyte numbers in blood, especially during the rest phase. However, genetic ablation does not confirm this observation, indicating different regulatory mechanisms in these animals.

4.7. Proposals

Taken together, we propose that a rhythmic food uptake shapes daily rhythms in microbiota. These release microbial factors or metabolites rhythmically into the host organism that are sensed via pattern recognition receptors, dependent on MyD88. This leads to a rhythmic release of TNFα which mediates rhythmic leukocyte mobilization into the blood stream (**Figure 4-1**).

On a molecular level, there are two possible scenarios on how this circadian microbiota-host leukocyte axis could be mediated.

4.7.1. Systemic influence of timed feeding

First, microbial factors or metabolites could leak into the circulation and act directly and systemically. This is supported by the finding of microbial-derived products in peripheral tissues, such as LPS on bone marrow and blood neutrophils or peptidoglycan in serum and bone marrow (Balmer et al., 2014; Zhang et al., 2015). Although the results do not indicate involvement of LPS or LPS detection in rhythmic leukocyte numbers in blood, peptidoglycan was not investigated and there can be many other potential factors released from commensal bacteria or also archaea, viruses and fungi, which were not studied so far. Additionally, metabolites such as short chain fatty acids (SCFAs), are able to influence the immune system systemically (Levy et al., 2016) although no effect on leukocyte numbers in blood has been studied so far. Additionally, SCFAs were shown to induce peripheral clock entrainment (Tahara et al., 2018), highlighting an additional level of entrainment in

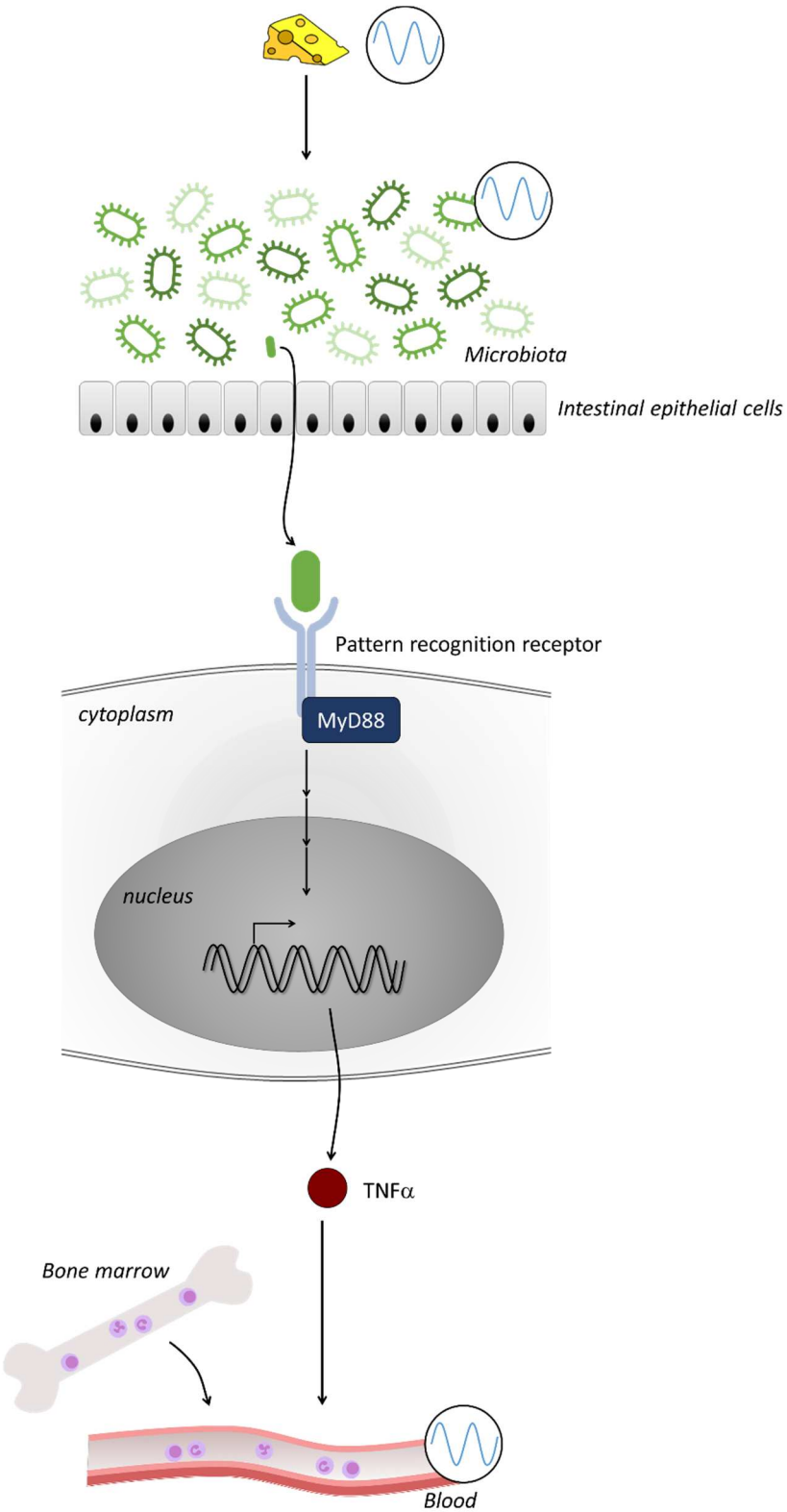

Figure 4-1: Proposed mechanism on how timed feeding influences rhythmic blood leukocyte numbers. Rhythmic food uptake shapes daily microbiota oscillations. Microbial products or metabolites can leak into the host organism and - either systemically or locally - induce signalling of pattern recognition receptors via MyD88. This leads to the rhythmic expression of TNFα which might induce the oscillatory leukocyte mobilization into the blood stream, resulting in circadian leukocyte numbers in the circulation.

the daily gut-immune system axis. However, since very low doses are potentially

mediating these effects as it was shown by maintained oscillations in leukocyte numbers upon insufficient depletion of microbiota, TLR4, MyD88 or TRIF, it will be a challenge to investigate these concentrations with current methodologies.

4.7.2. Local influence of timed feeding

Second, commensal bacteria intensely shape gut immunity locally (Hall et al., 2008; Uematsu et al., 2008) and several interactions at this site were shown to be under circadian control. For example, biogeography of microbiota is under daily control with oscillatory adherence to the intestinal epithelium (Thaiss et al., 2016a). Also, TLR expression on intestinal epithelial cells is under direct circadian control and might hence mediate oscillatory immune responses in this area (Mukherji et al., 2013). Especially type innate lymphoid cells (ILC3) were under recent investigation in this context. Two publications have highlighted the importance of clock gene expression in these cells on host metabolism, which was mediated by rhythmic microbiota (Godinho-Silva et al., 2019; Teng et al., 2019). ILC3s are tissue-resident cells, but they were also shown to migrate from the intestinal *lamina propria* to the mesenteric lymph node where they can interact with CD4+ T cells (Hepworth et al., 2013; Vivier et al., 2018). This provides a potential mechanism on how these highly clock-dependent cells might regulate rhythms distant from their site of residence, which is interesting since we have seen dampened clock gene oscillations in mesenteric lymph node after light-restricted feeding, but not in inguinal lymph node. Additionally, ILC3s also control Th17 cell responses and secrete IL-17 themselves, which was demonstrated to stimulate granulopoiesis (Schwarzenberger et al., 1998; Vivier et al., 2018), thus giving a hint on how these cells might modify the innate immune system as well. However, these cytokines are mostly released locally and it is not clear, how this could affect distant organs such as bone marrow. On the other side, it is also possible that timed feeding shapes the local clock machinery, as we have shown, and thereby controls ILC3 activity which subsequently regulates a microbial balance, indicating a symbiotic feedback loop.

4.8. Outlook

Presence of microbial products or metabolites in the host are usually only identified under pathological circumstances and hence do not provide information about the physiological relevance. Thus, our data provide insights into the steady-state relationship between microbiota and the host immune system. We propose a steady-state physiological state of low-level inflammation, mediated by low doses of microbial-derived products, which prime the immune system for a fast response upon infection. Additionally, this relationship seems to be under circadian control, mediated by rhythmic food uptake, to increase efficiency by timing leukocyte abundancies to risky times of infection. Future studies should focus on the role of rhythmic food uptake in combatting infections via our proposed pathway. Also, immunological diseases, which are linked to dysbiosis such as inflammatory bowel disease, multiple sclerosis, allergies and asthma (Petersen and Round, 2014), should be investigated concerning their susceptibility to timed feeding or eating patterns. Metabolic syndromes such as obesity or insulin resistance were already shown to be linked to altered eating patterns and even some diet metabolites, especially being important during circadian disruption (Chaix et al., 2019). Since different diets can influence the composition of commensal organisms and thereby also the metabolite configuration in the host (Brown et al., 2012), it might be of interest to investigate the role of nutrition in influencing the immune system. Ideally, a diet will be identified that leads to the mobilization of leukocytes into the blood stream, usually mediated in a rhythmic manner by the microbiota, and might thereby boost the immune system.

5. References

Adams, D.H., and Shaw, S. (1994). Leucocyte-endothelial interactions and regulation of leucocyte migration. Lancet *343*, 831-836.

Addison, C.L., Daniel, T.O., Burdick, M.D., Liu, H., Ehlert, J.E., Xue, Y.Y., Buechi, L., Walz, A., Richmond, A., and Strieter, R.M. (2000). The CXC chemokine receptor 2, CXCR2, is the putative receptor for ELR+ CXC chemokine-induced angiogenic activity. Journal of immunology *165*, 5269-5277.

Adrover, J.M., Del Fresno, C., Crainiciuc, G., Cuartero, M.I., Casanova-Acebes, M., Weiss, L.A., Huerga-Encabo, H., Silvestre-Roig, C., Rossaint, J., Cossio, I.*, et al.* (2019). A Neutrophil Timer Coordinates Immune Defense and Vascular Protection. Immunity *50*, 390-402 e310.

Akira, S. (2006). TLR signaling. Curr Top Microbiol Immunol *311*, 1-16.

Albrecht, U., Sun, Z.S., Eichele, G., and Lee, C.C. (1997). A differential response of two putative mammalian circadian regulators, mper1 and mper2, to light. Cell *91*, 1055-1064.

Alibhai, F.J., Tsimakouridze, E.V., Reitz, C.J., Pyle, W.G., and Martino, T.A. (2015). Consequences of Circadian and Sleep Disturbances for the Cardiovascular System. Can J Cardiol *31*, 860-872.

Anderson, D.C., Schmalstieg, F.C., Arnaout, M.A., Kohl, S., Tosi, M.F., Dana, N., Buffone, G.J., Hughes, B.J., Brinkley, B.R., Dickey, W.D.*, et al.* (1984). Abnormalities of polymorphonuclear leukocyte function associated with a heritable deficiency of high molecular weight surface glycoproteins (GP138): common relationship to diminished cell adherence. J Clin Invest *74*, 536-551.

Arjona, A., and Sarkar, D.K. (2005). Circadian oscillations of clock genes, cytolytic factors, and cytokines in rat NK cells. J Immunol *174*, 7618-7624.

Arumugam, M., Raes, J., Pelletier, E., Le Paslier, D., Yamada, T., Mende, D.R., Fernandes, G.R., Tap, J., Bruls, T., Batto, J.M.*, et al.* (2011). Enterotypes of the human gut microbiome. Nature *473*, 174-180.

Asher, G., and Sassone-Corsi, P. (2015). Time for food: the intimate interplay between nutrition, metabolism, and the circadian clock. Cell *161*, 84-92.

Balmer, M.L., Schurch, C.M., Saito, Y., Geuking, M.B., Li, H., Cuenca, M., Kovtonyuk, L.V., McCoy, K.D., Hapfelmeier, S., Ochsenbein, A.F.*, et al.* (2014). Microbiota-derived compounds drive steady-state granulopoiesis via MyD88/TICAM signaling. J Immunol *193*, 5273-5283.

Barbalat, R., Lau, L., Locksley, R.M., and Barton, G.M. (2009). Toll-like receptor 2 on inflammatory monocytes induces type I interferon in response to viral but not bacterial ligands. Nature immunology *10*, 1200-1207.

Basan, M., Elgeti, J., Hannezo, E., Rappel, W.J., and Levine, H. (2013). Alignment of cellular motility forces with tissue flow as a mechanism for efficient wound healing. Proc Natl Acad Sci U S A *110*, 2452-2459.

Bass, J., and Takahashi, J.S. (2010). Circadian integration of metabolism and energetics. Science *330*, 1349-1354.

Bell-Pedersen, D., Cassone, V.M., Earnest, D.J., Golden, S.S., Hardin, P.E., Thomas, T.L., and Zoran, M.J. (2005). Circadian rhythms from multiple oscillators: lessons from diverse organisms. Nat Rev Genet *6*, 544-556.

Bengmark, S. (1998). Ecological control of the gastrointestinal tract. The role of probiotic flora. Gut *42*, 2-7.

Bonilla, F.A., and Oettgen, H.C. (2010). Adaptive immunity. J Allergy Clin Immunol *125*, S33-40.

Brown, K., DeCoffe, D., Molcan, E., and Gibson, D.L. (2012). Diet-induced dysbiosis of the intestinal microbiota and the effects on immunity and disease. Nutrients *4*, 1095-1119.

Bruce, V.G.a.P., Colin S. (1957). Endogenous Rhythms in Insects and Microorganisms. The American Naturalist *91*, 179-195.

Bunger, M.K., Wilsbacher, L.D., Moran, S.M., Clendenin, C., Radcliffe, L.A., Hogenesch, J.B., Simon, M.C., Takahashi, J.S., and Bradfield, C.A. (2000). Mop3 is an essential component of the master circadian pacemaker in mammals. Cell *103*, 1009-1017.

Cario, E. (2008). Barrier-protective function of intestinal epithelial Toll-like receptor 2. Mucosal Immunol *1 Suppl 1*, S62-66.

Cario, E., Rosenberg, I.M., Brandwein, S.L., Beck, P.L., Reinecker, H.C., and Podolsky, D.K. (2000). Lipopolysaccharide activates distinct signaling pathways in intestinal epithelial cell lines expressing Toll-like receptors. Journal of immunology *164*, 966-972.

Caruso, R., Warner, N., Inohara, N., and Nunez, G. (2014). NOD1 and NOD2: signaling, host defense, and inflammatory disease. Immunity *41*, 898-908.

Carvas, J.M., Vukolic, A., Yepuri, G., Xiong, Y., Popp, K., Schmutz, I., Chappuis, S., Albrecht, U., Ming, X.F., Montani, J.P*., et al.* (2012). Period2 gene mutant mice show compromised insulin-mediated endothelial nitric oxide release and altered glucose homeostasis. Front Physiol *3*, 337.

Casanova-Acebes, M., Pitaval, C., Weiss, L.A., Nombela-Arrieta, C., Chevre, R., N, A.G., Kunisaki, Y., Zhang, D., van Rooijen, N., Silberstein, L.E*., et al.* (2013). Rhythmic modulation of the hematopoietic niche through neutrophil clearance. Cell *153*, 1025-1035.

Cermakian, N., Lange, T., Golombek, D., Sarkar, D., Nakao, A., Shibata, S., and Mazzoccoli, G. (2013). Crosstalk between the circadian clock circuitry and the immune system. Chronobiol Int *30*, 870-888.

Chaix, A., Lin, T., Le, H.D., Chang, M.W., and Panda, S. (2019). Time-Restricted Feeding Prevents Obesity and Metabolic Syndrome in Mice Lacking a Circadian Clock. Cell Metab *29*, 303-319 e304.

Cheng, M., and Qin, G. (2012). Progenitor cell mobilization and recruitment: SDF-1, CXCR4, alpha4-integrin, and c-kit. Prog Mol Biol Transl Sci *111*, 243-264.

Chu, H., and Mazmanian, S.K. (2013). Innate immune recognition of the microbiota promotes host-microbial symbiosis. Nature immunology *14*, 668-675.

Clarke, T.B., Davis, K.M., Lysenko, E.S., Zhou, A.Y., Yu, Y., and Weiser, J.N. (2010). Recognition of peptidoglycan from the microbiota by Nod1 enhances systemic innate immunity. Nature medicine *16*, 228-231.

Coban, C., Igari, Y., Yagi, M., Reimer, T., Koyama, S., Aoshi, T., Ohata, K., Tsukui, T., Takeshita, F., Sakurai, K*., et al.* (2010). Immunogenicity of whole-parasite vaccines against Plasmodium falciparum involves malarial hemozoin and host TLR9. Cell Host Microbe *7*, 50-61.

Corbitt, N., Kimura, S., Isse, K., Specht, S., Chedwick, L., Rosborough, B.R., Lunz, J.G., Murase, N., Yokota, S., and Demetris, A.J. (2013). Gut bacteria drive Kupffer cell expansion via MAMP-mediated ICAM-1 induction on sinusoidal endothelium and influence preservation-reperfusion injury after orthotopic liver transplantation. Am J Pathol *182*, 180-191.

Crosby, P., Hamnett, R., Putker, M., Hoyle, N.P., Reed, M., Karam, C.J., Maywood, E.S., Stangherlin, A., Chesham, J.E., Hayter, E.A*., et al.* (2019). Insulin/IGF-1 Drives PERIOD Synthesis to Entrain Circadian Rhythms with Feeding Time. Cell *177*, 896-909 e820.

Curtis, A.M., Bellet, M.M., Sassone-Corsi, P., and O'Neill, L.A. (2014). Circadian clock proteins and immunity. Immunity *40*, 178-186.

Curtis, A.M., Fagundes, C.T., Yang, G., Palsson-McDermott, E.M., Wochal, P., McGettrick, A.F., Foley, N.H., Early, J.O., Chen, L., Zhang, H*., et al.* (2015). Circadian control of innate immunity in macrophages by miR-155 targeting Bmal1. Proc Natl Acad Sci U S A *112*, 7231-7236.

Dallmann, R., Viola, A.U., Tarokh, L., Cajochen, C., and Brown, S.A. (2012). The human circadian metabolome. Proc Natl Acad Sci U S A *109*, 2625-2629.

Damiola, F., Le Minh, N., Preitner, N., Kornmann, B., Fleury-Olela, F., and Schibler, U. (2000). Restricted feeding uncouples circadian oscillators in peripheral tissues from the central pacemaker in the suprachiasmatic nucleus. Genes Dev *14*, 2950-2961.

Delezie, J., Dumont, S., Dardente, H., Oudart, H., Grechez-Cassiau, A., Klosen, P., Teboul, M., Delaunay, F., Pevet, P., and Challet, E. (2012). The nuclear receptor REV-ERBalpha is required for the daily balance of carbohydrate and lipid metabolism. FASEB J *26*, 3321-3335.

den Haan, J.M., Arens, R., and van Zelm, M.C. (2014). The activation of the adaptive immune system: cross-talk between antigen-presenting cells, T cells and B cells. Immunol Lett *162*, 103-112.

Dicksved, J., Halfvarson, J., Rosenquist, M., Jarnerot, G., Tysk, C., Apajalahti, J., Engstrand, L., and Jansson, J.K. (2008). Molecular analysis of the gut microbiota of identical twins with Crohn's disease. ISME J *2*, 716-727.

Dinarello, C.A. (2009). Immunological and inflammatory functions of the interleukin-1 family. Annu Rev Immunol *27*, 519-550.

Do, M.T., and Yau, K.W. (2010). Intrinsically photosensitive retinal ganglion cells. Physiol Rev *90*, 1547-1581.

Dong, W., Liu, Y., Peng, J., Chen, L., Zou, T., Xiao, H., Liu, Z., Li, W., Bu, Y., and Qi, Y. (2006). The IRAK-1-BCL10-MALT1-TRAF6-TAK1 cascade mediates signaling to NF-kappaB from Toll-like receptor 4. The Journal of biological chemistry *281*, 26029-26040.

Druzd, D., Matveeva, O., Ince, L., Harrison, U., He, W., Schmal, C., Herzel, H., Tsang, A.H., Kawakami, N., Leliavski, A*., et al.* (2017). Lymphocyte Circadian Clocks Control Lymph Node Trafficking and Adaptive Immune Responses. Immunity *46*, 120-132.

Durgan, D.J., Pulinilkunnil, T., Villegas-Montoya, C., Garvey, M.E., Frangogiannis, N.G., Michael, L.H., Chow, C.W., Dyck, J.R., and Young, M.E. (2010). Short communication: ischemia/reperfusion tolerance is time-of-day-dependent: mediation by the cardiomyocyte circadian clock. Circ Res *106*, 546-550.

Eastman, C.I., Mistlberger, R.E., and Rechtschaffen, A. (1984). Suprachiasmatic nuclei lesions eliminate circadian temperature and sleep rhythms in the rat. Physiol Behav *32*, 357-368.

Eckel-Mahan, K., and Sassone-Corsi, P. (2015). Phenotyping Circadian Rhythms in Mice. Curr Protoc Mouse Biol *5*, 271-281.

Ella, K., Mocsai, A., and Kaldi, K. (2018). Circadian regulation of neutrophils: Control by a cell-autonomous clock or systemic factors? Eur J Clin Invest *48 Suppl 2*, e12965.

Epelman, S., Lavine, K.J., and Randolph, G.J. (2014). Origin and functions of tissue macrophages. Immunity *41*, 21-35.

Ewald, S.E., Lee, B.L., Lau, L., Wickliffe, K.E., Shi, G.P., Chapman, H.A., and Barton, G.M. (2008). The ectodomain of Toll-like receptor 9 is cleaved to generate a functional receptor. Nature *456*, 658-662.

Fonken, L.K., Aubrecht, T.G., Melendez-Fernandez, O.H., Weil, Z.M., and Nelson, R.J. (2013). Dim light at night disrupts molecular circadian rhythms and increases body weight. J Biol Rhythms *28*, 262-271.

Fortier, E.E., Rooney, J., Dardente, H., Hardy, M.P., Labrecque, N., and Cermakian, N. (2011). Circadian variation of the response of T cells to antigen. J Immunol *187*, 6291-6300.

Frazer, L.C., Sullivan, J.E., Zurenski, M.A., Mintus, M., Tomasak, T.E., Prantner, D., Nagarajan, U.M., and Darville, T. (2013). CD4+ T cell expression of MyD88 is essential for normal resolution of Chlamydia muridarum genital tract infection. Journal of immunology *191*, 4269-4279.

Fu, L., and Kettner, N.M. (2013). The circadian clock in cancer development and therapy. Prog Mol Biol Transl Sci *119*, 221-282.

Gardner, M.J., Hubbard, K.E., Hotta, C.T., Dodd, A.N., and Webb, A.A. (2006). How plants tell the time. The Biochemical journal *397*, 15-24.

Gekle M, W.E., Gründer S, Petersen M, Schwab A, Markwardt F, Klöcker N, Baumann R, Marti H (2010). Taschenlehrbuch Physiologie (Thieme).

Gibbs, J.E., Blaikley, J., Beesley, S., Matthews, L., Simpson, K.D., Boyce, S.H., Farrow, S.N., Else, K.J., Singh, D., Ray, D.W*., et al.* (2012). The nuclear receptor REV-ERBalpha mediates circadian regulation of innate immunity through selective regulation of inflammatory cytokines. Proc Natl Acad Sci U S A *109*, 582-587.

Godinho-Silva, C., Domingues, R.G., Rendas, M., Raposo, B., Ribeiro, H., da Silva, J.A., Vieira, A., Costa, R.M., Barbosa-Morais, N.L., Carvalho, T*., et al.* (2019). Light-entrained and brain-tuned circadian circuits regulate ILC3s and gut homeostasis. Nature *574*, 254-258.

Green, D.J., and Gillette, R. (1982). Circadian rhythm of firing rate recorded from single cells in the rat suprachiasmatic brain slice. Brain Res *245*, 198-200.

Griffin, E.A., Jr., Staknis, D., and Weitz, C.J. (1999). Light-independent role of CRY1 and CRY2 in the mammalian circadian clock. Science *286*, 768-771.

Guillaumond, F., Dardente, H., Giguere, V., and Cermakian, N. (2005). Differential control of Bmal1 circadian transcription by REV-ERB and ROR nuclear receptors. J Biol Rhythms *20*, 391-403.

Hacker, H., Redecke, V., Blagoev, B., Kratchmarova, I., Hsu, L.C., Wang, G.G., Kamps, M.P., Raz, E., Wagner, H., Hacker, G*., et al.* (2006). Specificity in Toll-like receptor signalling through distinct effector functions of TRAF3 and TRAF6. Nature *439*, 204-207.

Halberg, F., Johnson, E.A., Brown, B.W., and Bittner, J.J. (1960). Susceptibility rhythm to E. coli endotoxin and bioassay. Proc Soc Exp Biol Med *103*, 142-144.

Hall, J.A., Bouladoux, N., Sun, C.M., Wohlfert, E.A., Blank, R.B., Zhu, Q., Grigg, M.E., Berzofsky, J.A., and Belkaid, Y. (2008). Commensal DNA limits regulatory T cell conversion and is a natural adjuvant of intestinal immune responses. Immunity *29*, 637-649.

Hara, R., Wan, K., Wakamatsu, H., Aida, R., Moriya, T., Akiyama, M., and Shibata, S. (2001). Restricted feeding entrains liver clock without participation of the suprachiasmatic nucleus. Genes Cells *6*, 269-278.

Haspel, J.A., Chettimada, S., Shaik, R.S., Chu, J.H., Raby, B.A., Cernadas, M., Carey, V., Process, V., Hunninghake, G.M., Ifedigbo, E.*, et al.* (2014). Circadian rhythm reprogramming during lung inflammation. Nat Commun *5*, 4753.

Hayashi, M., Shimba, S., and Tezuka, M. (2007). Characterization of the molecular clock in mouse peritoneal macrophages. Biol Pharm Bull *30*, 621-626.

He, W., Holtkamp, S., Hergenhan, S.M., Kraus, K., de Juan, A., Weber, J., Bradfield, P., Grenier, J.M.P., Pelletier, J., Druzd, D.*, et al.* (2018). Circadian Expression of Migratory Factors Establishes Lineage-Specific Signatures that Guide the Homing of Leukocyte Subsets to Tissues. Immunity *49*, 1175-1190 e1177.

Hepworth, M.R., Monticelli, L.A., Fung, T.C., Ziegler, C.G., Grunberg, S., Sinha, R., Mantegazza, A.R., Ma, H.L., Crawford, A., Angelosanto, J.M.*, et al.* (2013). Innate lymphoid cells regulate CD4+ T-cell responses to intestinal commensal bacteria. Nature *498*, 113-117.

Hill, D.A., Siracusa, M.C., Abt, M.C., Kim, B.S., Kobuley, D., Kubo, M., Kambayashi, T., Larosa, D.F., Renner, E.D., Orange, J.S.*, et al.* (2012). Commensal bacteria-derived signals regulate basophil hematopoiesis and allergic inflammation. Nature medicine *18*, 538-546.

Illing, H.P. (1981). Techniques for microfloral and associated metabolic studies in relation to the absorption and enterohepatic circulation of drugs. Xenobiotica *11*, 815-830.

Ip, W.K., and Medzhitov, R. (2015). Macrophages monitor tissue osmolarity and induce inflammatory response through NLRP3 and NLRC4 inflammasome activation. Nat Commun *6*, 6931.

Janeway CA, T.P., Walport M, Shlomchik M (2001). Immunobiology, Vol 5 (New York, USA: Garland Publishing).

Kawagoe, T., Sato, S., Matsushita, K., Kato, H., Matsui, K., Kumagai, Y., Saitoh, T., Kawai, T., Takeuchi, O., and Akira, S. (2008). Sequential control of Toll-like receptor-dependent responses by IRAK1 and IRAK2. Nature immunology *9*, 684-691.

Kawai, T., and Akira, S. (2010). The role of pattern-recognition receptors in innate immunity: update on Toll-like receptors. Nature immunology *11*, 373-384.

Keller, M., Mazuch, J., Abraham, U., Eom, G.D., Herzog, E.D., Volk, H.D., Kramer, A., and Maier, B. (2009). A circadian clock in macrophages controls inflammatory immune responses. Proc Natl Acad Sci U S A *106*, 21407-21412.

Kennedy, E.A., King, K.Y., and Baldridge, M.T. (2018). Mouse Microbiota Models: Comparing Germ-Free Mice and Antibiotics Treatment as Tools for Modifying Gut Bacteria. Front Physiol *9*, 1534.

Kim, K.S., Kim, Y.C., Oh, I.J., Kim, S.S., Choi, J.Y., and Ahn, R.S. (2012). Association of worse prognosis with an aberrant diurnal cortisol rhythm in patients with advanced lung cancer. Chronobiol Int *29*, 1109-1120.

Koblansky, A.A., Jankovic, D., Oh, H., Hieny, S., Sungnak, W., Mathur, R., Hayden, M.S., Akira, S., Sher, A., and Ghosh, S. (2013). Recognition of profilin by Toll-like receptor 12 is critical for host resistance to Toxoplasma gondii. Immunity *38*, 119-130.

Koeth, R.A., Wang, Z., Levison, B.S., Buffa, J.A., Org, E., Sheehy, B.T., Britt, E.B., Fu, X., Wu, Y., Li, L.*, et al.* (2013). Intestinal microbiota metabolism of L-carnitine, a nutrient in red meat, promotes atherosclerosis. Nature medicine *19*, 576-585.

Komatsu, T., Aida, Y., Fukuda, T., Sanui, T., Hiratsuka, S., Pabst, M.J., and Nishimura, F. (2016). Disaggregation of lipopolysaccharide by albumin, hemoglobin or high-density lipoprotein, forming complexes that prime neutrophils for enhanced release of superoxide. Pathog Dis *74*.

Krieger, D.T., Hauser, H., and Krey, L.C. (1977). Suprachiasmatic nuclear lesions do not abolish food-shifted circadian adrenal and temperature rhythmicity. Science *197*, 398-399.

Kubo, T., Ozasa, K., Mikami, K., Wakai, K., Fujino, Y., Watanabe, Y., Miki, T., Nakao, M., Hayashi, K., Suzuki, K.*, et al.* (2006). Prospective cohort study of the risk of prostate cancer among rotating-shift workers: findings from the Japan collaborative cohort study. Am J Epidemiol *164*, 549-555.

Kurosawa, G., Aihara, K., and Iwasa, Y. (2006). A model for the circadian rhythm of cyanobacteria that maintains oscillation without gene expression. Biophys J *91*, 2015-2023.

Kyoko, O.O., Kono, H., Ishimaru, K., Miyake, K., Kubota, T., Ogawa, H., Okumura, K., Shibata, S., and Nakao, A. (2014). Expressions of tight junction proteins Occludin and Claudin-1 are under the circadian control in the mouse large intestine: implications in intestinal permeability and susceptibility to colitis. PLoS One *9*, e98016.

Lahti, T.A., Partonen, T., Kyyronen, P., Kauppinen, T., and Pukkala, E. (2008). Night-time work predisposes to non-Hodgkin lymphoma. Int J Cancer *123*, 2148-2151.

Lampe, J.W. (2008). The Human Microbiome Project: getting to the guts of the matter in cancer epidemiology. Cancer Epidemiol Biomarkers Prev *17*, 2523-2524.

Larochelle, P. (2002). Circadian variation in blood pressure: dipper or nondipper. J Clin Hypertens (Greenwich) *4*, 3-8.

Lauw, F.N., Caffrey, D.R., and Golenbock, D.T. (2005). Of mice and man: TLR11 (finally) finds profilin. Trends Immunol *26*, 509-511.

Leone, V., Gibbons, S.M., Martinez, K., Hutchison, A.L., Huang, E.Y., Cham, C.M., Pierre, J.F., Heneghan, A.F., Nadimpalli, A., Hubert, N.*, et al.* (2015). Effects of diurnal variation of gut microbes and high-fat feeding on host circadian clock function and metabolism. Cell Host Microbe *17*, 681-689.

Leproult, R., Holmback, U., and Van Cauter, E. (2014). Circadian misalignment augments markers of insulin resistance and inflammation, independently of sleep loss. Diabetes *63*, 1860-1869.

Levi, F., Filipski, E., Iurisci, I., Li, X.M., and Innominato, P. (2007). Cross-talks between circadian timing system and cell division cycle determine cancer biology and therapeutics. Cold Spring Harb Symp Quant Biol *72*, 465-475.

Levy, M., Thaiss, C.A., and Elinav, E. (2016). Metabolites: messengers between the microbiota and the immune system. Genes & development *30*, 1589-1597.

Ley, K., Laudanna, C., Cybulsky, M.I., and Nourshargh, S. (2007). Getting to the site of inflammation: the leukocyte adhesion cascade updated. Nat Rev Immunol *7*, 678-689.

Liang, X., Bushman, F.D., and FitzGerald, G.A. (2015). Rhythmicity of the intestinal microbiota is regulated by gender and the host circadian clock. Proc Natl Acad Sci U S A *112*, 10479-10484.

Lippert, U., Zachmann, K., Henz, B.M., and Neumann, C. (2004). Human T lymphocytes and mast cells differentially express and regulate extra- and intracellular CXCR1 and CXCR2. Exp Dermatol *13*, 520-525.

Litinski, M., Scheer, F.A., and Shea, S.A. (2009). Influence of the Circadian System on Disease Severity. Sleep Med Clin *4*, 143-163.

Littman, D.R., and Pamer, E.G. (2011). Role of the commensal microbiota in normal and pathogenic host immune responses. Cell Host Microbe *10*, 311-323.

Loures, F.V., Pina, A., Felonato, M., Feriotti, C., de Araujo, E.F., and Calich, V.L. (2011). MyD88 signaling is required for efficient innate and adaptive immune responses to Paracoccidioides brasiliensis infection. Infect Immun *79*, 2470-2480.

Lu, Y.C., Yeh, W.C., and Ohashi, P.S. (2008). LPS/TLR4 signal transduction pathway. Cytokine *42*, 145-151.

Lucas, D., Battista, M., Shi, P.A., Isola, L., and Frenette, P.S. (2008). Mobilized hematopoietic stem cell yield depends on species-specific circadian timing. Cell stem cell *3*, 364-366.

Mahla, R.S., Reddy, M.C., Prasad, D.V., and Kumar, H. (2013). Sweeten PAMPs: Role of Sugar Complexed PAMPs in Innate Immunity and Vaccine Biology. Front Immunol *4*, 248.

Mancuso, G., Gambuzza, M., Midiri, A., Biondo, C., Papasergi, S., Akira, S., Teti, G., and Beninati, C. (2009). Bacterial recognition by TLR7 in the lysosomes of conventional dendritic cells. Nature immunology *10*, 587-594.

Manicassamy, S., and Pulendran, B. (2009). Modulation of adaptive immunity with Toll-like receptors. Seminars in immunology *21*, 185-193.

Marcheva, B., Ramsey, K.M., Buhr, E.D., Kobayashi, Y., Su, H., Ko, C.H., Ivanova, G., Omura, C., Mo, S., Vitaterna, M.H.*, et al.* (2010). Disruption of the clock components CLOCK and BMAL1 leads to hypoinsulinaemia and diabetes. Nature *466*, 627-631.

Marino, M.W., Dunn, A., Grail, D., Inglese, M., Noguchi, Y., Richards, E., Jungbluth, A., Wada, H., Moore, M., Williamson, B.*, et al.* (1997). Characterization of tumor necrosis factor-deficient mice. Proceedings of the National Academy of Sciences of the United States of America *94*, 8093-8098.

Marques, F.Z., Nelson, E., Chu, P.Y., Horlock, D., Fiedler, A., Ziemann, M., Tan, J.K., Kuruppu, S., Rajapakse, N.W., El-Osta, A.*, et al.* (2017). High-Fiber Diet and Acetate Supplementation Change the Gut Microbiota and Prevent the Development of Hypertension and Heart Failure in Hypertensive Mice. Circulation *135*, 964-977.

McEver, R.P., and Cummings, R.D. (1997). Role of PSGL-1 binding to selectins in leukocyte recruitment. J Clin Invest *100*, S97-103.

Mendez-Ferrer, S., Lucas, D., Battista, M., and Frenette, P.S. (2008). Haematopoietic stem cell release is regulated by circadian oscillations. Nature *452*, 442-447.

Miyake, S., Sumi, Y., Yan, L., Takekida, S., Fukuyama, T., Ishida, Y., Yamaguchi, S., Yagita, K., and Okamura, H. (2000). Phase-dependent responses of Per1 and Per2 genes to a light-stimulus in the suprachiasmatic nucleus of the rat. Neuroscience letters *294*, 41-44.

Mizrahi, K., and Askenasy, N. (2014). Physiological functions of TNF family receptor/ligand interactions in hematopoiesis and transplantation. Blood *124*, 176-183.

Mizutani, H., Tamagawa-Mineoka, R., Minami, Y., Yagita, K., and Katoh, N. (2017). Constant light exposure impairs immune tolerance development in mice. J Dermatol Sci *86*, 63-70.

Montagner, A., Korecka, A., Polizzi, A., Lippi, Y., Blum, Y., Canlet, C., Tremblay-Franco, M., Gautier-Stein, A., Burcelin, R., Yen, Y.C.*, et al.* (2016). Hepatic circadian clock oscillators and nuclear receptors integrate microbiome-derived signals. Sci Rep *6*, 20127.

Moore, R.Y. (1973). Retinohypothalamic projection in mammals: a comparative study. Brain Res *49*, 403-409.

Mrosovsky, N., Reebs, S.G., Honrado, G.I., and Salmon, P.A. (1989). Behavioural entrainment of circadian rhythms. Experientia *45*, 696-702.

Mukherji, A., Kobiita, A., Damara, M., Misra, N., Meziane, H., Champy, M.F., and Chambon, P. (2015). Shifting eating to the circadian rest phase misaligns the peripheral clocks with the master SCN clock and leads to a metabolic syndrome. Proc Natl Acad Sci U S A *112*, E6691-6698.

Mukherji, A., Kobiita, A., Ye, T., and Chambon, P. (2013). Homeostasis in intestinal epithelium is orchestrated by the circadian clock and microbiota cues transduced by TLRs. Cell *153*, 812-827.

Muller, E., Dagenais, P., Alami, N., and Rola-Pleszczynski, M. (1993). Identification and functional characterization of platelet-activating factor receptors in human leukocyte populations using polyclonal anti-peptide antibody. Proceedings of the National Academy of Sciences of the United States of America *90*, 5818-5822.

Nagy F, K.S., Chua N-H (1988). A circadian clock regulates transcription of the wheat Cab-1 gene. Genes Dev *2*, 376-382.

Nakajima, M., Imai, K., Ito, H., Nishiwaki, T., Murayama, Y., Iwasaki, H., Oyama, T., and Kondo, T. (2005). Reconstitution of circadian oscillation of cyanobacterial KaiC phosphorylation in vitro. Science *308*, 414-415.

Nguyen, K.D., Fentress, S.J., Qiu, Y., Yun, K., Cox, J.S., and Chawla, A. (2013). Circadian gene Bmal1 regulates diurnal oscillations of Ly6C(hi) inflammatory monocytes. Science *341*, 1483-1488.

O'Neill, L.A., and Bowie, A.G. (2007). The family of five: TIR-domain-containing adaptors in Toll-like receptor signalling. Nat Rev Immunol *7*, 353-364.

Oeckinghaus, A., and Ghosh, S. (2009). The NF-kappaB family of transcription factors and its regulation. Cold Spring Harb Perspect Biol *1*, a000034.

Ohno, T., Onishi, Y., and Ishida, N. (2007). The negative transcription factor E4BP4 is associated with circadian clock protein PERIOD2. Biochem Biophys Res Commun *354*, 1010-1015.

Oldenburg, M., Kruger, A., Ferstl, R., Kaufmann, A., Nees, G., Sigmund, A., Bathke, B., Lauterbach, H., Suter, M., Dreher, S*., et al.* (2012). TLR13 recognizes bacterial 23S rRNA devoid of erythromycin resistance-forming modification. Science *337*, 1111-1115.

Oosting, M., Cheng, S.C., Bolscher, J.M., Vestering-Stenger, R., Plantinga, T.S., Verschueren, I.C., Arts, P., Garritsen, A., van Eenennaam, H., Sturm, P*., et al.* (2014). Human TLR10 is an anti-inflammatory pattern-recognition receptor. Proceedings of the National Academy of Sciences of the United States of America *111*, E4478-4484.

Oster, H., Damerow, S., Kiessling, S., Jakubcakova, V., Abraham, D., Tian, J., Hoffmann, M.W., and Eichele, G. (2006). The circadian rhythm of glucocorticoids is regulated by a gating mechanism residing in the adrenal cortical clock. Cell Metab *4*, 163-173.

Panda, S., Antoch, M.P., Miller, B.H., Su, A.I., Schook, A.B., Straume, M., Schultz, P.G., Kay, S.A., Takahashi, J.S., and Hogenesch, J.B. (2002). Coordinated transcription of key pathways in the mouse by the circadian clock. Cell *109*, 307-320.

Pasparakis, M., Alexopoulou, L., Episkopou, V., and Kollias, G. (1996). Immune and inflammatory responses in TNF alpha-deficient mice: a critical requirement for TNF alpha in the formation of primary B cell follicles, follicular dendritic cell networks and germinal centers, and in the maturation of the humoral immune response. J Exp Med *184*, 1397-1411.

Pendergast, J.S., and Yamazaki, S. (2018). The Mysterious Food-Entrainable Oscillator: Insights from Mutant and Engineered Mouse Models. J Biol Rhythms *33*, 458-474.

Petersen, C., and Round, J.L. (2014). Defining dysbiosis and its influence on host immunity and disease. Cellular microbiology *16*, 1024-1033.

Petrovsky, N., and Harrison, L.C. (1998). The chronobiology of human cytokine production. Int Rev Immunol *16*, 635-649.

Pezuk, P., Mohawk, J.A., Yoshikawa, T., Sellix, M.T., and Menaker, M. (2010). Circadian organization is governed by extra-SCN pacemakers. J Biol Rhythms *25*, 432-441.

Piras, V., and Selvarajoo, K. (2014). Beyond MyD88 and TRIF Pathways in Toll-Like Receptor Signaling. Front Immunol *5*, 70.

Pittendrigh, C.S. (1993). Temporal organization: reflections of a Darwinian clock-watcher. Annu Rev Physiol *55*, 16-54.

Pobezinskaya, Y.L., Kim, Y.S., Choksi, S., Morgan, M.J., Li, T., Liu, C., and Liu, Z. (2008). The function of TRADD in signaling through tumor necrosis factor receptor 1 and TRIF-dependent Toll-like receptors. Nature immunology *9*, 1047-1054.

Premack, B.A., and Schall, T.J. (1996). Chemokine receptors: gateways to inflammation and infection. Nature medicine *2*, 1174-1178.

Rausch, P., Basic, M., Batra, A., Bischoff, S.C., Blaut, M., Clavel, T., Glasner, J., Gopalakrishnan, S., Grassl, G.A., Gunther, C*., et al.* (2016). Analysis of factors contributing to variation in the C57BL/6J fecal microbiota across German animal facilities. Int J Med Microbiol *306*, 343-355.

Reddy, P., Zehring, W.A., Wheeler, D.A., Pirrotta, V., Hadfield, C., Hall, J.C., and Rosbash, M. (1984). Molecular analysis of the period locus in Drosophila melanogaster and identification of a transcript involved in biological rhythms. Cell *38*, 701-710.

Robles, M.S., Cox, J., and Mann, M. (2014). In-vivo quantitative proteomics reveals a key contribution of post-transcriptional mechanisms to the circadian regulation of liver metabolism. PLoS Genet *10*, e1004047.

Rosenfeld, P., van Eekelen, J.A., Levine, S., and de Kloet, E.R. (1993). Ontogeny of corticosteroid receptors in the brain. Cell Mol Neurobiol *13*, 295-319.

Rothfuchs, A.G., Bafica, A., Feng, C.G., Egen, J.G., Williams, D.L., Brown, G.D., and Sher, A. (2007). Dectin-1 interaction with Mycobacterium tuberculosis leads to enhanced IL-12p40 production by splenic dendritic cells. Journal of immunology *179*, 3463-3471.

Round, J.L., and Mazmanian, S.K. (2009). The gut microbiota shapes intestinal immune responses during health and disease. Nat Rev Immunol *9*, 313-323.

Round, J.L., O'Connell, R.M., and Mazmanian, S.K. (2010). Coordination of tolerogenic immune responses by the commensal microbiota. J Autoimmun *34*, J220-225.

Sampson, T.R., Debelius, J.W., Thron, T., Janssen, S., Shastri, G.G., Ilhan, Z.E., Challis, C., Schretter, C.E., Rocha, S., Gradinaru, V*., et al.* (2016). Gut Microbiota Regulate Motor Deficits and Neuroinflammation in a Model of Parkinson's Disease. Cell *167*, 1469-1480 e1412.

Sangoram, A.M., Saez, L., Antoch, M.P., Gekakis, N., Staknis, D., Whiteley, A., Fruechte, E.M., Vitaterna, M.H., Shimomura, K., King, D.P*., et al.* (1998). Mammalian circadian autoregulatory loop: a timeless ortholog and mPer1 interact and negatively regulate CLOCK-BMAL1-induced transcription. Neuron *21*, 1101-1113.

Sato, K., Yang, X.L., Yudate, T., Chung, J.S., Wu, J., Luby-Phelps, K., Kimberly, R.P., Underhill, D., Cruz, P.D., Jr., and Ariizumi, K. (2006). Dectin-2 is a pattern recognition receptor for fungi that couples with the Fc receptor gamma chain to induce innate immune responses. The Journal of biological chemistry *281*, 38854-38866.

Scheiermann, C., Kunisaki, Y., and Frenette, P.S. (2013). Circadian control of the immune system. Nat Rev Immunol *13*, 190-198.

Scheiermann, C., Kunisaki, Y., Lucas, D., Chow, A., Jang, J.E., Zhang, D., Hashimoto, D., Merad, M., and Frenette, P.S. (2012). Adrenergic nerves govern circadian leukocyte recruitment to tissues. Immunity *37*, 290-301.

Schernhammer, E.S., Laden, F., Speizer, F.E., Willett, W.C., Hunter, D.J., Kawachi, I., Fuchs, C.S., and Colditz, G.A. (2003). Night-shift work and risk of colorectal cancer in the nurses' health study. J Natl Cancer Inst *95*, 825-828.

Schwarzenberger, P., La Russa, V., Miller, A., Ye, P., Huang, W., Zieske, A., Nelson, S., Bagby, G.J., Stoltz, D., Mynatt, R.L*., et al.* (1998). IL-17 stimulates granulopoiesis in mice: use of an alternate, novel gene therapy-derived method for in vivo evaluation of cytokines. Journal of immunology *161*, 6383-6389.

Sender, R., Fuchs, S., and Milo, R. (2016). Are We Really Vastly Outnumbered? Revisiting the Ratio of Bacterial to Host Cells in Humans. Cell *164*, 337-340.

Seong, S.Y., and Matzinger, P. (2004). Hydrophobicity: an ancient damage-associated molecular pattern that initiates innate immune responses. Nat Rev Immunol *4*, 469-478.

Sephton, S.E., Sapolsky, R.M., Kraemer, H.C., and Spiegel, D. (2000). Diurnal cortisol rhythm as a predictor of breast cancer survival. J Natl Cancer Inst *92*, 994-1000.

Shackelford, P.G., and Feigin, R.D. (1973). Periodicity of susceptibility to pneumococcal infection: influence of light and adrenocortical secretions. Science *182*, 285-287.

Shen, Y., Giardino Torchia, M.L., Lawson, G.W., Karp, C.L., Ashwell, J.D., and Mazmanian, S.K. (2012). Outer membrane vesicles of a human commensal mediate immune regulation and disease protection. Cell Host Microbe *12*, 509-520.

Shi, Z., Cai, Z., Sanchez, A., Zhang, T., Wen, S., Wang, J., Yang, J., Fu, S., and Zhang, D. (2011). A novel Toll-like receptor that recognizes vesicular stomatitis virus. The Journal of biological chemistry *286*, 4517-4524.

Silver, A.C., Arjona, A., Hughes, M.E., Nitabach, M.N., and Fikrig, E. (2012a). Circadian expression of clock genes in mouse macrophages, dendritic cells, and B cells. Brain Behav Immun *26*, 407-413.

Silver, A.C., Arjona, A., Walker, W.E., and Fikrig, E. (2012b). The circadian clock controls toll-like receptor 9-mediated innate and adaptive immunity. Immunity *36*, 251-261.

So, A.Y., Bernal, T.U., Pillsbury, M.L., Yamamoto, K.R., and Feldman, B.J. (2009). Glucocorticoid regulation of the circadian clock modulates glucose homeostasis. Proc Natl Acad Sci U S A *106*, 17582-17587.

Stappenbeck, T.S., and Gordon, J.I. (2001). Extranuclear sequestration of phospho-Jun N-terminal kinase and distorted villi produced by activated Rac1 in the intestinal epithelium of chimeric mice. Development *128*, 2603-2614.

Stenzinger, M., Karpova, D., Unterrainer, C., Harenkamp, S., Wiercinska, E., Hoerster, K., Pfeffer, M., Maronde, E., and Bonig, H. (2019). Hematopoietic-Extrinsic Cues Dictate Circadian Redistribution of Mature and Immature Hematopoietic Cells in Blood and Spleen. Cells *8*.

Stephan, F.K., Swann, J.M., and Sisk, C.L. (1979). Entrainment of circadian rhythms by feeding schedules in rats with suprachiasmatic lesions. Behav Neural Biol *25*, 545-554.

Stephan, F.K., and Zucker, I. (1972). Circadian rhythms in drinking behavior and locomotor activity of rats are eliminated by hypothalamic lesions. Proceedings of the National Academy of Sciences of the United States of America *69*, 1583-1586.

Stevens, C.E., and Hume, I.D. (1998). Contributions of microbes in vertebrate gastrointestinal tract to production and conservation of nutrients. Physiol Rev *78*, 393-427.

Stevens, R.G. (2009). Working against our endogenous circadian clock: Breast cancer and electric lighting in the modern world. Mutat Res *680*, 106-108.

Stevens, R.G., Blask, D.E., Brainard, G.C., Hansen, J., Lockley, S.W., Provencio, I., Rea, M.S., and Reinlib, L. (2007). Meeting report: the role of environmental lighting and circadian disruption in cancer and other diseases. Environ Health Perspect *115*, 1357-1362.

Storch, K.F., Lipan, O., Leykin, I., Viswanathan, N., Davis, F.C., Wong, W.H., and Weitz, C.J. (2002). Extensive and divergent circadian gene expression in liver and heart. Nature *417*, 78-83.

Stratmann, M., and Schibler, U. (2006). Properties, entrainment, and physiological functions of mammalian peripheral oscillators. J Biol Rhythms *21*, 494-506.

Sunderkotter, C., Nikolic, T., Dillon, M.J., Van Rooijen, N., Stehling, M., Drevets, D.A., and Leenen, P.J. (2004). Subpopulations of mouse blood monocytes differ in maturation stage and inflammatory response. J Immunol *172*, 4410-4417.

Suwa, T., Hogg, J.C., English, D., and Van Eeden, S.F. (2000). Interleukin-6 induces demargination of intravascular neutrophils and shortens their transit in marrow. Am J Physiol Heart Circ Physiol *279*, H2954-2960.

Tahara, Y., and Shibata, S. (2013). Chronobiology and nutrition. Neuroscience *253*, 78-88.

Tahara, Y., Yamazaki, M., Sukigara, H., Motohashi, H., Sasaki, H., Miyakawa, H., Haraguchi, A., Ikeda, Y., Fukuda, S., and Shibata, S. (2018). Gut Microbiota-Derived Short Chain Fatty Acids Induce Circadian Clock Entrainment in Mouse Peripheral Tissue. Sci Rep *8*, 1395.

Takahashi, K., Kawai, T., Kumar, H., Sato, S., Yonehara, S., and Akira, S. (2006). Roles of caspase-8 and caspase-10 in innate immune responses to double-stranded RNA. Journal of immunology *176*, 4520-4524.

Takeuchi, O., Sato, S., Horiuchi, T., Hoshino, K., Takeda, K., Dong, Z., Modlin, R.L., and Akira, S. (2002). Cutting edge: role of Toll-like receptor 1 in mediating immune response to microbial lipoproteins. Journal of immunology *169*, 10-14.

Tani, K., Su, S.B., Utsunomiya, I., Oppenheim, J.J., and Wang, J.M. (1998). Interferon-gamma maintains the binding and functional capacity of receptors for IL-8 on cultured human T cells. Eur J Immunol *28*, 502-507.

Teng, F., Goc, J., Zhou, L., Chu, C., Shah, M.A., Eberl, G., and Sonnenberg, G.F. (2019). A circadian clock is essential for homeostasis of group 3 innate lymphoid cells in the gut. Sci Immunol *4*.

Tenoever, B.R., Ng, S.L., Chua, M.A., McWhirter, S.M., Garcia-Sastre, A., and Maniatis, T. (2007). Multiple functions of the IKK-related kinase IKKepsilon in interferon-mediated antiviral immunity. Science *315*, 1274-1278.

Thaiss, C.A., Levy, M., Korem, T., Dohnalova, L., Shapiro, H., Jaitin, D.A., David, E., Winter, D.R., Gury-BenAri, M., Tatirovsky, E.*, et al.* (2016a). Microbiota Diurnal Rhythmicity Programs Host Transcriptome Oscillations. Cell *167*, 1495-1510 e1412.

Thaiss, C.A., Levy, M., Suez, J., and Elinav, E. (2014a). The interplay between the innate immune system and the microbiota. Curr Opin Immunol *26*, 41-48.

Thaiss, C.A., Zeevi, D., Levy, M., Zilberman-Schapira, G., Suez, J., Tengeler, A.C., Abramson, L., Katz, M.N., Korem, T., Zmora, N.*, et al.* (2014b). Transkingdom control of microbiota diurnal oscillations promotes metabolic homeostasis. Cell *159*, 514-529.

Thaiss, C.A., Zmora, N., Levy, M., and Elinav, E. (2016b). The microbiome and innate immunity. Nature *535*, 65-74.

Ueda, H.R., Hayashi, S., Chen, W., Sano, M., Machida, M., Shigeyoshi, Y., Iino, M., and Hashimoto, S. (2005). System-level identification of transcriptional circuits underlying mammalian circadian clocks. Nature genetics *37*, 187-192.

Uematsu, S., Fujimoto, K., Jang, M.H., Yang, B.G., Jung, Y.J., Nishiyama, M., Sato, S., Tsujimura, T., Yamamoto, M., Yokota, Y.*, et al.* (2008). Regulation of humoral and cellular gut immunity by lamina propria dendritic cells expressing Toll-like receptor 5. Nature immunology *9*, 769-776.

Uematsu, S., Jang, M.H., Chevrier, N., Guo, Z., Kumagai, Y., Yamamoto, M., Kato, H., Sougawa, N., Matsui, H., Kuwata, H.*, et al.* (2006). Detection of pathogenic intestinal bacteria by Toll-like receptor 5 on intestinal CD11c+ lamina propria cells. Nature immunology *7*, 868-874.

Van Bezooijen, R.L., Farih-Sips, H.C., Papapoulos, S.E., and Lowik, C.W. (1998). IL-1alpha, IL-1beta, IL-6, and TNF-alpha steady-state mRNA levels analyzed by reverse transcription-competitive PCR in bone marrow of gonadectomized mice. J Bone Miner Res *13*, 185-194.

van Damme, J., Opdenakker, G., de Ley, M., Heremans, H., and Billiau, A. (1986). Pyrogenic and haematological effects of the interferon-inducing 22K factor (interleukin 1 beta) from human leukocytes. Clin Exp Immunol *66*, 303-311.

van Kooyk, Y. (2008). C-type lectins on dendritic cells: key modulators for the induction of immune responses. Biochem Soc Trans *36*, 1478-1481.

Viswanathan, A.N., Hankinson, S.E., and Schernhammer, E.S. (2007). Night shift work and the risk of endometrial cancer. Cancer research *67*, 10618-10622.

Vivier, E., Artis, D., Colonna, M., Diefenbach, A., Di Santo, J.P., Eberl, G., Koyasu, S., Locksley, R.M., McKenzie, A.N.J., Mebius, R.E.*, et al.* (2018). Innate Lymphoid Cells: 10 Years On. Cell *174*, 1054-1066.

Wen, L., Ley, R.E., Volchkov, P.Y., Stranges, P.B., Avanesyan, L., Stonebraker, A.C., Hu, C., Wong, F.S., Szot, G.L., Bluestone, J.A.*, et al.* (2008). Innate immunity and intestinal microbiota in the development of Type 1 diabetes. Nature *455*, 1109-1113.

Whitman, W.B., Coleman, D.C., and Wiebe, W.J. (1998). Prokaryotes: the unseen majority. Proceedings of the National Academy of Sciences of the United States of America *95*, 6578-6583.

Wolf, Y., Shemer, A., Polonsky, M., Gross, M., Mildner, A., Yona, S., David, E., Kim, K.W., Goldmann, T., Amit, I.*, et al.* (2017). Autonomous TNF is critical for in vivo monocyte survival in steady state and inflammation. J Exp Med *214*, 905-917.

Yamamoto, M., Sato, S., Hemmi, H., Hoshino, K., Kaisho, T., Sanjo, H., Takeuchi, O., Sugiyama, M., Okabe, M., Takeda, K.*, et al.* (2003). Role of adaptor TRIF in the MyD88-independent toll-like receptor signaling pathway. Science *301*, 640-643.

Yamazaki, S., Kerbeshian, M.C., Hocker, C.G., Block, G.D., and Menaker, M. (1998). Rhythmic properties of the hamster suprachiasmatic nucleus in vivo. J Neurosci *18*, 10709-10723.

Yarovinsky, F., Zhang, D., Andersen, J.F., Bannenberg, G.L., Serhan, C.N., Hayden, M.S., Hieny, S., Sutterwala, F.S., Flavell, R.A., Ghosh, S.*, et al.* (2005). TLR11 activation of dendritic cells by a protozoan profilin-like protein. Science *308*, 1626-1629.

Yoo, S.H., Ko, C.H., Lowrey, P.L., Buhr, E.D., Song, E.J., Chang, S., Yoo, O.J., Yamazaki, S., Lee, C., and Takahashi, J.S. (2005). A noncanonical E-box enhancer drives mouse Period2 circadian oscillations in vivo. Proceedings of the National Academy of Sciences of the United States of America *102*, 2608-2613.

Young, M.R., Matthews, J.P., Kanabrocki, E.L., Sothern, R.B., Roitman-Johnson, B., and Scheving, L.E. (1995). Circadian rhythmometry of serum interleukin-2, interleukin-10, tumor necrosis factor-alpha, and granulocyte-macrophage colony-stimulating factor in men. Chronobiol Int *12*, 19-27.

Zarrinpar, A., Chaix, A., Xu, Z.Z., Chang, M.W., Marotz, C.A., Saghatelian, A., Knight, R., and Panda, S. (2018). Antibiotic-induced microbiome depletion alters metabolic homeostasis by affecting gut signaling and colonic metabolism. Nat Commun *9*, 2872.

Zarrinpar, A., Chaix, A., Yooseph, S., and Panda, S. (2014). Diet and feeding pattern affect the diurnal dynamics of the gut microbiome. Cell Metab *20*, 1006-1017.

Zehring, W.A., Wheeler, D.A., Reddy, P., Konopka, R.J., Kyriacou, C.P., Rosbash, M., and Hall, J.C. (1984). P-element transformation with period locus DNA restores rhythmicity to mutant, arrhythmic Drosophila melanogaster. Cell *39*, 369-376.

Zhang, D., Chen, G., Manwani, D., Mortha, A., Xu, C., Faith, J.J., Burk, R.D., Kunisaki, Y., Jang, J.E., Scheiermann, C*., et al.* (2015). Neutrophil ageing is regulated by the microbiome. Nature *525*, 528-532.

Zhang, Q., Zmasek, C.M., and Godzik, A. (2010). Domain architecture evolution of pattern-recognition receptors. Immunogenetics *62*, 263-272.

Zhang, S.Y., Jouanguy, E., Ugolini, S., Smahi, A., Elain, G., Romero, P., Segal, D., Sancho-Shimizu, V., Lorenzo, L., Puel, A*., et al.* (2007). TLR3 deficiency in patients with herpes simplex encephalitis. Science *317*, 1522-1527.

Zhao, L. (2013). The gut microbiota and obesity: from correlation to causality. Nat Rev Microbiol *11*, 639-647.

Zhao, Y., Liu, M., Chan, X.Y., Tan, S.Y., Subramaniam, S., Fan, Y., Loh, E., Chang, K.T.E., Tan, T.C., and Chen, Q. (2017). Uncovering the mystery of opposite circadian rhythms between mouse and human leukocytes in humanized mice. Blood *130*, 1995-2005.

6. Appendix

6.1. List of publications

09/2019 de Juan A, Ince LM, Pick R, Chen CS, Molica F, Zuchtriegel G, Wang C, Zhang D, Druzd D, Hessenauer MET, Pelli G, Kolbe I, Oster H, Prophete C, **Hergenhan SM**, (…), Scheiermann C: Artery-Associated Sympathetic Innervation Drives Rhythmic Vascular Inflammation of Arteries and Veins, *Circulation*; 140(13):1100-1114

12/2018 He W, Holtkamp S, **Hergenhan SM**, (…), Scheiermann C: Circadian Expression of Migratory Factors Establishes Lineage-Specific Signatures that Guide the Homing of Leukocyte Subsets to Tissues, *Immunity*; 49(6):1175-1190

01/2017 Druzd D, Matveeva O, Ince L, Harrison U, He W, Schmal C, Herzel H, Tsang AH, Kawakami N, Leliavski A, Uhl O, Yao L, Sander LE, Chen CS, Kraus K, de Juan A, **Hergenhan SM**, (…), Scheiermann C: Lymphocyte Circadian Clocks Control Lymph Node Trafficking and Adaptive Immune Responses, *Immunity*; 46(1):120-132

6.2. Affidavit

Hergenhan, Sophia Martina
Winzererstraße 49b
80797 München
Germany

I hereby declare, that the submitted thesis entitled

“Circadian Control of Leukocyte Numbers in the Circulation”

is my own work. I have only used the sources indicated and have not made unauthorised use of services of a third party. Where the work of others has been quoted or reproduced, the source is always given. I further declare that the submitted thesis or parts thereof have not been presented as part of an examination degree to any other university.

Munich, 01.05.2020 — Sophia Martina Hergenhan

Place, date — *Signature doctoral candidate*

6.3. Confirmation of congruency between printed and electronic version of the doctoral thesis

Hergenhan, Sophia Martina
Winzererstraße 49b
80797 München
Germany

I hereby declare that the electronic version of the submitted thesis, entitled

"Circadian Control of Leukocyte Numbers in the Circulation"

is congruent with the printed version both in content and format.

Munich, 01.05.2020 — Sophia Martina Hergenhan

Place, date — *Signature doctoral candidate*